The Kondo Effect in a Single-Electron Transistor

by

David Joshua Goldhaber-Gordon

A.B. Physics and A.M. History of Science
Harvard University, 1994

Submitted to the Department of Physics
in partial fulfillment of the requirements for the degree of

Doctor of Philosophy

at the

MASSACHUSETTS INSTITUTE OF TECHNOLOGY

June 1999

Author .....
Department of Physics
May 18, 1999

Certified by .....
Marc A. Kastner
Donner Professor of Physics and Department Head
Thesis Supervisor

Accepted by .....
Thomas J. Greytak
Professor and Associate Department Head for Education

The Kondo Effect in a Single-Electron Transistor

by

David Joshua Goldhaber-Gordon

Submitted to the Department of Physics
on May 18, 1999, in partial fulfillment of the
requirements for the degree of
Doctor of Philosophy

Abstract

The Kondo effect, which occurs when a metal with magnetic impurities is cooled to low temperatures, has been a focus of research in solid-state physics for several decades. I have designed, fabricated, and measured a system which behaves as a single "artificial" impurity in a metal, displaying the Kondo effect. This so-called Single-Electron Transistor (SET) has several advantages over the classic bulk Kondo systems. Most obviously, only one impurity is involved, so there is no need to worry about interactions between impurities, or different impurities feeling different environments. But even more importantly all the parameters of the system, such as the binding energy of electrons on the impurity and the tunneling rate between metal and impurity, can be tuned in-situ, allowing detailed quantitative comparison to thirty years of theoretical developments whose details could not be tested in previously-studied Kondo systems.

Thesis Supervisor: Marc A. Kastner
Title: Donner Professor of Physics and Department Head

Acknowledgments

When I read a thesis, I always like to read the acknowledgements first. They give a sense of the writer's personality in an otherwise stiff and regimented document. Though I've tried to adopt an informal tone in my thesis as a whole, I find I'm still enjoying this opportunity to recall and thank the many people who played a positive role in my scientific and personal odyssey of the last five years.

I did my graduate work in two places: MIT and the Weizmann Institute of Science in Israel. In each place I learned a great deal, did essential parts of the work, and had the opportunity to meet and interact with a wonderful group of people.

The making of the SETs featured in this thesis was a laborious process to which many people contributed over the course of the year I spent at the Braun Center for Submicron Research at Israel's Weizmann Institute of Science. I would particularly like to single out for mention: Udi Meirav, who acted *in loco consuasoris* during that year and strongly supported the idea of making very small nanostructures using very shallow 2DEGs, providing advice and help at many stages of fabrication and characterization; Hadas Shtrikman, MBE grower extraordinaire, who was willing to try pushing the limits on shallow heterostructures, and succeeded brilliantly; Rachel Goldman of the University of Michigan, and Randy Feenstra of Carnegie-Mellon, who did the high-resolution XSTM characterizations of the heterostructures, as described in Appendix B; Diana Mahalu, the e-beam lithography expert who achieved the remarkable 20 to 30 nm lines and spaces in the smallest devices; Grisha Bunin, who made reactive ion etching a bit more predictable; Kostya Gartsman, who helped train me on the SEM, and Vladimir Umansky, who took some of the beautiful SEM pictures shown here, all the while giving me a proper perspective on the craziness of America; Sorina Neagu, who gave helpful recommendations on many aspects of processing, maintained the metal evaporator, and was always a cheering presence in the clean room; Nathalie Questembert Balaban and Yael Hanein, who enjoyed chatting about physics or politics, patiently conveyed their knowledge of processing, and were delightful officemates, with the right mix of vitality and wry humor; and of course Yoram and Ofer, the twin pillars of the center, who kept everything running by dint of incredible skill and hard work, and always eventually good-humoredly did what I asked after I learned to hound them incessantly.

Outside the Braun Center, I also had the privilege of interacting with some of Weizmann's distinguished condensed-matter theorists. In particular, Joe Imry, one of the founding theorists of mesoscopic physics in the mid-'80s, offered simple, clear

explanations of the basics of the field, the fruit of a decade's thought. His sense for simple but not obvious concepts and experiments has left its imprint on everyone in the Braun Center and on the beautiful experiments they have produced. I feel fortunate to have been able to audit his class on mesoscopic physics.

Of the other Weizmann theorists, I had especially fruitful discussions both during my time at Weizmann and on later occasions with Ady Stern, Yehoshua Levenson, Shimon Levit, and Yuval Gefen.

Many other students, postdocs, and alumni of the Weizmann physics department made me feel welcome and helped me in myriad ways. I feel fortunate to have had the opportunity to interact with a group of such outstanding people and scientists: Rafa Almuhannad, Boaz Brill, Eyal Buks, Eyal Comforti, Guy Eytan, Gleb Finkelstein, Avi Messica, Yossi Paltiel, Rafi de Picciotto, Misha Reznikov, Ralf Schuster, Rafi Shikler, Sasha Soibel, and David Sprinzak. It has been a pleasure to meet many of these friends again at MIT, on return visits to Weizmann, and at conferences.

It was also nice to be part of a small American expatriate community at the Braun Center. Two other couples (David and Denise Cheskis, and Charles and Monica Sharman) were also spending a year in Rehovot while David and Charles worked with Udi, and we all helped each other with the cultural adjustment, went to *ulpan* together in the evenings, and became friends in the process. David generously shared with me his expert knowledge of processing, high-mobility MESFETs, and microwave techniques; his smile could always (and I mean *always*) be seen in the clean room. Charles and Monica were fun bridge opponents, and Ilana and I passed many a *shabbat* afternoon with them playing cards and discussing theology.

I must especially salute Moty Heiblum, who designed and orchestrated at Weizmann what is today perhaps the world's foremost center for mesoscopic physics research. I couldn't have accomplished what I did without his efforts on myriad fronts over many years. In addition, he and his students and postdocs continue to perform many of the exciting experiments that have made the Braun Center such an exciting place to be.

The year I spent in Israel was, like all years there, an eventful one for the country. The bombings of buses and plazas fades from memory, but the spirit and legacy of Yitzhak Rabin live on. He was assassinated at a peace rally shortly after I arrived in Israel, and my wife and I joined more than a million mourners paying their respects to him in Jerusalem. It was a terrible, heart-wrenching time. I believe and pray that over the next decade the Israeli and Palestinian peoples will find the trust and inner strength to enact the necessary transfers of power, with their concomitant

compromises.

Even before I left for Israel, I spent more than a year at MIT, where Marc Kastner welcomed me into his lab, and shared with me his excitement and insight into physics. When in my reading I run across a physical phenomenon that is new to me, Marc shows a remarkable ability to give a concise, correct explanation of the concept. He also gives excellent guidance, often suggesting the perfect measurement or approach to clarify puzzling data. After giving advice, Marc also knows to step back and give his students room to explore, a freedom I've really valued. Finally, Marc gives his students opportunities to participate in, and learn from, the broader physics community, by inviting us to speak with the many distinguished visitors passing through MIT, and by sending us to conferences. These interactions have made my graduate school years rich and exciting, and have given me a sense of the broad sweep of the field I could never have achieved just by doing my own experiments and reading PRL.

In Marc Kastner's lab I met Olivier Klein, a creative and insightful physicist and one of the best experimenters I know. Olivier doesn't sit still: he had done optical and microwave studies on superconductors as a grad student, making his rapid success in quantum dots (a new field with new techniques) all the more impressive. It was great fun working together and doing exciting and publishable work with Olivier my first year of grad school, and in the process he gave me an excellent crash course on how to be an experimental physicist.

Olivier and I worked closely on interpreting our results with Claudio Chamon, then a student of the theorist Xiao-Gang Wen, and now a professor at B.U. Claudio has the rare knack of explaining the essence of his often esoteric calculations in simple language. He also always seems to carry the Brazilian sun in his smile. Claudio used to keep me in shape as my regular squash partner at MIT (now he's a father and professor, with more pressing responsibilities to his respective wards).

Steve Simon, besides generally being a pleasure to talk with, helped me as I struggled to understand why Fano resonances were occurring in my single-electron transistors. The care he takes in crafting clear and simple talks has inspired me to work toward the same goal. I've missed Steve since he finished his theory postdoc at MIT, but I've fortunately had frequent occasions to see him since then during visits to Bell Labs or at conferences.

Along with Olivier, David Abusch-Magder was my other young mentor at MIT. He shared his enthusiasm for our common subject even as he suffered through two years of fabrication under much less congenial conditions than I would experience at Weizmann. I'm glad to still be able to benefit from David's physics insights, ranging

from calculational tricks to new ways of seeing a topic I thought I understood. We can also commiserate about all the technical work that goes into building a lab, as I'm installing a new dilution fridge, and David's building up an entire lab as a new staff member at Bell Labs. David is my acknowledged master of interpersonal relations: he showed me by example how to remain good-natured while also standing up for myself, whether dealing with colleagues or with company representatives. David's teaching has been crucial both to my confidence and to my effectiveness in handling the political scrapes of life. Finally, David and his wonderful wife Ruti remain great friends of me and Ilana. The phone tides us over between insufficiently frequent visits here or in New Jersey, but each time I see their brilliant and charming baby Oren I'm shocked by how much he's changed (and impressed by what good parents David and Ruti are — they can be models for yet another phase of life).

Recently, I had the privilege of working with Jörn Göres. He came to the lab as a beginning grad student, but he already had quite a lot of experimental and theoretical experience, having benefited from Germany's more rigorous undergrad program plus an extra year of lab work at UConn in the U.S. Jörn and I were able to teach each other a lot, but it was also a pleasure having an enthusiastic and smart partner in experiments, brainstorming, and more mundane matters, after a year and a half of working on my own. The material of Chapter 6 represents some of the fruit of our work together. Jörn has just returned to Germany to continue graduate work at the Max Planck Institut in Stuttgart. I know he will succeed brilliantly in all that he undertakes there. Since then, I've enjoyed beginning to work with Ian Zacharia, a grad student who's recently joined the lab, and I look forward to spending more time with him now that I've finished my thesis.

Nicole Morgan has been my compatriot in the lab almost from the start. It has been wonderful to have someone at the same stage with whom to discuss physics, study for exams, and share the inevitable frustrations of research. Nicole took on a very demanding project, and I'm delighted that it's producing exciting results. I'm sure you'll be hearing more about her work in the years to come.

Misha Brodsky, in Ray Ashoori's lab, is a good friend with whom I often benefit from discussing the related physics of our respective experiments. He's done very interesting work in the Ashoori lab, and I've also grown to enjoy his dry sense of humor and to appreciate his personal generosity.

I have had many productive discussions with Sven Heemeyer and Joel Moore. Their interesting calculations and clear explanations on many-body aspects of SET behavior have helped me interpret existing data and plan for future experiments.

I've long appreciated Adam Polcyn's broad knowledge of physics, spanning atomic and solid-state, and his patient sharing of his experimental tricks and techniques. So of course I frequently go to him for advice. In the process, he's become a good friend as well. I wish him well in his move to California.

Tom Killian and Dale Fried, Adam's fellows in Tom Greytak's group, also could be relied on for friendly and insightful suggestions on low-temperature techniques, machining, electronics or, in a pinch, for a supply of liquid helium. With their graduation as well, the second floor of Building 13 won't be the same.

I enjoyed interactions with many other students and postdocs in Marc Kastner's group and others on the corridor. Only writing this do I realize how much this community made physics grad school lively, interesting, and cheerful when I needed cheer. Among those I will (or already do) miss are Jessica Thomas, for her friendliness and her depth of perspective on the world at large; Beth Parks, for her amazing energy, good cheer, and articulate discussion of physics; Fang Chen Chou and Pam Blakeslee, each of whom exudes an unusual personal warmth; Gleb Finkelstein, for hours of fascinating discussions. It has been a pleasure to interact with Dave Carter, Ila Prasad, Danielle (*née* Kleinberg), Yuki Ono, Yuki Nihey, Barry Wells, Martin Greven, Young Lee, Rebecca Christianson, Young-June Kim, Sungil Park, Yujie Wang, Mike Young, Vijay Pande, Ho-Bun Chan, Paul Glicofridis, David Berman, Bob Leheny, Valery Kiryukhin, Kolya Zhitenev, Neer Asherie, Zhenya Zastavker, Jens Siewert, David Landhuis, Steve Moss, Lorenz Willmann, Kent Thurber, Allen Hunt, and too many more to list here.

The staff of the CMSE have always been kind and gracious, unstinting of their time and effort in helping with administrative tasks, even well beyond the call of duty. I've also enjoyed their friendship over the past five years, so it is a pleasure to thank Carol Breen, Virginia Esau, Karen Fosher, Ron Hasseltine, Debra Henry, Susan Rosevear, and Amanda Tat. Amongst other administrators, I would particularly like to thank Peggy Berkovitz and Pat Solakoff for really caring about students and giving the physics department a human and compassionate face.

I am very grateful to Felice Frankel for teaching me a great deal about presenting data in visual form, and to Jen Cook-Chrysos for expertly drawing many of the figures presented in this thesis. Patrick Winston taught me important lessons about how to give a talk, and the thought processes he initiated have also improved my writing. Matthew Gray provided invaluable and sustained help installing Linux on my home computer, enabling me to write my thesis in a quiet environment. Marc Kastner, Ray Ashoori, and Wolfgang Ketterle served on my thesis committee. I appreciate their

supportive attitudes during the process, and thank them for comments that made this thesis stronger and clearer.

MIT has one of the most exciting set of physics professors anywhere, in condensed-matter and beyond. Discussions with quite a few of these professors have enriched my MIT experience greatly. In particular, it has been a pleasure to discuss with Ray Ashoori the broad range of fascinating results on electrons in reduced dimensions that keep coming out of his group. Having such an exciting group down the hall doing research related to mine is a rare opportunity in today's university environment, and it has really helped my scientific growth. Peter Wolff encouraged me to think broadly about what areas would be exciting to work on next, and shared his enthusiasm for the future of nanoscience at a time when I was temporarily jaded. Bob Birgenau generously took the time to give me valuable perspective and advice on career paths. Patrick Lee, besides suggesting a decade ago that the Kondo effect could be observed in a single-electron transistor, has shared with me some of his broad knowledge of the Anderson model when I was trying to puzzle out some unexpected wrinkles in the Kondo effect. Leonid Levitov has inspired me and shown me how to start thinking about localized electrons using analogies from areas as far-removed as nuclear physics. Xiao-Gang Wen has recently helped me start thinking about extensions to the simple Kondo system, including two-channel Kondo. Supriyo Datta, a visiting professor from Purdue for a semester, helped make the formalism of mesoscopic electron transport simple and intuitive. Takashi Imai has shared his insights on spin resonance when I was contemplating an ESR experiment. Moungi Bawendi, who studies chemically-synthesized quantum dots, has helped me see how the relevant physics and experimental techniques change with the size of a dot. In addition, his worked has spurred my imagination about the diverse and powerful possibilities of chemically-synthesized nanostructures. Martin Deutsch has shared with me his enthusiasm for my work, along with insights on its striking parallels to ideas in nuclear physics. Finally, Gene Fitzgerald, who develops remarkable and novel SiGe-based heterostructures, has inspired me to consider how nanostructure physics might be changed when the band structure of the host is made more complicated than that of GaAs.

Last Fall I spent an interesting and productive three weeks visiting the Quantum Transport group at TU Delft in the Netherlands. The data on state filling presented in Figures 4-6, 4-7, and 4-8 of Chapter 4 were taken during this stay in Delft. I had fun working with Wilfred van der Wiel, Silvano de Franceschi, Jeroen Elzerman, and Leo Kouwenhoven. Wilfred was so amazingly generous as to let me live in his apartment

during my visit. He also taught me that the way to get around Delft is by bike, and I was very grateful for the resultant exercise and freedom from the bus schedules (which had put a damper on working till the wee hours of the morning)! Many others also extended lovely hospitality to me: Nina Markovič and Silvano welcomed me into their respective homes, where Silvano acted as master chef; and my visit was highlighted by interesting conversations with Tjerk Oosterkamp, Hans Mooij, Cees Dekker, Peter Hadley, Yuli Nazarov, Kees Harmans, Ramon Aguado, David Dixon, Caspar van der Wal, Bram van der Enden, Danny Porath, Nina Markovič, Leonid Gurevich, Jorg Janssen, and Henk Postma.

Much of my last two years has been focused on designing, purchasing, and implementing a new measurement setup, including a new dilution refrigerator. In the process, it has been a pleasure to work with Giorgio Frossati, low-temperature physicist and fridge designer *par excellence*, and a true gentleman. Matt Reynolds, of the MIT Media Lab, has generously applied his electronics and microwave wizardry to the project. It has been a joy to learn from him. The design of the wiring and microwave filters on the new fridge owes much to both Giorgio and Matt, and I'm sure this work will achieve fruition in well-chilled electrons for many theses to come.

When I asked Michel Devoret for advice on setting up a dilution fridge, he graciously invited me to spend a week at Saclay, where I had the opportunity to learn about exciting experiments and see well-designed fridges first-hand. Many thanks to Christian Glattli, Michel Devoret, Daniele Esteve and the entire Saclay Quantronics Group for making my visit productive, delightful, and memorable.

Over my entire graduate career, I have also had the privilege to learn from conversations with many other researchers from outside MIT, many of them theorists due to the strong theoretical ties of my chosen research area. Yigal Meir, Ned Wingreen, Leonid Glazman, and Theo Costi in particular stand out for their patience, the clarity of their explanations, and their influence on my thinking about the Kondo effect. Yigal and Ned first got me excited about Kondo, and later pointed out ways of quantitatively testing theory with my experiments. Leonid has come closer to anyone else to suggesting an intuitive way of understanding the Kondo effect. And Theo, besides having performed the beautiful calculations to which I compare my data in Chapter 6, generously modified his calculations to account for the geometrical difference between a bulk Kondo system and my SETs (the results were strikingly similar). The many others who have augmented and challenged my understanding of physics, and particularly the Kondo effect, over the last five years include Oded Agam, Igor Aleiner, Yoram Alhassid, Jim Allen, Boris Altshuler, Vinay Ambegaokar, Nathan Argaman,

Guy Austing, Dima Averin, Yshai Avishai, Leon Balents, Israel Bar-Yosef, Harold Baranger, Sean Barrett, Bertram Batlogg, Alexey Bezryadin, Gene Bickers, David Bishop, Chuck Black, Robert Blick, Eberhard Bodenschatz, Greg Boebinger, Piet Brouwer, Christoph Bruder, Bob Buhrman, Federico Capasso, Tapash Chakraborty, Albert Chang, Mitya Chklovskii, David Cobden, Peter Coleridge, Barbara Cooper, Mike Crommie, Sara Cronenwett, Catherine Crouch, Karin Dahmen, Sankar Das Sarma, Drago Davidovic, David Duncan, Laurence Eaves, Jim Eisenstein, Lloyd Engel, Klaus Ensslin, Mark Eriksson, Saro Fazio, Herb Fertig, Matthew Fisher, Misha Fogler, Carl Franck, Toshimasha Fujisawa, Antoine Georges, David Gershoni, Bennett Goldberg, Yehuda Goldin, Vladimir Goldman, Hermann Grabert, Bob Grober, George Grüner, Bert Halperin, Alex Hamilton, Rolf Haug, Pawel Hawrylak, Jack Hergenrother, Selman Hershfield, Wilson Ho, Michel Horvatič, Wataru Izumida, Jainendra Jain, Hong-Wen Jiang, David Khmelnitskii, Jay Kikkawa, Steve Kivelson, Jörg Kotthaus, Alexay Kozhevnikov, Bernhard Kramer, Herb Kroemer, Arvind Kumar, Rolf Landauer, Rob Liu, Carol Livermore, Daniel Loss, Allan MacDonald, Michael Manfra, Jan Marek, Charlie Marcus, Kostya Matveev, Paul McEuen, Emilio Mendez, Anurag Mittal, Raj Mohanty, Laurens Molenkamp, Don Monroe, Cherry Murray, Chris Murray, L. Ravi Narasimhan, Doug Natelson, Yehuda Naveh, Chetan Nayak, Peter Nordlander, Jacob Oaknin, Yuval Oreg, Richard Packard, Juanjo Palacios, Jeevak Parpia, Pierre Petroff, Danielle Pfannkuche, Loren Pfeiffer, Aron Pinczuk, Philip Phillips, Phil Platzman, Walter Pötz, Bob Pohl, Dan Prober, Karin Rabe, Dan Ralph, Emmanuel Rashba, Nick Read, Mark Reed, Michael Roukes, Subir Sachdev, Andy Sachrajda, Hugo Saïar, Osamu Sakai, Avi Schiller, Rob Schoelkopf, Gerd Schön, Christian Schoenenberger, Anirvan Sengupta, Jim Sethna, Danny Shahar, Shye Shapira, Herb Shea, Efrat Shimshoni, Boris Shklovskii, Bob Silsbee, Uri Sivan, Lydia Sohn, Paul Solomon, Shivaji Sondhi, Boris Spivak, Srinivas Sridhar, Andy Steinbach, Horst Störmer, Doug Stone, Charlie Stafford, Hideaki Takayanagi, Seigo Tarucha, Carlos Tejedor, Mike Tinkham, Chang Tsuei, Sergio Ulloa, Jan van Ruitenbeek, Chandra Varma, Giovanni Vignale, Jan von Delft, Felix von Oppen, Watt Webb, Dietmar Weinmann, Jürgen Weis, Jeff Welser, Bob Westervelt, Bob Willet, Frank Wise, Amir Yacoby, P.D. Ye, Gergely Zimanyi, and Ulrich Zuelicke.

I look forward to enjoying continued interactions with this friendly and stimulating community over the years to come.

Finally, I come to the people I knew even before I entered the (infinite) corridors of MIT.

My parents, Suzan and Fred Goldhaber, taught me that I could pursue my dreams, wherever they might lie. It's not their fault that I ended up back in physics, and it's much to their credit that I'm here because I want to be, not by default. They also showed me by example how to appreciate life, and to live it well, instilling in me a love for Judaism, good food, music, art, literature, and the wilderness of the American southwest. Equally important, they showed me how to treat my fellows from all walks of life with openness and respect. Thank you for making me who I am today.

My grandparents too made strong impressions on me. My mother's parents, Eva and Walter Kress, died when I was very young, but I can still remember the warmth with which they held me and played with me. Even after they were gone, they left fragments of their lives to remember them by: the raspberry bushes Eva planted beside their house continued to bring forth fruit, and Walter's quirkily meticulous system for filing household supplies kept yielding up surprising delights. I still smile when I think of the box of "pieces of string too small to use". Perhaps he was wise before his time — I'm sure today's physicists could find a use for them.

My father's parents, Gertrude (Trude) Scharff Goldhaber and Maurice Goldhaber, have inspired me in other ways. Both achieved great distinction through their careers in nuclear and particle physics. Not only was Trude an outstanding scientist, but to get there she had to overcome the gross discrimination faced by women scientists of her generation. In turn, she actively mentored and encouraged many younger women establishing their own careers in physics. Trude died recently, but I was privileged to see her regularly for many years, into my adulthood. I am sorry that she could not be here to read this thesis. Maurice continually astounds me. Not only does he participate actively in an exciting neutrino oscillation experiment and continue to spend every day working at Brookhaven lab, but he swims, plays tennis, and travels so much that he hasn't had time to write his memoirs. I hope I've inherited half his insight, charm, vitality, and staying power.

Discussions with my sister Sara Goldhaber-Fiebert constantly challenge and refine my feelings on a broad range of religious, ethical and societal issues. Her love and support have sustained me during the more trying times of graduate school. And I'm delighted to have recently gained an intelligent, sensitive, generous and fun friend in my brother-in-law Jeremy Goldhaber-Fiebert.

I thank Ilana's family, Robert, Evvy, Tamar, and Dov, for wholeheartedly welcoming me as a family member. It is always a pleasure to discuss physics with Robert,

and to learn about his pioneering experiments in the field of coherent control. Not only have these been exciting in their own right, but they have also encouraged me to think about new directions for my own work on artificial atoms. Evvy is the central pillar of a warm and loving family, and it has been inspiring to watch her follow her dream and forge a new career in family counseling after many years in teaching. Tamar's forthrightness, wit, and deep caring have made her an increasingly important part of my life over the past few years. Finally, I have enjoyed sharing my love of board games with Dov, in whom I have found a worthy opponent. As he has grown and matured, I have watched him become a considerate and thoughtful *mensch*, wise beyond his teenage years and articulate in defending his passionate ethical views.

My high school science teacher, Mrs. Melanie Krieger, gave me and hundreds of others the freedom and encouragement to do scientific research even in high school, through her fabulous "Westinghouse Prep" course.

James Ellenbogen of the MITRE Corporation was one of my first and most important physics mentors outside of my family, and our active and fruitful relationship continues to this day. James' vision and leadership brought me together with other bright young scientists in different specialties, and inspired us to write an overview of nanoelectronics for computing. Two years ago this article was published as the review article in a special nanoelectronics issue of the Proceedings of the IEEE, and later it was selected as MITRE's best paper of the year.

My enthusiasm for condensed-matter experiment was first sparked by a flexible and challenging undergraduate lab course with Bob Westervelt and Costas Papaliolios. To their credit, I can look back on the experience and see that I really got a taste of what research in the field is like.

In addition to my family and my friends within the physics community, friends outside of physics have sustained me with their warmth and companionship. This is not the place to describe each of my friends and say what makes them so special, but I would at least like to name some who are very important to me. Thank you Marc Kuchner, Joshua Newman, Badsah Mukherji and David Miller. Thank you Matthew Gray and Carrie Heitman — your friendship in particular has carried me and Ilana through the last three years.

I dedicate this thesis to my wife Ilana, my soulmate for the past seven years. Her perceptive editing and ear for language have made this thesis much more of a pleasure to read. And her support, understanding, and delicious meals when I needed them have kept me working and in good spirits as the writing dragged on. It has been a revelation to wrestle together with issues in physics, biology, and every aspect of life,

and I look forward to many more years of a partnership that only gets better with time.

The work described in this thesis was supported by the grants from the National Science Foundation, the US Army's Army Research Office, the MINERVA foundation (Munich, Germany) and the Israeli Science Foundation (administered by the Israeli Academy of Science and Humanities). I gratefully acknowledge financial support during my graduate studies through a Graduate Fellowship from the Fannie and John Hertz Foundation and through the K.T. Compton Fellowship of the MIT Physics Department.

Contents

List of Figures

Chapter 1

Introduction

If you take a chunk of a metal like copper and cool it down to low temperature, its resistivity decreases monotonically before saturating to a finite value at very low temperature. In fact, this resistivity decrease is a hallmark of conductors as contrasted with semiconductors or insulators whose conduction is thermally activated so that resistivity increases with decreasing temperature. The resistivity of a metal decreases with decreasing temperature because there are fewer (and lower energy) phonons for the conduction electrons to scatter off of, and it saturates because the copper is never a perfect crystal — there are always impurities which can scatter conduction electrons. This is all very well understood using the Drude model of conduction [1], cited in [2].

However, starting in the 1930s, people began to observe a very strange phenomenon: sometimes, when they cooled down a piece of metal, it would behave as expected at high temperatures, but then at very low temperatures, typically 1–20 K, the resistivity would hit a minimum and begin to rise again. The reasons for this were mysterious for a long time (I'll outline the history briefly in the next chapter), but in the end the culprit turned out to be very dilute, initially unintentional, magnetic impurities: a few parts per million of iron in gold, for example. These impurity atoms were so dilute that, to first approximation, they didn't feel each other's presence, so the phenomenon could be considered a property of a *single* magnetic impurity in a metal. This begs the question: what *is* a single magnetic impurity? We are used to thinking of magnetism as a cooperative behavior — ferromagnetism, in which the spins of the unpaired electrons on all the individual iron atoms lock together to form a very large magnetic moment. But this is really a quite complex phenomenon. A single magnetic impurity is just an atom with an unfilled shell, so that the unpaired electrons form a net magnetic moment. While most atoms in isolation have unpaired

electrons, when they are put in a metallic host this property generally goes away, but the "ferromagnetic" transition elements tend to retain their unpaired electrons.[1]. We can see the unpaired electrons by making magnetic susceptibility measurements and observing a Curie law. What we have, then, is an atom with an unfilled shell, bathed in a sea of conduction electrons: the simplest combination of magnetism and conduction electrons, and perhaps a basis for trying to understand more complex materials like bulk iron.

Getting back to our puzzle, it took fifty years to work out what was happening, but here's the upshot. Atoms with unpaired electrons tend to form bonds or spin singlet states to spread out their electrons over a larger area and hence reduce their kinetic energy. As I mentioned before, the impurity atoms are ideally so dilute that they don't interact with each other, but each impurity *can* form a bond with the surrounding conduction electrons, as illustrated in Figure 1-1. This is just like a bond between two Hydrogen atoms, except that only one of the electrons starts out localized—the other is a conduction electron and hence starts out delocalized and must be localized somewhat to form the bond (costing energy). As a result, the bond is rather weak. Unlike molecular hydrogen, which is stable to well above room temperature, this type of bond forms only at very low temperatures, tens of Kelvin at most. But when the bond does form, because it involves conduction electrons it has a dramatic effect on electron transport. If an electron sent in from far away passes close to an ordinary impurity, it has some chance to scatter off the impurity and head off in a new direction, increasing resistivity. When these special bonds form, the behavior is more dramatic. *Every* electron passing near to our impurity *must* hang around for a while, participating in the bond, before leaving in a new, random direction. This situation is referred to as the unitarity limit of scattering [3, pp. 34, 121], and only occurs when the bond is well developed, at extremely low temperatures. At these temperatures, the resistivity stops rising, and saturates at a new level, the Curie part of the magnetic susceptibility disappears (localized spins are paired with surrounding conduction electron spins), the spin-related specific heat vanishes, and a whole host of other measurements corroborate this picture [3, 4, 5, 6, 7]. This set of phenomena is collectively known as the Kondo effect [8].

Not only has the Kondo effect been a challenging and exciting realm for experiments, but it has been one of the classic problems in condensed-matter many-body theory over the past forty years, demanding, and serving as a proving ground for, ever

[1]This can also depend on the host metal

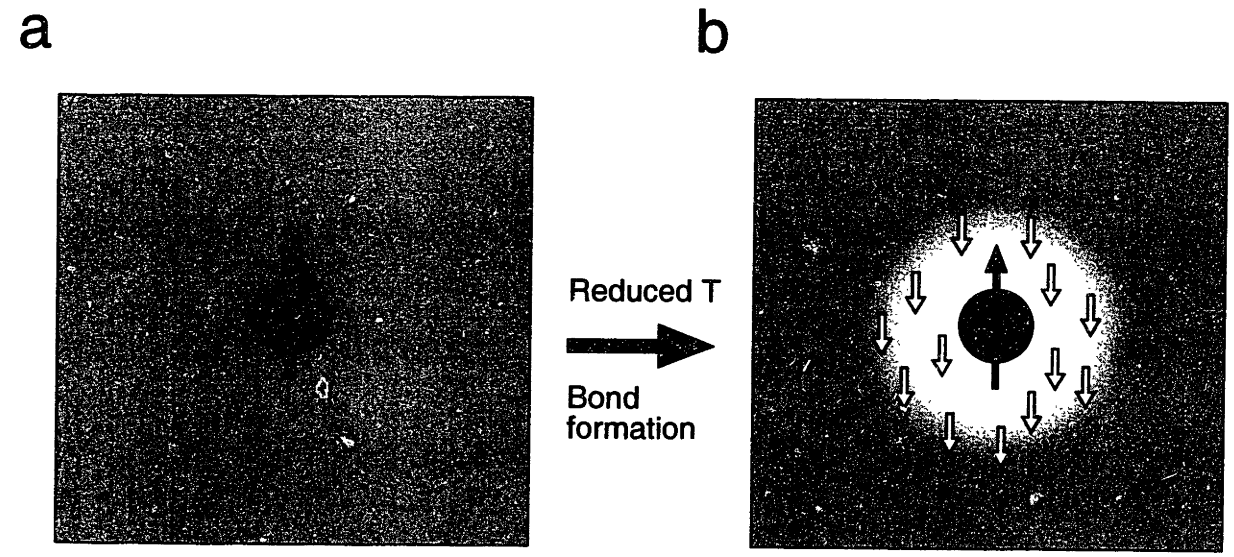

Figure 1-1: A magnetic impurity in a metal has one or more unpaired electrons, and hence a net spin magnetic moment. At low temperature, the unpaired electron(s) form a bond with a conduction electron in the surrounding metal. This bond compensates the magnetic moment of the impurity spin and has dramatic effects on electronic conduction in the metal host.

more sophisticated non-perturbative techniques.[2] The reason for this is that it offers exactly the right combination of a conceptually simple model, broad interest as the simplest example of magnetism combined with conduction electrons, and stubborn refusal to yield up its secrets to simple treatments.

It took thirty years after the first experiments to understand the Kondo effect on even a basic level, but eventually the theorists got ahead. They can now predict the detailed temperature dependence of resistivity as the bond gradually forms, and even the strength of the bond as a function of parameters of the impurity atom, the host metal, and their coupling. Unfortunately, these parameters cannot easily be tuned but are fixed for each combination of impurity and host. Furthermore, the values of these parameters are not known from first principles, and they are difficult to determine with accuracy. So we're left with a situation in which theory makes rich predictions about the relation of the emergent bond energy scale to other parameters of the system, and experiment can't test any of them.

Enter the artificial atom. For ten years, advances in semiconductor processing technology have enabled physicists to create small droplets containing one to a thousand electrons. These droplets, variously termed quantum dots or artificial atoms

[2]The bond does not appear, even to infinite order, in perturbation theory [3, p. xix]

(AAs), will be discussed more in Chapter 3, but for now the important thing is that they really act like atoms in important ways: they hold a fixed, integer number of electrons; and it takes energy to change that number (ionization) or to excite the electrons to higher quantum states. But unlike real atoms their shape, size and number of electrons can be chosen by design, and these properties are even tunable. For example we can add electrons one at a time. This has allowed some very interesting spectroscopic studies of the ground and excited states of artificial atoms over the past decade [9, 10, 11, 12, 13], but it also held out the possibility of juxtaposing these artificial atoms controllably and tunably with an external environment [14, 15, 16, 17, 18].

In particular, we could imagine placing an artificial atom near a reservoir of mobile conduction electrons—an artificial metal—so that electrons can tunnel back and forth between the "impurity atom" and the "metal". Since electrons could be added to the system one at a time, the impurity could be converted from even occupancy/paired electrons/non-magnetic to odd occupancy/unpaired electron/magnetic. I set out to create a system like this in order to study the Kondo effect in an idealized single, highly tunable "impurity", testing theoretical work on both artificial atoms and bulk Kondo systems [18]. What followed forms the bulk of this thesis, but suffice it to say that I've been able to quantitatively test theoretical predictions both longstanding and recent, and the match is astonishingly good.

In Chapter 2, I will describe the current theoretical understanding of the Kondo effect in bulk systems. Since I cannot do justice to this lively field in the space available, I refer interested readers to the excellent book by Alex Hewson [3]. For the experimental picture, I recommend the review by Grüner [5].

In Chapter 3, I will explain the basics of transport studies of artificial atoms, including the Coulomb blockade. This will form an essential basis for the less familiar and intuitive phenomena of the Kondo effect. For readers who want to know more, I recommend several theses: Ethan Foxman's [19], as an excellent introduction to transport phenomena in artificial atoms; David Dixon's [20] and Carol Livermore's [21], on coupled artificial atoms ("artificial molecules", of course); and Tjerk Oosterkamp's [22] for several interesting spectroscopic studies on artificial atoms. There are also multiple good reviews and paper collections, for example References [23, 24, 25].

In Chapter 4, I will describe the conditions under which an artificial atom connected to an artificial metal might be expected to display the Kondo effect, as well as the basic phenomenology of the Kondo effect in such a coupled system. This will require me to introduce a simple model of how electrons fill states in an artificial

atom. These phenomenological discussions will be paired with supporting data.

Chapters 5 and 6 are more succint, as they are directed at those already familiar with the field of semiconductor nanostructures. Chapter 5 will cover the basic experiments which demonstrate all the qualitatively-expected aspects of the Kondo effect in an SET.

Chapter 6 will go on to explain some more detailed and quantitative theoretical predictions, along with the experimental data that match them. In one case, the data vindicate for the first time a thirty-year-old prediction.

Finally, Chapter 7 will briefly explore puzzles in the Kondo measurements, along with other interesting phenomena that occur in the same SETs, before wrapping up with some hints as to where the research might go from here.

For the diehard, details on fabrication may be found in Appendices A and B, and a brief discussion of measurement techniques and associated issues in Appendix C.

Chapter 2

Kondo effect

2.1 Background and History

To recap the discussion in Chapter 1, the Kondo effect refers to the behavior of a metal with magnetic impurities cooled down to low temperature, especially the anomalous temperature-dependence of the resistivity. At relatively high temperatures, metallic resistivity is typically dominated by electron-phonon scattering. As the temperature is lowered well below the Debye temperature, this scattering rate, and hence the resistivity, decreases as T^5, due to a combination of three factors: (i) $E_{\text{phonon}} \leq kT$ or equivalently $q_{\text{phonon}} \leq kT/\hbar c$: only phonons coupling electron states near the Fermi surface can scatter electrons, so the number of phonons effective in scattering decreases as T^2; (ii) the square of the electron-phonon coupling matrix element decreases linearly with q_{phonon} and hence with T; (iii) since we're well below the Debye temperature, $q_{\text{phonon}} \ll k_{\text{F}}$, so a single phonon can't change an electron's momentum or velocity dramatically. The resulting predilection for forward scattering of electrons by phonons weakens the momentum (current) relaxation by phonons by a further factor T^2. These three factors combine to produce the dramatic T^5 decrease in phonon-related resistivity [2]. At sufficiently low temperatures (a few Kelvin), this scattering rate becomes insignificant, but imperfections in the crystal lattice cause residual scattering and hence finite resistance as $T \to 0$ even in very pure and carefully-prepared samples.

More than sixty years ago, in the 1930s, researchers began noticing that this simple picture didn't always hold. Gold cooled to 10 K sometimes showed a resistivity *rise* rather than the typical saturation as temperature was lowered still further [26, 3]. The origin of this behavior remained a complete enigma through the mid-1950s [3, p.

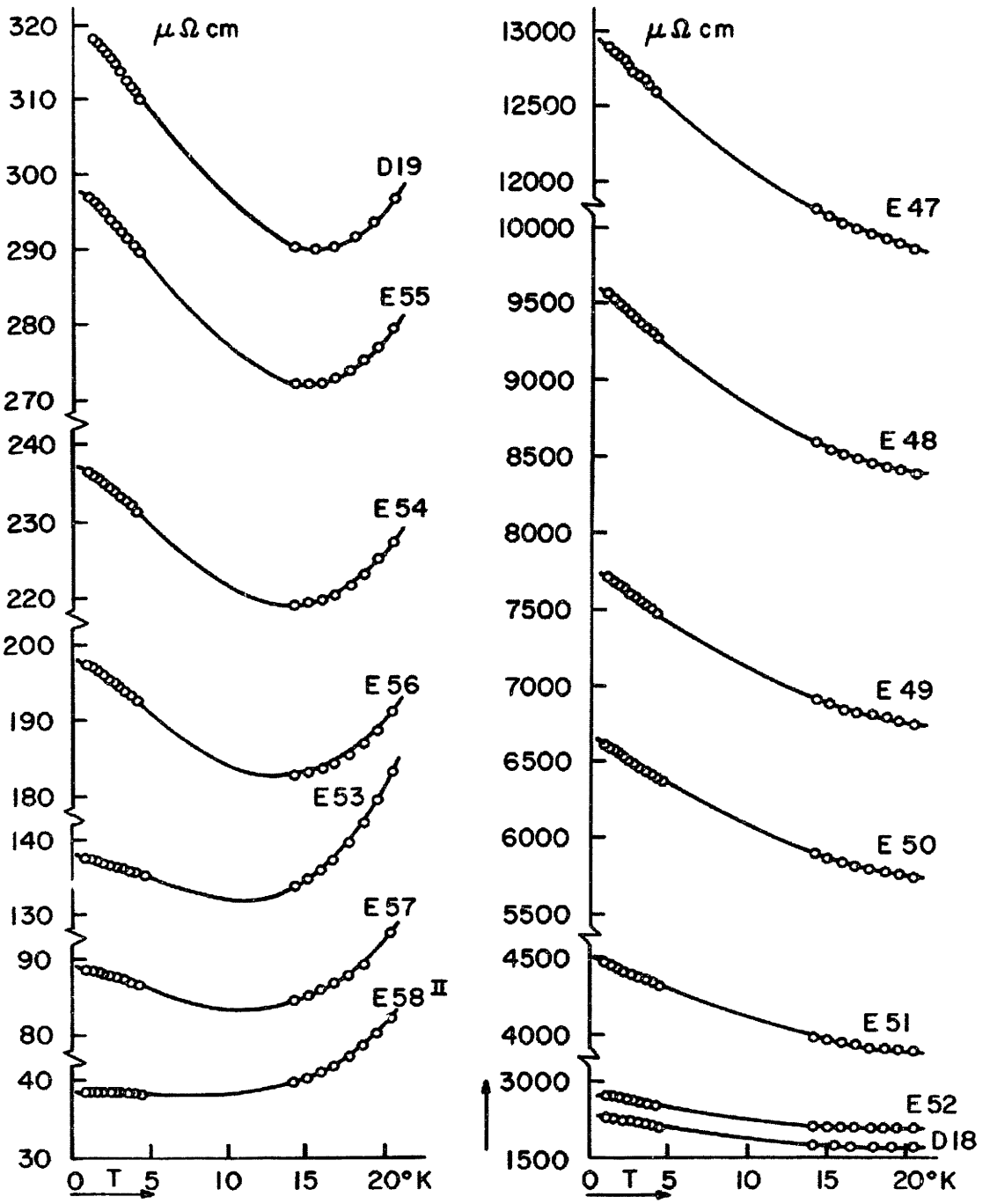

Figure 2-1: The results of a systematic study of resistivity vs. temperature for various Cu/Au alloys with intentional Fe impurities (reproduced from Reference [27]). Note that resistivity decreases with decreasing temperature, then reaches a minimum and increases again. The temperature at which the minimum occurs is rather insensitive to impurity concentration, but highly sensitive to the composition of the host alloy (different for each curve in the figure). As described in the main text, this type of behavior was first observed in the 1930s.

xviii]. In the late '50s and early '60s several theorists formulated models of the phenomenon based on scattering from impurities [28, 29], but it was not until 1964 that experimenters conclusively correlated the resistivity anomaly with the now-intentional presence of magnetic impurities in the metal: the presence of impurity atoms which retained a magnetic moment despite immersion in the host metal appeared to be connected to the rise in resistivity [4] (see Figure 2-1 for an example of the low-T increase in resistivity. Inspired by this result [3], Jun Kondo shortly thereafter made the first theoretical steps toward an explanation of the effect [30].

2.2 A magnetic atom: concepts and models

Before explaining Kondo's insight, I would like to address a more basic issue: What is a magnetic atom? For isolated atoms, the answer is simple: any atom with an unfilled shell is paramagnetic (i.e. has a permanent moment which aligns with an externally-applied field). Some elements form bulk magnetic solids, again with moments that align with an external field, however here the correlations among the moments of electrons on neighboring atoms are important, and so the phenomenon is more complex and less well understood. For example, in Fe the moments all align ferromagnetically while in Cr they alternate direction antiferromagnetically. There is really quite a leap from individual magnetic atoms to bulk magnetic metals: not only do we immerse each magnetic atom in a sea of mobile electrons, but we also place many magnetic atoms in close proximity. Our understanding of the final result may be aided if we can understand the result of just the first of these steps: placing an isolated magnetic atom in a metallic environment. The first important question that arises is whether the magnetic atom remains magnetic in its new environment, retaining a magnetic moment which can align with an externally-applied field. This question was first properly treated by Anderson, who articulated criteria for the survival of magnetism in the context of a simple two-parameter model [29]. The model Hamiltonian, known as the Anderson Hamiltonian, is

$$\mathcal{H}_{\mathrm{A}} = \sum_{\sigma;k<k_{\mathrm{F}}} \epsilon_{k\sigma} c^{\dagger}_{k\sigma} c_{k\sigma} + \sum_{\sigma} \epsilon_{\sigma} d^{\dagger}_{\sigma} d_{\sigma}$$
$$+\frac{1}{2} U n_{\sigma} n_{\sigma'} + \sum_{\sigma;k<k_{\mathrm{F}}} t_{k\sigma} c^{\dagger}_{k\sigma} d_{\sigma} + \mathrm{H.c.} \tag{2.1}$$

The Anderson model starts with localized and delocalized electrons, represented by creation operators $d^{\dagger}_{\sigma}$ and $c^{\dagger}_{k\sigma}$, respectively. The index σ indicates the spin of an electron, while k indicates its momentum, and thus is only included for the delocalized electrons. The first term represents the energy of all the delocalized electrons in the Fermi sea of the metal. The second term represents the energy of localized electrons in a single impurity atom. Here I have followed Anderson in considering just a single localized "d" state which can hold zero, one, or two electrons (of opposite spin), the simplest possible model of an atomic shell. This constitutes both a simplification which doesn't change any of the important physics [31], and is a good approximation: first, we ignore the five-fold degeneracy in the atomic d-orbitals of real magnetic impurities; second, we assume that the many other orbital states on the same atom are either full or empty, and hence in both cases inert — only the partially-filled orbital near the Fermi level is of interest to us. Even our single d-orbital has Kramers degeneracy: it can be filled by a spin up or down electron with the same energy $\epsilon_{\uparrow/\downarrow} = \epsilon_{\sigma}$. Were electrons non-interacting, it would be impossible for such a localized state in equilibrium with a Fermi liquid reservoir to have an unpaired electron (one state filled and the other empty). Instead, either both degenerate spin states would be empty or both full, depending on whether their energy is greater or less than the Fermi energy. However, experiment tells us that it is possible to have an unpaired electron (and hence a net magnetic moment) on the localized site. This is possible because electrons *do* interact with each other via the Coulomb repulsion. When one electron is added to a small region, the energy for adding a second electron is increased by a Coulomb charging energy U, possibly preventing the second electron from entering. This charging effect is described by the third term in the Hamiltonian. Finally, the fourth term describes transitions between localized and delocalized states.

Now that I've laid out the Anderson model, I can articulate the criteria for the model impurity to display magnetism. For an isolated atom, having an unfilled shell is enough to produce a net paramagnetic moment, but in a metallic environment such

a conclusion is less obvious. Certainly, as a first condition, the impurity state must be partially filled, occupied by one electron. We can now imagine two limiting situations for the localized electron: either a spin up or spin down electron, with a corresponding moment, on the localized site, in which case the impurity is magnetic; or half a spin-up electron and half a spin-down electron, producing no moment. It's not immediately obvious which of these two scenarios gives the lower energy. However, in the limit of strong on-site Coulomb repulsion U and weak hybridization t with the conduction band, Anderson's Hartree-Fock (HF) analysis shows that the magnetic case wins and we can speak of the impurity atom as a magnetic impurity [29, 32]. Anderson was able to determine the relative values of U and t required for a crossover between magnetic and nonmagnetic configurations, and hence to explain the empirical observation that some but not all transition elements with partially-filled d-shells remain magnetic when diluted in some but not all host metals [28]. In the following discussion, we will generally be concerned only with this regime in which the impurity is magnetic.

2.3 Coupling a localized moment to a reservoir

Once we know that the localized electron has a net moment, an even more interesting issue arises: how does this localized moment interact with the moments of electrons in the surrounding metal? A handwaving perturbation-theory argument based on the Anderson model shows that the coupling should be antiferromagnetic (i.e. electrons in the Fermi sea surrounding the impurity should prefer to have their spin aligned antiparallel to that of the localized electron) [33] [32, p. 302]. To wit, imagine that the localized electron has spin up. Then it can lower its energy by virtually hopping to an unoccupied spin up state (the partner to an excess spin down electron) at the Fermi surface, and back again. The energy lowering is of order t^2/U, and due to the Pauli exclusion principle this stabilization is not available if the extra electron at the Fermi surface is spin up (see Figure 2-2), so it is energetically favorable for conduction electrons to have spin down. This suggests the following effective Hamiltonian for the coupling between conduction and localized electrons:

$$H_{s-d} = -JS \cdot s, \tag{2.2}$$

where $J \simeq -t^2/U$ is called an antiferromagnetic exchange integral, S is the impurity spin, and s is the spin of a conduction electron. This is termed the $s-d$ model, and

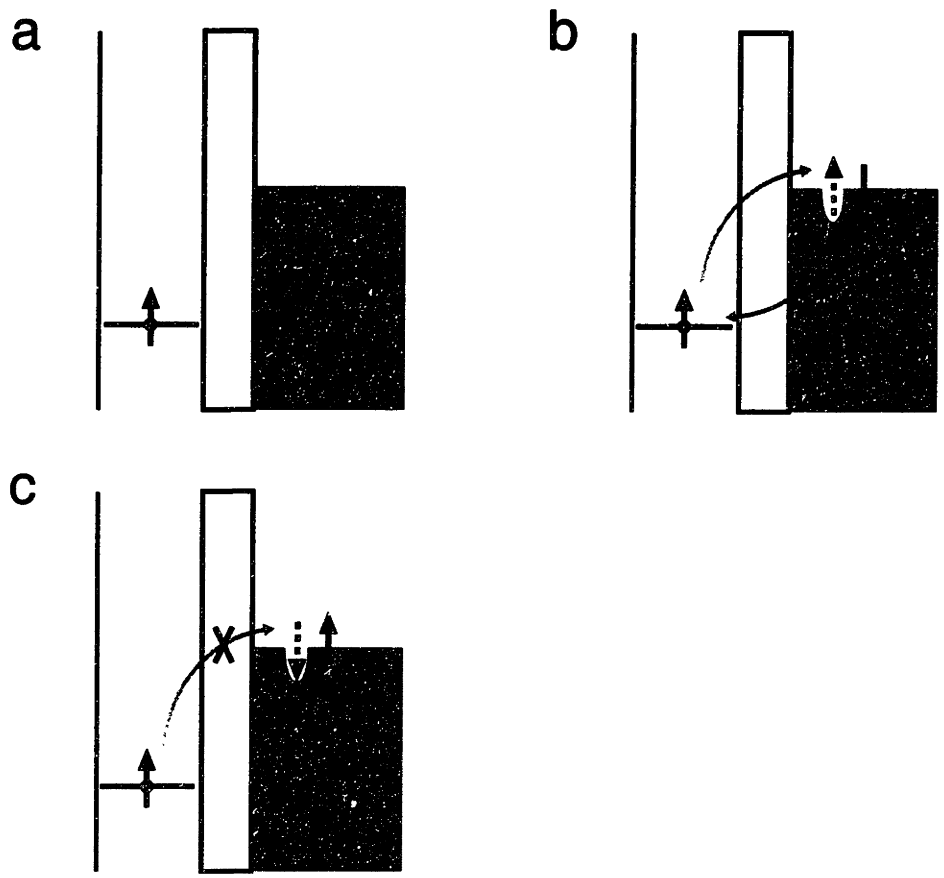

Figure 2-2: The reason for antiferromagnetic coupling. (a) A magnetic impurity in the Anderson model: a single-electron state is below the Fermi level, and hence is filled, while the state with a second electron added is raised far above the Fermi level by Coulomb repulsion, and is not shown. (b) The localized electron can make virtual transitions on and off the impurity state, lowering its kinetic energy. But by the Pauli exclusion principle this is only possible if an electron with the same spin is missing from the Fermi sea (i.e. there is an extra electron with opposite spin in the Fermi sea). (c) If the extra electron in the Fermi sea has spin parallel to that of the localized electron, the localized electron cannot make these virtual transitions, and hence cannot lower its energy. Together, these phenomena produce an antiferromagnetic coupling between localized and delocalized electrons (Eq. 2.2), allowing bond formation.

was the basis of Kondo's original treatment of scattering from magnetic impurities.[1] This model was later rigorously shown by Schrieffer and Wolff to be equivalent to the Anderson model in the limit of weak hybridization ($t \ll U, |\epsilon_0|$) [34], in which fluctuation of charge on and off the impurity site may be treated as a perturbation. Hence, although the Anderson model is a more general and physically intuitive description of an impurity coupled to a metallic reservoir, and I will return to it in analyzing my experiments, it is worthwhile to briefly explore the ramifications of the $s-d$ model.

As a consequence of the antiferromagnetic coupling made explicit in the $s-d$ model, conduction electrons in the surrounding metal try to screen the spin of the impurity, forming at zero temperature a spin-singlet or bond with the impurity electron(s) [35, 3]. As this bond forms, the impurity becomes a more efficient scatterer for conduction electrons, so the resistivity of the host metal increases. Though this bond has a characteristic energy kT_K, where T_K is termed the Kondo temperature, it begins to manifest itself at temperatures far above T_K as a logarithmic increase in resistivity with decreasing temperature. In fact, Kondo's original calculation was perturbational, reproducing this logarithmic behavior of resistivity at temperatures well above T_K. Extrapolation of this result to lower temperatures is clearly unphysical, since it would predict that the dilute collection of magnetic impurities cause a divergent resistivity at zero temperature. This failure of perturbation theory in describing the true low temperature behavior of the system became known as the Kondo problem [3].

The correct low-temperature properties, which I have summarized as resulting from bond formation, were understood using a variety of theoretical techniques in the 1970s and early '80s [36, 37, 38], and confirmed by many experiments [5]. Interestingly, though these calculations accurately described the temperature-dependence of such thermodynamic properties as specific heat and magnetization, the measurements of *resistivity* versus temperature that started the whole business proved harder to account for in detail. Only in 1994 did Costi and Hewson virtuosically adapt Ken Wilson's renormalization-group approach [36] to calculate resistivity over the entire

[1] The $s-d$ model, like the Anderson model, shows no essential change in behavior if more degenerate states or more electrons are added to the impurity, so long as the localized electrons have a net moment. However, it is simplest to consider the case of a singly-occupied localized state with only spin degeneracy. A larger set of localized d-electrons, as is found in most real Kondo impurities, simply combines to form a single effective spin $S > 1/2$. Interestingly, the multiple d-electrons are still screened by only a *single* conduction s-electron. This condition changes if there are several varieties of conduction electrons, each of which can couple to — and hence screen — the localized spin. This is the so-called multi-channel Kondo system, which displays physics quite different from that of the simple one-channel Kondo system we will be studying.

temperature range from zero to well above T_K [39], in the context of the Anderson model.

I will return to these calculations later, since they also beautifully describe results of my own measurements on a single artificial impurity. However, before discussing these results I must explain the physics of the artificial atoms which I will later exploit as artificial, tunable Kondo impurities.

Chapter 3

Quantum Confinement of Electrons or The Single-Electron Transistor

3.1 Electrons in Reduced Dimensions

When I took my first quantum mechanics class eight years ago, the first thing we calculated was the energy spectrum of a particle in a box. I naturally supposed that physicists routinely placed particles in boxes of various sizes, providing a firm experimental basis for what I was learning. In my naïveté, I would have been shocked to discover that the particle in a box held its privileged pedagogical position by virtue of the rare tractability of calculations on it, not thanks to any contact with experimental reality. Not that there was much doubt about how a particle in a box would behave: nearly a century of studying the spectra of atoms, Nature's electron boxes, had put quantum mechanics on firm ground. But it still would have offended my sensibilities to know that a thought experiment so central to my education was basically a lie. In fact, in the preceding years, experiments had finally begun to catch up. Instead of being based on disembodied electric fields as I had imagined, the new boxes were made from semiconductors patterned on submicroscopic scales.

First, the invention of molecular beam epitaxy (MBE) by Al Cho at Bell Labs opened the way to growing perfect crystals of semiconductors, layer by atomic layer, with the concomitant ability to switch abruptly back and forth between different semiconductor materials, forming an arbitrary and intricate sandwich structure. Since conduction electrons have a different minimum energy in each material, the sandwich produces an artificial one-dimensionally modulated potential for electrons. In particular, a thin layer of a low band-gap semiconductor sandwiched between two

thick layers with higher band-gap makes a box for electrons: a "quantum well". The next important development was modulation doping: Horst Stormer and Art Gossard added electron donors *outside* the quantum well. When the donated electrons flowed to the lower potential in the well, they could move quite freely in the plane of the well, nearly free from scattering, while remaining in one or a few quantized states normal to the plane. Here was a perfect one-dimensional box. That it held many electrons, not one, might have introduced two complexities, but neither entered in an important way: 1. The Pauli exclusion principle doesn't allow two electrons to occupy exactly the same quantum state, yet here were millions of electrons expected to sit in the same state of the quantum well. Since electrons in the well had complete freedom of motion within the plane, they all simply took on different in-plane momenta, filling up a two-dimensional Fermi sea, while all remaining in the ground state normal to the plane. 2. Electrons interact, and their mutual repulsion might be expected to change the energy of states, or even prevent multiple occupancy. In fact, the shape of the well, and hence the energy of states in it, *is* changed by the presence of many electrons. The effect on the well potential can be calculated classically by adding an appropriate density of charge to the well, solving Poisson's equation in the dimension normal to the plane to find the resulting modification of potential, then modifying the charge to suit the new potential and iterating until a self-consistent solution emerges. However, this classical mean-field accounting for charge is enough. We don't need to worry about correlations among individual pairs of electrons, since electrons in a Fermi sea screen each other so well.

Now we have electrons trapped in a box in one dimension, with quantized energy levels. But within the plane of the quantum well, electrons can still move freely, with a continuum of energies, so their total energy is *not* quantized. To achieve that, we would have to confine electrons to a small region in the plane of the quantum well, to a three-dimensional box: an artificial atom. Like a real atom, this box would hold a small, integer number of electrons, and its states would be quantized so that exciting the electrons, even without changing their number, would require a finite energy. Such artificial atoms were first made in the late '80s and early '90s [40, 41, 42, 43, 44, 13]. They have several interesting advantages over "real" atoms for experiments: for example, their size and shape can be chosen, and even tuned *in-situ*; and electrons can be added or removed one at a time.

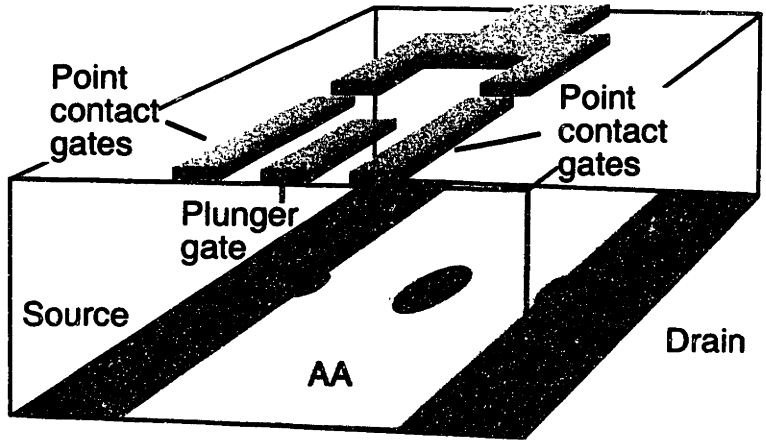

Figure 3-1: An AA can be made from a 2DEG by two common methods. In the first, shown here, the entire heterostructure is left intact, but gate electrodes are placed on the surface in the shape of a box. When these gate electrodes are biased negatively, they deplete electrons beneath them, leaving a small puddle of electrons "inside" the box. This is the basic method I used. The second method is illustrated in Figure 3-2.

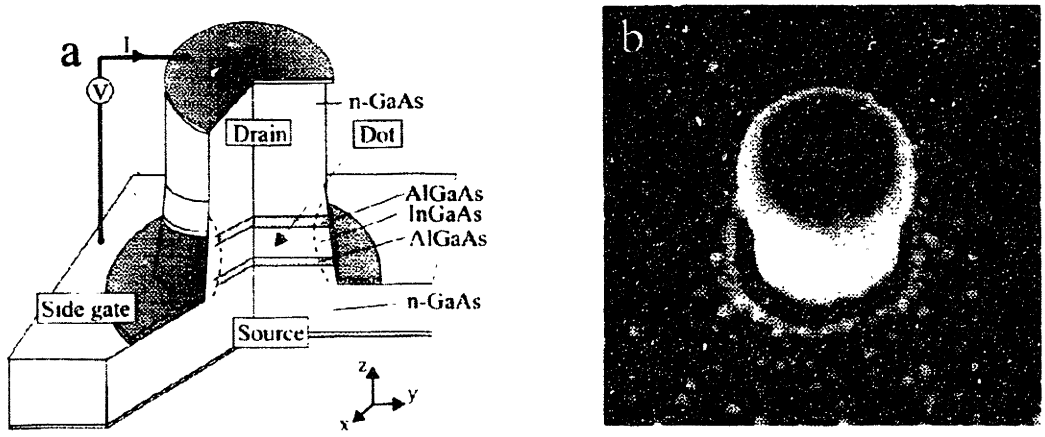

Figure 3-2: (a) A second common method for making an AA from a 2DEG involves etching a slender pillar in the heterostructure, leaving only a small region of 2DEG. Electrical contact is then made to the AA from top and bottom. (b) shows an electron micrograph of the finished structure. This figure was taken from Reference [22]. As discussed in Appendix A, I began with the electrode-based method illustrated in Figure 3-1, but eventually combined it with etching to create my AAs.

3.2 The Single-Electron Transistor

One fruitful way of studying these artificial atoms involves connecting them to two leads or reservoirs (allowing electrons to tunnel between each lead and the atom). Now applying a small voltage between the two leads and measuring the current that flows, one electron at a time, through the atom, can give detailed spectroscopic information about the electronic states of the atom. Of course, it is also possible to do spectroscopy of these systems using light (here, microwaves or far-infrared are the frequencies appropriate to the artificial atom's (AA's) energy scales). However, I do transport measurements, so that's what I'll focus on. Much of the popular interest in these structures is based on the fact that once leads are connected, the system acts as a sort of transistor, termed a single-electron transistor or SET, since it turns on and off every time a single electron is added to the AA.

Transistors, the building blocks of modern computers, are simple electrical switches (see Figure 3-3): a current flowing through a wire is controlled by the voltage on a nearby gate electrode. Following traditional FET terminology, I sometimes refer to the two leads of my SETs as drain and source, and to the voltage applied between them as V_{ds}. But I often simply retain the intuitive terminology V_{LR} for the voltage between left and right leads. If the gate voltage is very negative, electrons are depleted from the central region or channel of the transistor, and no current can flow. When the voltage is made less negative, electrons accumulate, and the current through the transistor turns on. A single-electron transistor follows the same basic principle: a nearby gate can accumulate or deplete electrons from the channel (now the AA), changing the conductance through the AA. As noted above, the conductance turns on and off each time a *single* electron is added to the AA. Let's see how this works. The AA, like a real atom, holds at any given time a fixed, integer number of electrons, generally determined by its equilibrium ground state. This means that it takes a finite energy either to either remove an electron from or add an electron to the AA. If the energy to change the charge state of the AA is unavailable, no current flows (see Figure 3-4(a)). This energy could be made available by raising the temperature sufficiently high (see Figure 3-4(b)): for a real atom, temperatures of thousands of degrees are required for ionization, while AAs generally require only 1 to 100 K. Alternately, we could provide this energy by raising the electrochemical potential in one lead relative to that in the other by applying a large bias across the AA (see Figure 3-4(c)). However, if we want to study the ground state of the AA we should restrict ourselves to equilibrium measurements, in which only a small bias is applied

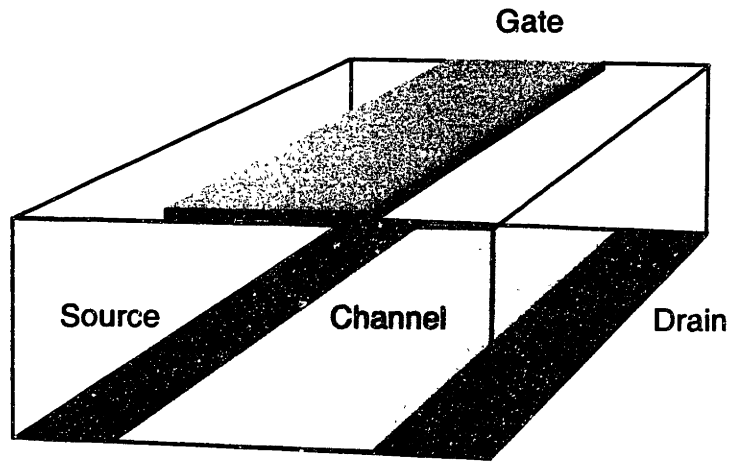

Figure 3-3: A conventional transistor Metal-Oxide-Semiconductor Field Effect Transistor (MOSFET) is a voltage-controlled current switch, used by the millions in a modern computer. A similar device termed a Metal-Semiconductor Field Effect Transistor (MESFET), shown here, can be made using a GaAs-based semiconductor heterostructure. Except for differences in gate patterning, the technology for making a MESFET is identical to that used for making an SET. When the gate bias on a MESFET is sufficiently negative, as is depicted here, electrons are depleted from the channel beneath the gate and no current can flow. If electrons are present in the channel, current can flow from source to drain.

across the AA in order to define a direction of current flow. Even in this situation it is possible to get current to flow. Recall that we can use a nearby gate electrode to change the confining potential of the electron droplet in the AA. Making this gate's voltage less negative pulls all the electronic states of the AA down in energy relative to the Fermi level in the leads, eventually aligning the energy for adding the next (N+1st) electron exactly with the Fermi level (see Figure 3-4(d)). Now, the N+1st electron can come on from one lead and off onto the other, a new N+1st electron comes on and off, and this repeats perhaps a million times a second. A small but measurable current flows, one electron at a time. Finally, we can make the gate's voltage less negative still. Now the N+1st electron comes onto the AA and stays on: the energy for adding it is below the Fermi level, so it is energetically unfavorable for it to return to the leads. Thus, no current flows under most conditions. Current only flows at charge degeneracy points, each time the number of electrons on the AA is being increased by one.

As the name suggests, single-electron transistors have been proposed as devices for computation or memory. They have the advantages of being compact, and of having a mechanism that takes advantage of the quantized nature of electron charge rather than breaking down when there are only a few electrons in the channel. Some have

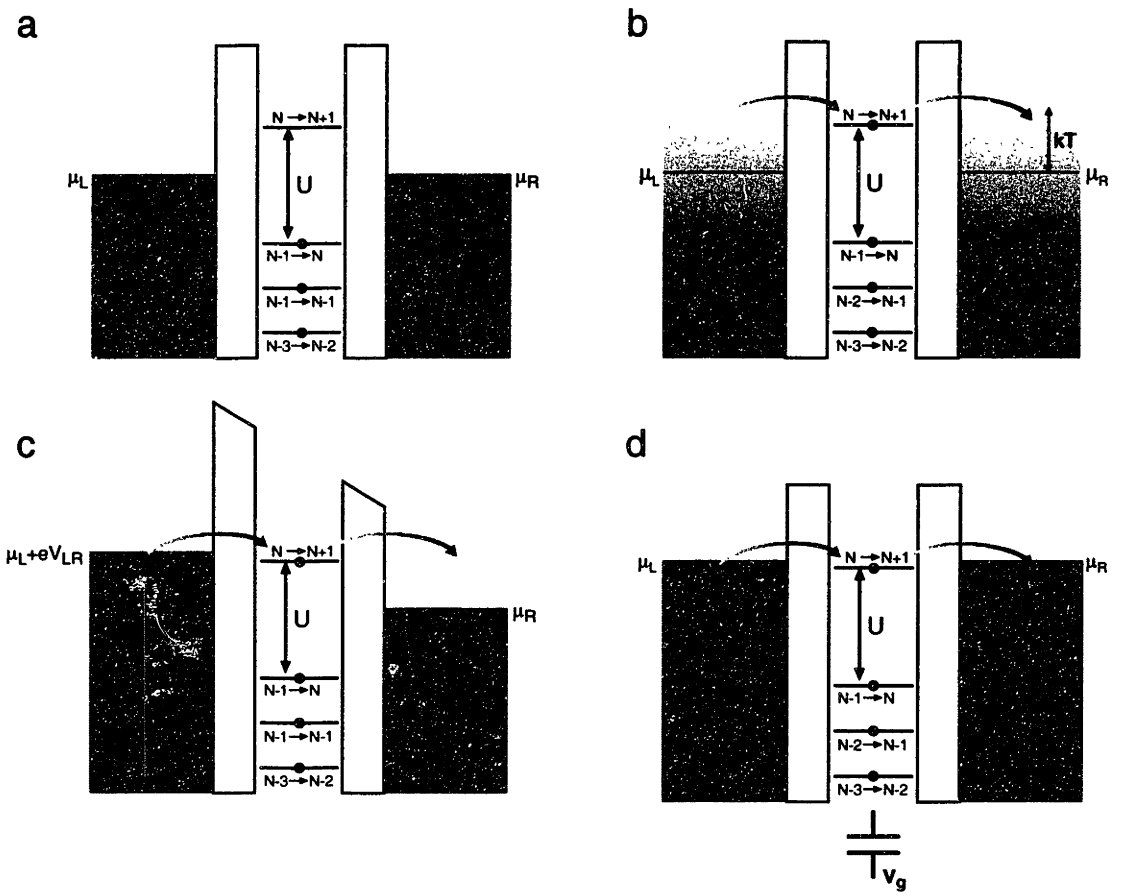

Figure 3-4: Conditions for current flow through a SET. Throughout, the chemical potentials in the left and right leads (μ_L and μ_R, respectively) are assumed equal, but a voltage bias $V_{\rm LR}$ can be applied across the AA to separate the two Fermi levels. (a) At low temperature and low voltage bias $V_{\rm LR}$ across the AA, it is energetically impossible to add an electron to the AA, and no current flows. (b) At high temperature, even with low applied bias an electron can be thermally excited from the Fermi sea to the AA, and can then exit on the other side, so current flows. (c) At low temperature but high bias, the bias provides enough energy to inject an extra electron into the AA. It can exit to the other lead above its Fermi level, so current flows. (d) At low temperature and low bias, the voltage $V_{\rm g}$ on a nearby gate can be made less negative, pulling all the energies for electron addition down. When it becomes equally favorable for the AA to be occupied by N or $N+1$ electrons, the $N+1$st electron can enter and then exit to the other lead, so current flows. If $V_{\rm g}$ is adjusted further, the $N+1$st electron will enter the AA and remain inside, so again no current flows.

even been made to run at room temperature, meeting the most obvious objection to their use in applications [45, 46]. Other problems will keep workers busy for years though: it's difficult to make them run fast (as we shall see below), and switching on and off each time an electron is added to the central region means that the SET is exquisitely sensitive to the configuration of charged impurities around it — one impurity can totally change the threshold for conduction, causing the transistor to be on when it's supposed to be off and vice versa. Some progress is being made on isolating SETs from such problematic environments, using special substrates or even suspension in vacuum. For a more detailed discussion of some of the issues involved in computing with SETs, see References [47, 48].

Getting back to physics, we can use the SET behavior to accurately measure the energy required to add each successive electron to the AA, since that energy is proportional to the gate voltage which produces the corresponding conductance peak. To allow good spectroscopy of the AA, the leads should be connected as weak probes — the tunneling rate should correspond to an energy smaller than kT, to avoid Lorentzian broadening of all spectroscopic lines due to the finite lifetime of electrons in the AA. Since temperature can be made so low (50-100 mK, typically 1 percent of the charging/ionization energy or less), these line positions can be determined quite precisely, enabling a wide range of spectroscopic studies, which have revealed such beautiful behavior as atom-like shell structures [12] and high-B phase transitions in AAs [10, 13]. It is also interesting from several perspectives to study what happens when the AA is *strongly* coupled to its nearby reservoirs. Then we can no longer think of the AA as an isolated object, but must consider the reservoirs as part of the system. The artificial atom becomes an artificial impurity coupled to an artificial metal, and we can hope to study in this new, tunable system the rich physics of impurities in metals, most notably the Kondo effect. It is worth noting that Kondo behavior will always emerge when the rate of tunneling from AA to leads is maximized, as is desirable for fast operation of an SET. Thus, though my studies have focused on behavior at dilution-refrigerator temperatures, they may be equally important in designing any practical SET for use in room-temperature computers.

3.3 Refining the analogy and motivation of an SET as a model, tunable Anderson/Kondo impurity

As I've just mentioned, an SET may be thought of as an artificial impurity coupled to artificial metal, and hence Kondo physics might be expected to emerge when the coupling is strong so that $T_K \gtrsim T$. Now I'd like to explain under what conditions an SET is a good model for a Kondo system, and revisit the reasons for studying an SET in this light, focusing on its tunability. The Kondo effect occurs when an impurity atom with an unpaired electron is placed in a metal, and the energy of the unpaired electron is far below the Fermi energy. At low temperatures a spin singlet state is formed between the unpaired localized electron and delocalized electrons at the Fermi energy. The consequences of this singlet formation were first observed over sixty years ago in metals with magnetic impurities, but full theoretical understanding was slow to come. Today, the situation has reversed: scaling theories and recent renormalization group calculations [39] can predict quantitatively the bonding strength of the singlet state, and the singlet's effect on the conduction electrons at all temperatures. The detailed dependence of these properties on parameters such as the energy of the localized electron cannot be tested experimentally in the classic Kondo systems, since the relevant parameters cannot easily be tuned for impurities in a metal. Recently I have been able to test these predictions with a new experimental approach: creating an artificial Kondo system by nanofabricatcn [18]. The confined droplet of electrons interacting with the leads of a single electron transistor (SET) is closely analogous to an impurity atom interacting with the delocalized electrons in a metal, as described by the Anderson model [49]. When the number of electrons in the droplet is odd, and hence one electron is unpaired, the SET exhibits the Kondo effect [18] in electronic transport. In an SET, this condition of odd occupancy is only one of many properties which may be selected by changing the voltages on various gate electrodes or leads: the number of electrons on the artificial atom can be changed from odd to even; the difference in energy between the localized state and the Fermi energy can be tuned; the coupling to the leads can be adjusted; and voltage differences can be applied between the leads revealing non-equilibrium Kondo phenomena [50]. An added advantage relative to bulk Kondo systems is that a single localized state can be studied rather than a statistical distribution of many impurity states. However, for SETs fabricated previously, the binding energy of the spin singlet has been too small

to observe Kondo phenomena. Ralph and Buhrman [51] observed the Kondo singlet at a single accidental impurity in a metal point contact, but with no gate electrodes and without control over the structure, they were not able to observe all the features and dependences predicted. In a very interesting recent experiment, Madhavan *et al.* [52] observed a Kondo-related zero-bias resonance in tunneling from an STM tip through a single Co atom to a Au surface.

In Chapter 4, I will review measurements on a new generation of SETs that display all the aspects of the Kondo effect: the spin singlet forms and causes an enhancement of the zero-bias conductance when the number of electrons on the artificial atom is odd but not when it is even. The singlet is altered by applying a voltage or magnetic field or by increasing the temperature, all in ways that agree with predictions [53, 50, 39, 54, 18, 55].

I have fabricated SETs using multiple metallic gates (electrodes) deposited on a GaAs/AlGaAs heterostructure containing a 2-dimensional electron gas (see Figure 1a). First, the electrons are trapped in a plane by differences in the electronic properties of the heterostructure's layers. Second, they are excluded from regions of the plane beneath the gates when negative voltages are applied to those gates. This creates a droplet of about 50 electrons separated from the leads by tunnel junctions formed by the narrow constrictions between electrodes. This basic technique has been used previously [56, 57, 40, 58, 9]. To make my SETs smaller than earlier ones, I collaborated with researchers at the Weizmann Institute to fabricate shallower 2DEG heterostructures [59] as well as finer metallic gate patterns by electron-beam lithography. In trying to make small patterns in the 2DEG, the importance of small gate structures is clear. It is equally important to avoid having the electron gas far beneath the gate electrodes, since then the gate-induced potential felt by the electrons would be smeared out, losing features smaller than the depth of the 2DEG (see Appendix B for more details.) The central droplet of an SET has a diameter defined by the distance between confining gates on the surface, decreased on each side by a "depletion width" [60] comparable to the depth of the 2DEG. This is another manifestation of the potential smearing due to the finite separation between gates and 2DEG. The smaller diameter of the central droplet in my SETs (100 nm compared to 200–500 nm in most previous work) is critical to the observation of the Kondo effect, as described below. Dimensions are given in Figure 3-6(a). For details of device fabrication see Appendix A and References [18, 59].

Several important energy scales and their relative sizes determine the behavior of an SET (see Figure 3-6(a)). At low temperature, the number of electrons N on

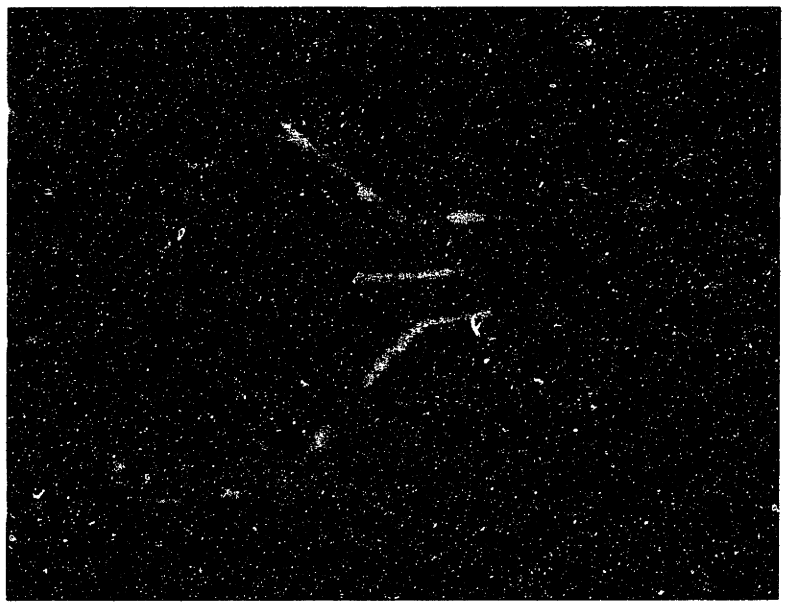

Figure 3-5: Electron micrograph of the electrodes that define the SET. Three gate electrodes (gray), the one on the right and the upper and lower ones on the left, control the tunnel barriers between reservoirs of the 2-dimensional electron gas (2DEG) and the droplet of electrons. The middle left electrode is used to change the energy of the droplet relative to the Fermi level in the 2DEG. The space enclosed by the four electrodes is approximately 150 nm square; extra lateral depletion leads to an electron droplet about 100 nm in diameter.

the droplet is a fixed integer. This number may be changed by raising the voltage of a nearby gate, thereby lowering the energy of electrons on the droplet relative to the Fermi level in the leads. The change in energy necessary to add an electron is called U, and in a simple model is the charging energy $e^2/2C_\Sigma$, where C_Σ is the total capacitance of the droplet to the outside world. Since U is determined by the Coulomb repulsion between pairs of electrons in the droplet, it scales approximately inversely with the droplet's radius.

For small droplets, the quantized energy difference between different spatial electronic states becomes important. We call the typical energy spacing between spatial states $\Delta\varepsilon$. It should scale with the curvature of the confining potential, or inversely with the square of the droplet's radius. So $\Delta\varepsilon$ increases even faster than U with decreasing droplet size. Another important energy Γ is the coupling of electronic states on the artificial atom to those on the leads, resulting from tunneling.

I will now consider the same energies in the context of the Anderson model (Eq. 2.2) of an impurity in a metal. In the Anderson model, the SET is approx-

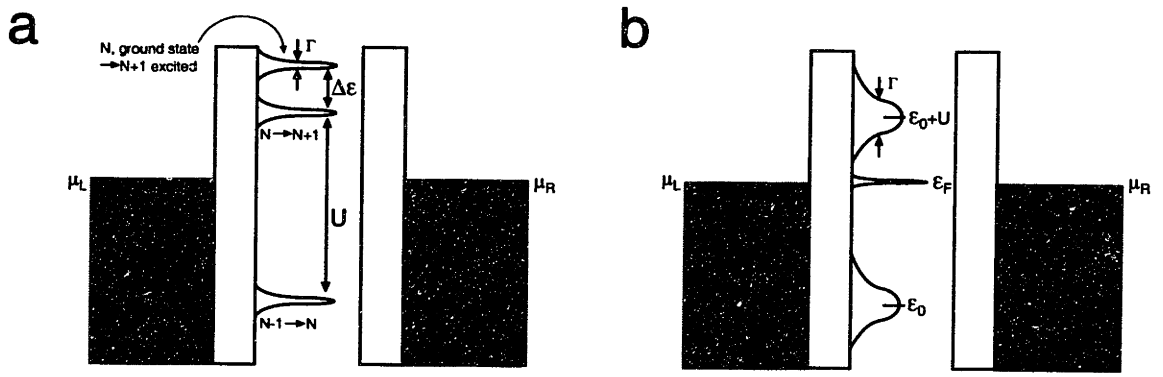

Figure 3-6: (a) Schematic energy diagram of the SET, showing an electron droplet separated by tunnel barriers from conducting leads. Adding an extra electron to the ground state requires a charging energy U. Adding it to an excited state takes an extra quantized level energy $\Delta\varepsilon$. Electrons can tunnel between droplet and leads with rate $\Gamma/\hbar$. The resulting finite lifetime of electrons in localized levels broadens the density of states corresponding to each such level into a Lorentzian with FWHM Γ. (b) A similar diagram, treating the central electron droplet in the context of the Anderson model. Higher levels are now neglected, and lifetime broadening Γ is enhanced to emphasize strong coupling between droplet and leads. Since the number of electrons in the droplet is odd, the (inset) local density of states exhibits a sharp Kondo resonance at the Fermi level. The broad resonance with width Γ at energy ϵ_0 represents a transition from $n_d = 0$ to $n_d = 1$, while the one at $\epsilon_0 + U$ corresponds to a transition from $n_d = 1$ to $n_d = 2$.

imated as a single localized state, coupled by tunneling to two electron reservoirs. The state can be occupied by $n_d = 0, 1$, or 2 electrons with opposite spin; couplings to all other filled and empty states of the droplet are neglected.[1] Adding the first electron takes an energy ϵ_0 referenced to the Fermi level in the leads, but the second electron requires $\epsilon_0 + U$, where the extra charging energy U (1.9 ± 0.05 meV in our SET) results from Coulomb repulsion. In the diagram of Fig. 3-6(b), $\epsilon_0 < 0$, but $\epsilon_0 + U > 0$, so there is one electron in the orbital. However, this electron can tunnel into the leads, with rate Γ/h, leading to Lorentzian broadening of the localized-state energies with full width at half maximum (FWHM) $\Gamma = t^2\rho(E_F)$, where ρ is the density of states in the leads. The energy ϵ_0 can be raised by increasing the negative voltage V_g on a nearby electrode (the middle left "plunger gate" electrode in Fig. 3-5)[2]

[1]This assumption is basically equivalent to assuming $\Delta\varepsilon \gg kT, \Gamma$. These inequalities are not held so strongly in my SETs for the data presented in Chapters 4, 5, and 6; in particular $\Delta\varepsilon \gtrsim \Gamma$. I will examine the expected and observed consequences of this in Chapter 6, but they do not drastically modify the picture obtained from the simple single-state Anderson model described here.

[2]Changes in gate voltage can be converted to energetic changes in states on the AA by the relation

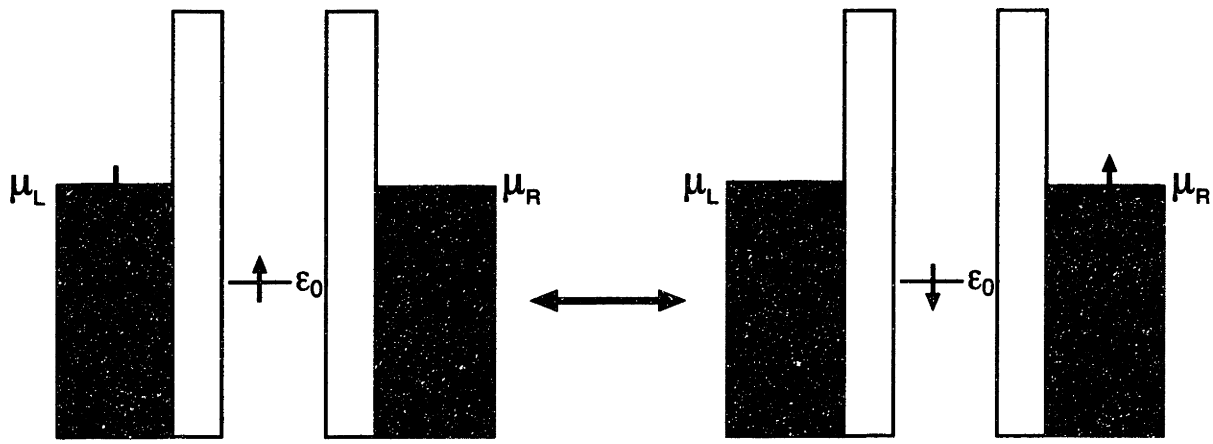

Figure 3-7: The Kondo bond which carries extra conductance through the SET is a spin-singlet composed of an electron on the AA and another electron spread between both leads. This figure illustrates two components of this spin singlet, both part of the ground state of the system. Since they are both part of the ground state, I envision electrons to be capable of "sloshing" back and forth between these two configurations, carrying a charge across the SET without changing the AA occupancy, which is well-quantized! Note that the process depicted is always possible, but suppressed approximately as $(\Gamma/\epsilon_0)^2$ by the two requisite virtual transitions. This is simply an expression of the Lorentzian shape of lifetime-broadened peaks. When both initial and final states are part of the ground state, the amplitude for the "sloshing" process can be much higher. The Kondo bond, and hence the sharp density-of-states feature seen in Figure 3-6(b), is formed with electrons at the Fermi level, since higher-energy states in the leads are empty, and lower-energy states are all full, leaving no freedom for electrons to choose their spin.

and Γ can be tuned by adjusting the voltages on the gates that form the constrictions. Two other important energies (not shown) are the spacing between quantized single-particle levels $\Delta\varepsilon \approx$400–500 μeV, and the thermal broadening of the Fermi level in the leads kT, which for our measurements is between 8 and 350 μeV. The Kondo temperature T_K is a new, many-body energy scale that emerges for a singly-occupied Anderson impurity [3]. It is essentially the binding energy of the spin singlet formed between the localized, unpaired electron and electrons in the surrounding reservoirs; we have measured values of kT_K between 4 and 250 μeV in SETs, depending on the other tunable parameters.[3]

Now we come to the motivation for making the AA of the SET small. To observe the Kondo effect clearly, it is important to be able to access the regime $kT \lesssim kT_K$, ideally $kT \ll kT_K$. Since the value of T_K depends on the other parameters of the system, we need to understand these dependences to design structures which allow T_K to be large as desired. For now, we are guided by two important relations: First, kT_K will always be smaller than Γ [50], so we need to make Γ large. Second, if Γ is made greater than $\Delta\varepsilon$, the electrons spread from the artificial atom into the leads, and quantization of charge and energy is lost, even at $T = 0$ [19, 61].[4] So as a first step toward making the Kondo effect strong without delocalizing the electrons of the AA we need to make $\Delta\varepsilon$ large. I have achieved this by making smaller SETs, thereby permitting large Γ and thus T_K comparable to or even greater than accessible temperatures. In semiconductor SETs, Γ can be tuned *in situ* by changing the voltage on the gates which define the barriers between artificial atom and leads. I find that with these new SETs I can vary Γ slowly as it approaches $\Delta\varepsilon$, and thus optimize T_K.

It is interesting to note that these considerations might be germane to technologically-useful devices. For an SET to operate at room temperature, the charging energy U would have to be increased by making the central AA smaller (one can't run an SET much above $kT = 0.1U$). This would cause an even larger increase in $\Delta\varepsilon$, which goes inversely as the AA area rather than its radius, so $\Delta\varepsilon$ would be comparable to U rather than five times smaller as in my devices. Then, since switching speed is limited by RC times, with R being the resistance through the transistor in its on

---

$\Delta\epsilon_0 = \alpha e V_g$, where $\alpha \equiv C_g/C_\Sigma$ is the separately measurable ratio between the capacitance of the AA to the gate being swept and that of the AA to the outside world. See Reference [19] for a more detailed discussion.

[3] All the values given in the last paragraph are typical for my SETs in general, but were determined quantitatively for the specific SET featured in Chapter 6.

[4] At this crossover, the conductance through the transistor is of order e^2/h — a full quantized channel; in general, once the electrons are delocalized, $G \propto (\Gamma/\Delta\varepsilon)(e^2/h)$.

state, we would want to tune Γ to be comparable to $\Delta\varepsilon$ to maximize the conductance (minimizing R). Finally, we end up with $\Gamma \geq 10kT$, and the Kondo effect will play a major role in device behavior. So it's important to understand this "low temperature" physics for operation of any practical semiconductor SETs designed for room temperature operation! In fact, it turns out that the Kondo effect doubles the possible conductance of the device to $2e^2/h$, also doubling its maximum speed. Finally, the Kondo effect creates interesting I-V characteristics. It should be possible without careful tuning of gate voltage to make a device whose conductance drops dramatically, perhaps by a factor of two or more, if more than 25 or 50 mV are applied across it.[5]

However, since my present interest is to exploit an SET as a model Kondo impurity, I should clarify the analogy between the artificial and "natural" systems. The conductance G of an SET is analogous to the resistivity ρ of a bulk Kondo system. Hence, when the Kondo singlet forms in an SET it causes an increase in *conductance* rather than *resistance* as we might have expected from bulk systems. This interchange is simply understood as resulting from the different geometry of the two systems. In the bulk, the impurities can be seen as creating an obstacle course through which the conduction electrons must pass for current to flow. Scattering from these impurities impedes this flow, giving rise to resistivity, and the increased coupling between conduction electrons and localized impurity electrons in the singlet state simply enhances this effect, *ergo* Kondo = higher resistivity. In contrast, in an SET electrons must go *through* the "impurity" to carry current from one reservoir to the other. Increasing the coupling between conduction electrons and localized electrons simply enhances the flow of current, so the Kondo effect gives rise to higher conductance. Although the reasons are not obvious, the analogy between resistivity in the bulk geometry and conductance in an SET works even better than I've justified — the calculated (and measured) temperature dependence of the two quantities is almost indistinguishable [62].

Some of the calculations to which I'll be comparing data in the coming chapters are remarkably new, given the long history of the Kondo effect. Although one thinks of the increase in resistivity at low T as the hallmark of the Kondo effect, transport properties such as resistivity have proven more difficult to calculate than thermodynamic properties except in special cases. For $T \ll T_K$, ρ is theoretically and experimentally known to equal $\rho_0 - cT^2$ (termed Fermi liquid behavior) [7] and for $T_K < T < 10\,T_K$, ρ is roughly logarithmic in T [8, 63], but the crossover regime has

[5]Note that differential conductance would decrease with increasing bias, but would never become negative.

only recently been successfully treated [39].

Chapter 4

Experiments on State Filling and The Kondo Effect

4.1 A Simple Phenomenological Model for State Filling

What phenomenology should we expect for the Kondo effect in an SET? First, at low temperature, the formation of a Kondo singlet should produce extra conductance. The Kondo singlet can form only when the electrons in the droplet have a net spin, so let's investigate when this should occur. In a simple model, each electron occupies a single-particle quantized state in the droplet, and two electrons with opposite spin can fit in each spatial state. This is a sort of simple shell structure. Unlike in a Hydrogen atom, the confining potential of my SET is sufficiently disordered to have no special degeneracies, but time-reversal invariance still produces a Kramers degeneracy between states of opposite spin. Since different spatial states have different energies, naïvely one should expect two successive electrons to doubly occupy a spatial state before the next electron would enter the next, higher-energy state, as illustrated in Figure 4-1. Since the two electrons in a given spatial state have opposite spin, a doubly-occupied state has no net spin and is unable to support a Kondo singlet. Hence, in this naïve model, a Kondo singlet can only form when the number of electrons is odd, so that one spatial state is only singly occupied. For an even number of electrons in the droplet the conductance will remain low. Recall that varying V_g on an SET typically results in adding an electron to the droplet each time the voltage is increased by an increment proportional to U. Since in most SETs $\Gamma < k_B T \ll U$, current can generally flow through the SET only when the occupancy of the island

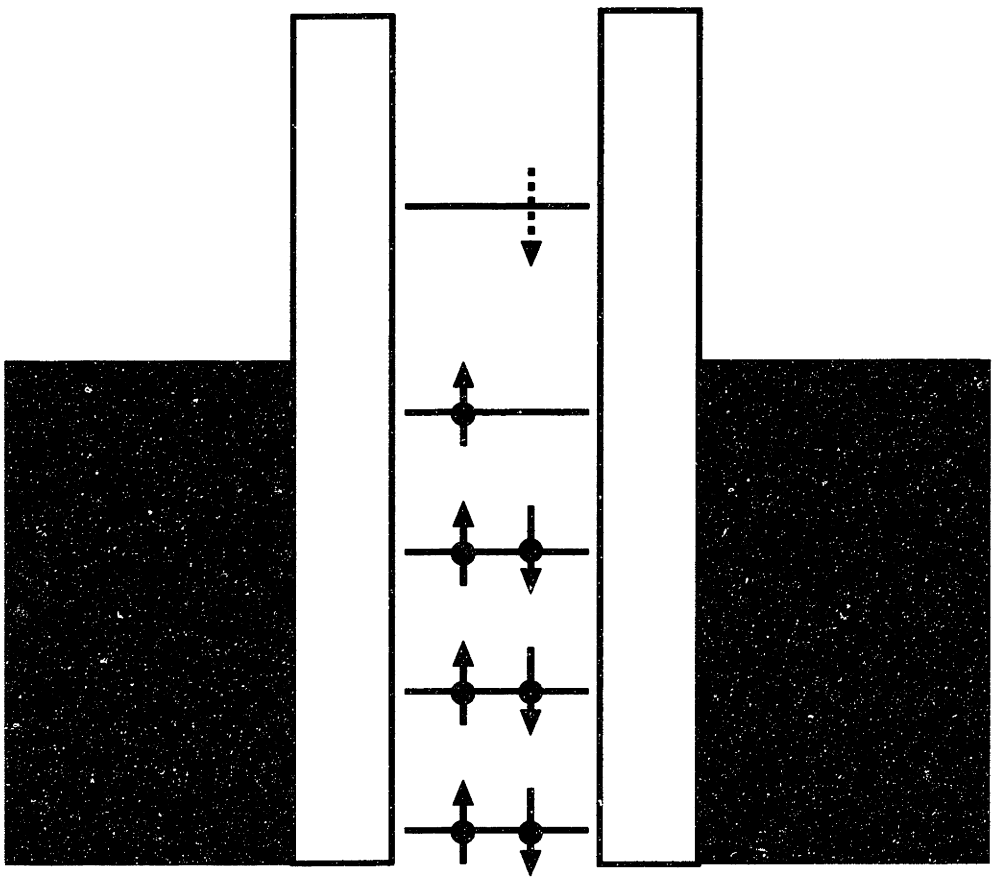

Figure 4-1: In a simple model of our AA, electrons occupy single-electron spatial states in a potential well. In absence of interactions, two electrons with opposite spin will fill each spatial state. If the number of electrons is odd, the electrons will still fill spatial states in pairs, but the leftover electron will half-fill its own spatial state.

is free to fluctuate between N and $N+1$, hence conductance versus V_g normally shows a series of sharp, periodically-spaced peaks [40, 58, 9]. Figure 4-2(b) shows this behavior in one of my SETs when Γ is tuned to be relatively small. The position of each peak measures the energy required to add the corresponding electron. Raising T broadens the peaks by broadening the Fermi distribution: as illustrated in Figure 3-4(b), conductance can occur even in the valley so long as temperature is sufficiently high to ionize the AA.

When Γ is tuned to be large, as in Figs. 4-2(a), these peaks form pairs, with deep inter-pair valleys and shallow intra-pair valleys. I have observed several consecutive pairs of peaks with this property (see Figure 4-4), demonstrating clearly that the extra conductance depends on the parity of the number of electrons as expected.[1] At this stage in the discussion, it's not experimentally clear whether the extra conductance is occurring for even or for odd numbers of electrons; we only know that it appears in alternate valleys. In structures made by others, in which tunneling occurs vertically, across a thin barrier of fixed height [13, 12] (see Figure 3-2), the electron droplet can be depleted all the way to zero electrons. Then, watching each electron enter, starting with the first, tells researchers exactly how many electrons are present. SETs with lateral transport such as mine (see Figure 3-1) generally cannot be depleted all the way to zero electrons: as the electron droplet shrinks, the barriers to tunneling become effectively wider and higher, and eventually no measurable current can pass through them. So I know the number of electrons only approximately. In the following section, I shall present evidence in support of the naïve model introduced above, in the process arriving at a Kondo-independent way of determining when the electron occupancy is odd and when even.

In our simple model, we assumed that electrons would successively fill the lowest-lying single-particle states of the droplet. This amounted to temporarily ignoring Coulomb interactions, which are certainly important in our small droplets. Without interactions the two electrons occupying a given spatial state would enter at the same gate voltage, the droplet would never have odd occupancy, and the Kondo effect could never be observed. Now we need to reintroduce the Coulomb interactions, but in a simplified way: adding each successive electron requires more energy than the last, and the increment is assumed to be a constant U. On top of this, we have the energy

[1] This strict alternation of valley conductance with occupancy is not always observed: sometimes a single "Kondo pair" will appear, surrounded by unpaired peaks. It's not yet understood what breaks the simple picture of state filling in these cases, nor what is the physics of the valleys surrounding the Kondo pair (see Chapter 7 for more discussion of this issue).

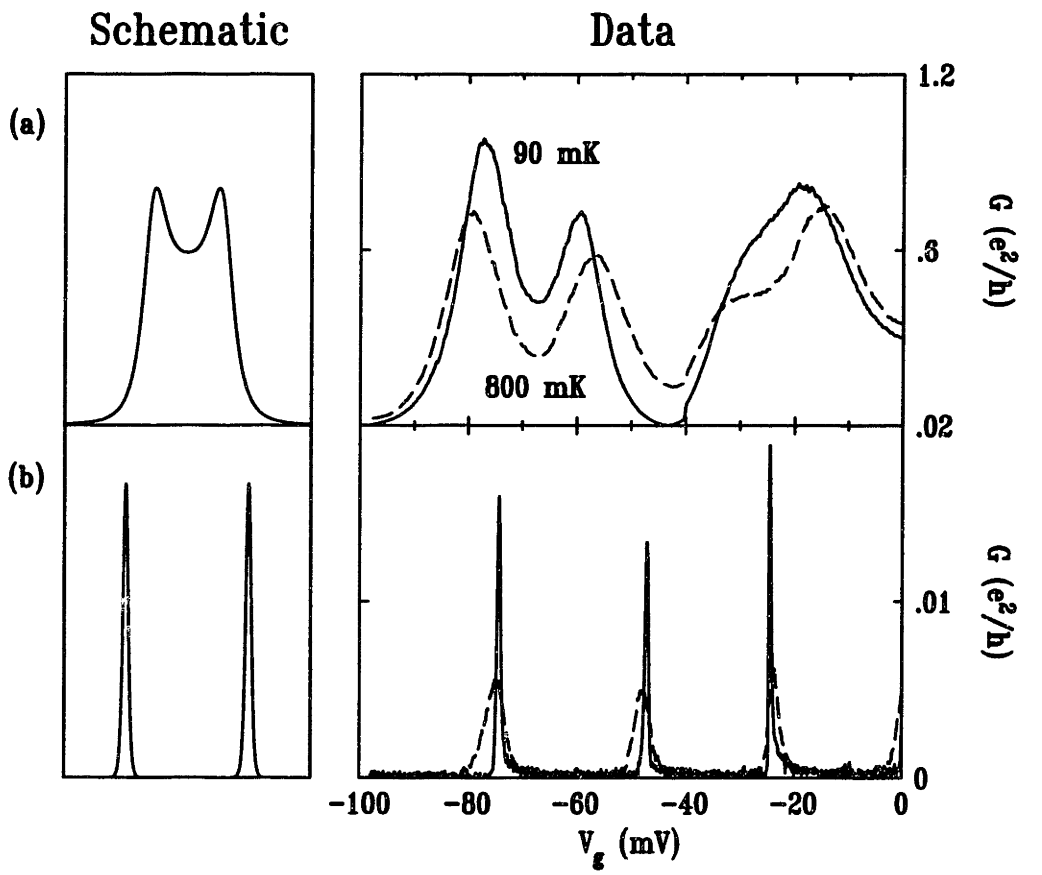

Figure 4-2: Temperature dependence of zero-bias conductance through two different spatial states on the droplet. The qualitatively-expected behavior is shown on the left, and actual measurements on the right. (a) Paired peaks corresponding to the two spin states for each spatial state move apart with *increasing* temperature, while the intrapair valleys become deeper. The paired peaks near $V_g = -70mV$ are resolved at 90 mK but become increasingly well-resolved with increasing temperature, up to about 1 K. In contrast, the peaks near $V_g = -25$ mV are completely unresolved at 90 mK, and can only be identified as separate features (a peak and a shoulder) when increased temperature suppresses the Kondo-related conductance between the peaks. The difference in behavior is due to the larger Γ (and hence larger T_K) for the peak pair near $V_g = -25$ mV. (b) When Γ is reduced (as illustrated by shorter and narrower peaks), U increases relative to $\Delta\epsilon$, so peak pairing is no longer evident. Since the Kondo phenomenon is suppressed, peaks become narrower as temperature is decreased at all T. Note: The peaks in (b) have been shifted by +120 mV in V_g and do not correspond to the addition of the same electrons as those in (a).

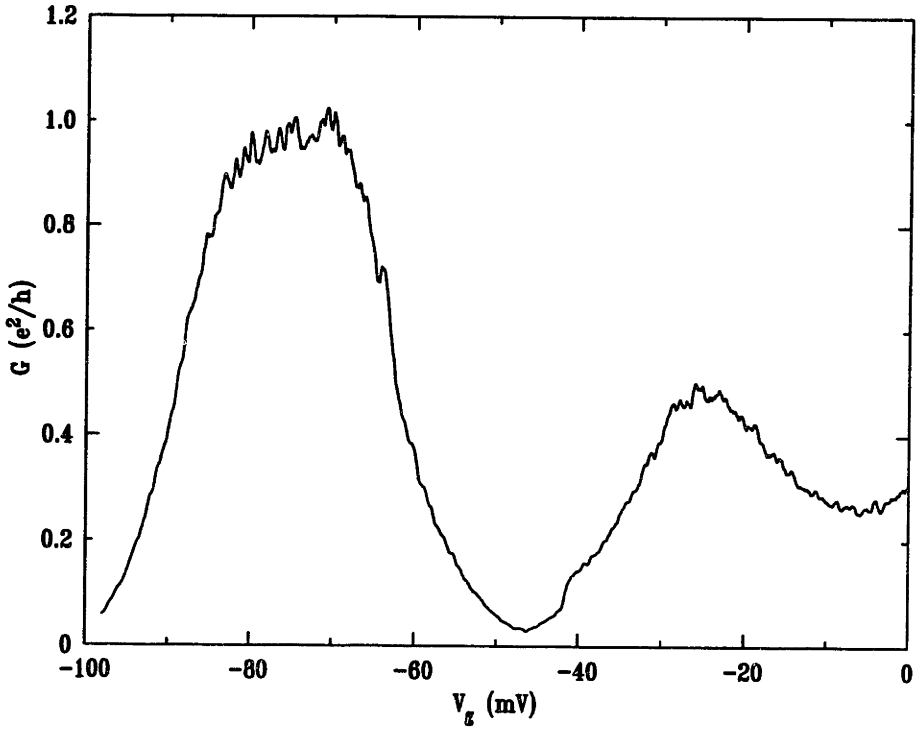

Figure 4-3: When $\Gamma \gg kT, T_K$ can also be greater than temperature in the entire valley between two Coulomb blockade peaks (see Chapter 6 for details on how T_K depends on Γ and on distance from a peak). This means that the Kondo bond is fully formed, and hence conductance is maximized, in this whole "valley". The two peaks grow together completely, with a flat top, so no valley is visible. This behavior was predicted a decade ago [64, 65], and may be seen in this figure as the broad feature centered around $V_g = -75$ mV. The height of the top conductance plateau should theoretically be $2e^2/h$ if the two barriers separating AA from leads are symmetric. The reduction below this value is probably due to an accidental asymmetry, since under other conditions I have observed peak pairs up to $1.7e^2/h$ in height.

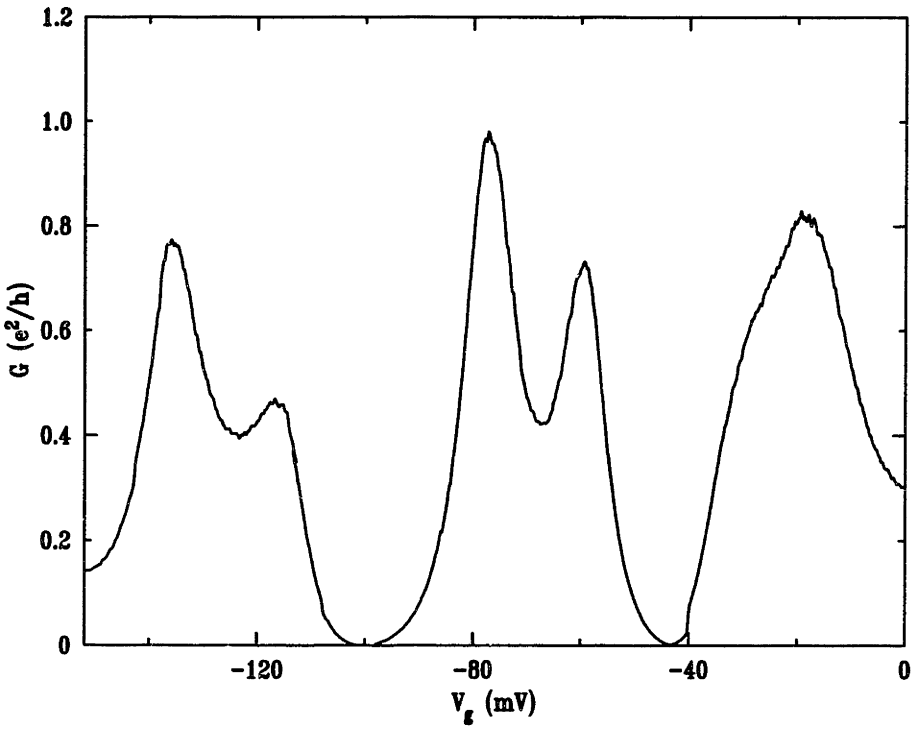

Figure 4-4: The two peak "pairs" of Figure 4-2 are shown on the right, along with an additional pair on the left. The appearance of the Kondo effect depends on the parity of the number of electrons, as indicated by the fact that the intrapair valleys are much higher than the interpair valleys. In addition, a zero-bias peak in differential conductance, associated with the Kondo resonance, is seen in all the intrapair valleys, and not in the interpair valleys (see Figure 5-1 for an example and explanation).

of the quantized state the electron is entering. Two successive electrons entering the same spatial state require the same quantized energy, so the peaks corresponding to their addition are merely spaced by U. In contrast, if two successive electrons enter two *different* spatial states, the second electron will require a quantized energy greater by $\Delta\varepsilon$, so the two peaks will be spaced by $U+\Delta\varepsilon$. These two conditions should alterate, with the first two electrons entering the same state, the next two entering a second state, and so on. This means that the peak spacing should alternate between small and large, U and $U + \Delta\varepsilon$.

In addition, Coulomb blockade peaks corresponding to transport through individual spatial states can have widely varying heights and widths depending on the overlap of the wavefunction for the particular state in question with wavefunctions of electrons at the Fermi level in the leads [19]. Our simple model suggests that each closely-spaced pair of peaks corresponds to a single spatial state, and hence should have a common height and width, whereas two consecutive widely-spaced peaks correspond to different spatial states and hence should generally have different heights and widths.[2] These predictions can be tested simply by looking at a series of Coulomb blockade peaks, and this has been done by many groups, most significantly by those led by Charlie Marcus, Albert Chang, and Uri Sivan [66, 67, 68, 69]. The surprising answer is that while variation in peak height and spacing is observed, there's no trace of the expected peak pairing. There is not even a bimodal distribution of peak spacings, with a small spacing corresponding to U and a large spacing corresponding to $U+\Delta\varepsilon$. In fact, Marcus' group has even studied the low-field "magneto-fingerprints" of a series of peaks (each wiggles in a different way as a function of magnetic field), concluding that no two electrons enter the same spatial state [70].

All these measurements were made on SETs with an electron droplet several hundred nm in diameter. My much smaller dots have displayed very suggestive evidence that pairs of electrons enter the same quantum state, as I will outline below.

Charlie Marcus has since informed me [71] that his group has recently seen similar behavior when the central droplet in an SET is particularly small. The reasons for this change in behavior, presumably related to the change in droplet size, are unclear, but so are the reasons for the absence of pairing in general.

[2]Width and height should gradually change as depletion of the droplet increases the opacity of the barriers, but this monotonic behavior should be enlivened by random variations in overlap (tunneling matrix element) from one state to the next.

4.2 When does the model work, and why?

Let me give a handwaving argument, inspired partially by discussions with Leonid Glazman. What would prevent electrons from pairing in a single quantum state? It must be Coulomb interactions, since as noted above the two spin states corresponding to a single spatial state are degenerate for non-interacting electrons. Now there are several possibilities:

1. The Coulomb energy will tend to be larger for two electrons in the same spatial state than for two electrons in different states, simply due to larger overlap. Hence, placing the second electron in a different state saves on Coulomb energy even as it costs quantum confinement energy. If the savings is greater than the cost, no two electrons will occupy the same spatial state. For a small droplet, it may be impossible to find a low-lying quantum state whose wavefunction is well-separated from that of the first state, reducing the savings. This could explain the recovery of pairing behavior when the droplet is made smaller.

2. All else being equal, electrons would prefer to have their spins aligned parallel rather than antiparallel, since Pauli exclusion then helps them avoid each other and decrease their Coulomb energy. This phenomenon can be expressed as the exchange part of the Coulomb energy. If the exchange energy W can overcome the cost $\Delta\varepsilon$ to populate a higher state, it will drive successive electrons into a series of distinct states to allow them to align their spins parallel. Since $\Delta\varepsilon$ is not a well-defined property of the droplet, but rather has an average value and a distribution, for some states W should exceed $\Delta\varepsilon$ and break pairing. However, $< \Delta\varepsilon >$ and W both scale inversely with droplet area [72], so this mechanism for pair breaking should not depend on droplet size.

3. More exotically, exchange could drive the electrons in a droplet to exhibit non-trivial spin order (for example, ferromagnetism), breaking the degeneracy between spin up and spin down states. Again, it's not clear how this should depend on droplet size, but evidence for a similar phenomenon has been seen in an experiment on a segment of carbon nanotube [73]. Hopefully future experiments will elucidate the conditions and mechanisms that defeat pairing in most semiconductor SETs.[3]

[3]In this context, it's also worth noting that, beyond mere spin degeneracy, the full Hydrogen-like shell structure expected for electrons in a 2D harmonic oscillator potential has been observed in a beautiful series of experiments by groups led by Leo Kouwenhoven and Seigo Tarucha [12]. In these experiments, great care was taken to make the confining potential perfectly cylindrically symmetric to preserve the extra degeneracies. In addition, screening by conducting layers above and below the droplet strongly reduced the effect of Coulomb interactions relative to that of quantized states

4.3 Experimental results on state filling

Now to the data. To elucidate the filling of successive quantum states, I focus on a situation where the barriers are tuned to be relatively opaque, suppressing the Kondo effect which produces its own form of peak pairing. As explained above, in this situation intrapair peak spacing should be smaller than interpair spacing. The two peaks within a pair should have comparable widths and heights, while between pairs both should vary significantly. Unfortunately, in our SETs it is difficult to study the successive addition of many electrons to the central AA. The problem is unexpected jumps in the conductance as a function of gate voltage, termed "switches". See Appendix C for more details on this behavior, and its probable causes. The SET studied here proved more stable in the presence of a magnetic field in the plane of the 2DEG, enabling the unusual addition of eight electrons (Fig. 4-6) without serious problems from switches. Fortunately, I was able to trace peaks from zero field to high field without interruption, allowing me to identify some of the peaks occurring at high field with their zero-field counterparts.

Even in high field, peaks form pairs with similar height and width (Figs. 4-6, 4-7), but the intrapair spacing is larger than the interpair spacing (Fig. 4-7)! These observations strongly suggest that each pair of peaks corresponds to two electrons of different spin occupying a single spatial state. To understand the strange behavior of peak spacing, we examine the expected effects of applying a magnetic field within the plane of the 2DEG. Unlike a field normal to the 2DEG, which produces major changes in orbital states in the leads, giving rise to the quantized Hall effects at high fields, a field in the plane couples primarily to the electron spin, splitting each spin-degenerate state into a doublet separated by the Zeeman energy $E_Z \equiv g\mu_B B$.

If two electrons enter the same spatial state, the first will lower its energy as B increases, while the second will raise its energy. The consequence will be that the peaks of a close-spaced pair will move apart as field is increased, eventually approaching closer to their unmatched neighbors than to their true partners. The consequence of this at high field is precisely what we see in Figures 4-6 and 4-7, demonstrating that electrons indeed form pairs in the same spatial state and opposite spin states, and unambiguously marking which valleys correspond to odd electron number and hence net spin 1/2 on the droplet at $B = 0$. Within this series of peaks

in the confinement potential, so much of the behavior could be understood in the context of the simple constant-U picture which I was just forced to question as a model for state filling in most semiconductor SETs.

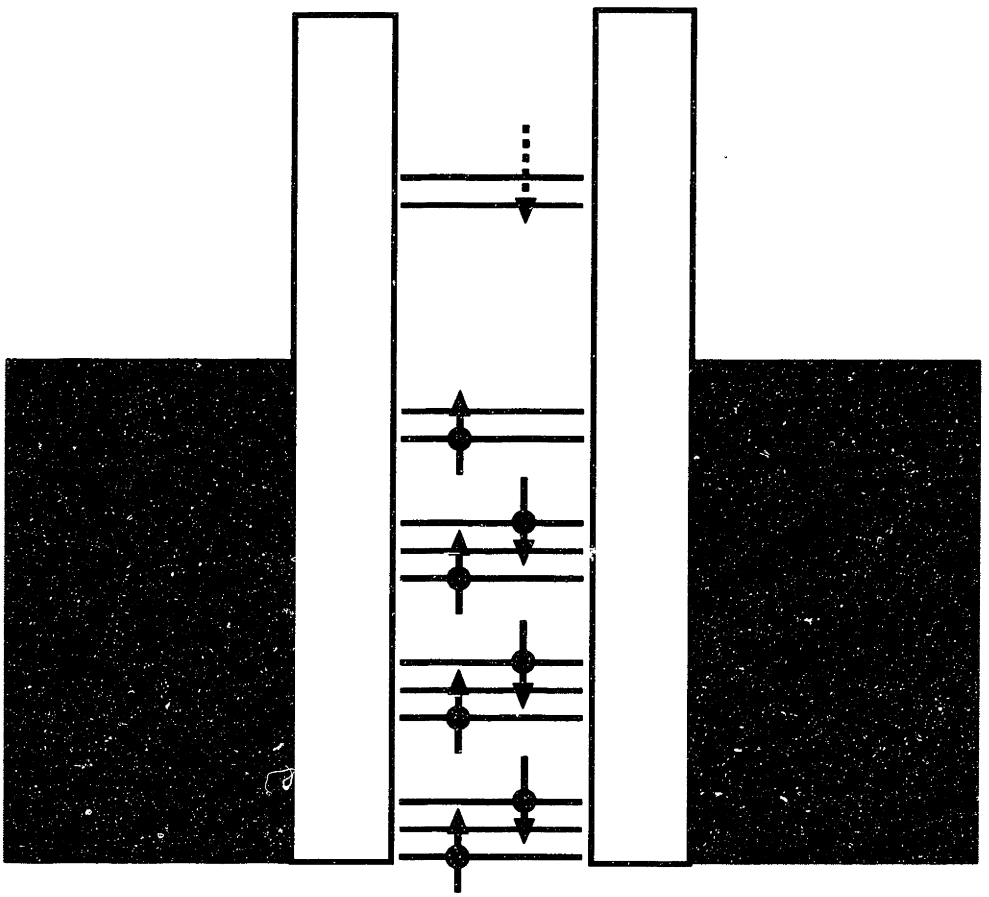

Figure 4-5: Retaining the simple model illustrated in Figure 4-5, the application of an in-plane magnetic field B should split each spatial state from Figure 4-1 into a Zeeman doublet separated by an energy $g\mu_B B$.

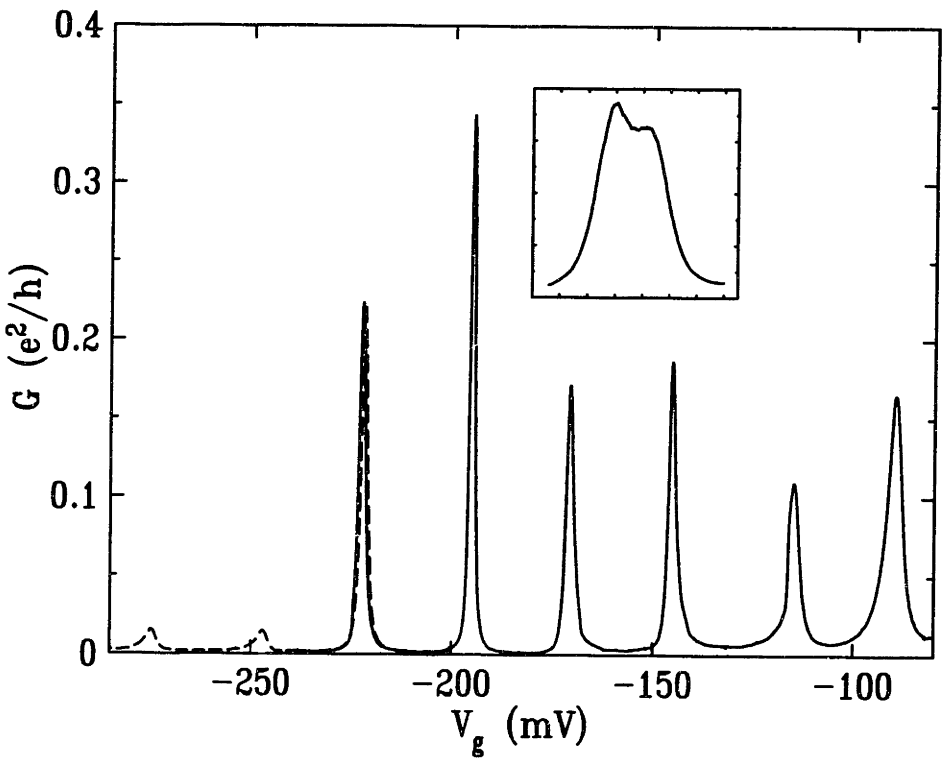

Figure 4-6: Coulomb blockade peaks in our SETs form pairs with similar width and height. This figure shows four such pairs(1-2, 3-4, 5-6, and 7-8), as measured in an in-plane magnetic field of 15.2 T. An in-plane magnetic field has only a weak effect on spatial states of electrons, since the electrons are already strongly confined in the direction normal to the plane. Hence, the dominant effect of such a field is the Zeeman splitting it induces between spin states. Empirically, the two peaks in a pair move apart as the in-plane B field is increased, resulting in intrapair spacing even larger than interpair spacing at $B = 15.2$T, as seen in this figure and as displayed quantitatively in Figure 4-7. The solid and dashed curves were measured in separate but consecutive gate voltage sweeps. Inset: Pair 5-6 displays Kondo effect at $B = 0$.

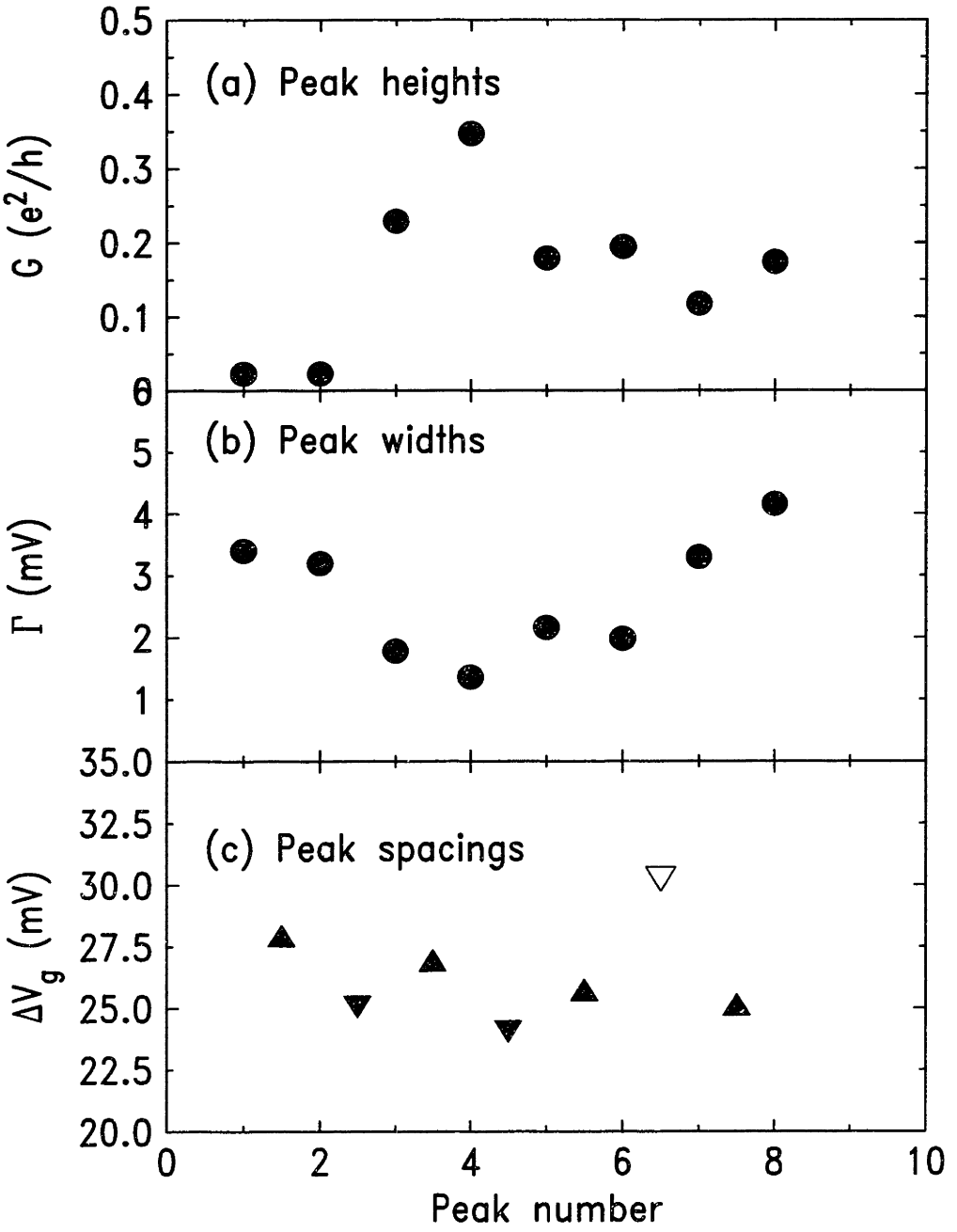

Figure 4-7: Quantitative demonstration that paired peaks move apart due to Zeeman energy. This figure shows quantitative information extracted from Figure 4-6. (a) Though the four pairs of peaks (1-2,3-4,5-6, and 7-8) have quite different heights, within each pair the heights are similar. (b) The same is true for widths. (c) Intrapair spacings (up triangles) are higher than surrounding interpair spacings (down triangles), due to Zeeman splitting. Interpair splitting 6-7 (unfilled down triangle) is anomalously large, perhaps due to an unnoticed "switch" in that valley.

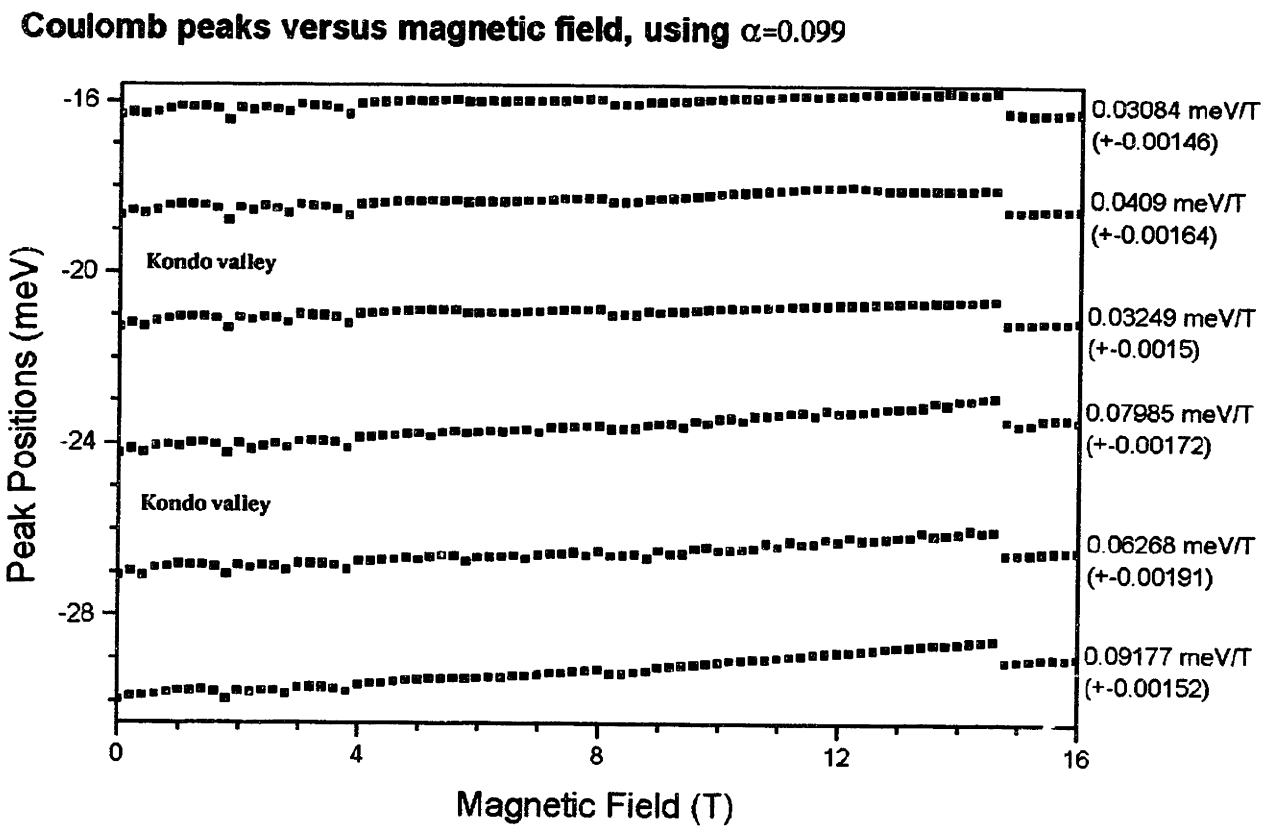

Figure 4-8: B-field dependence of peak positions. The second and third, and fourth and fifth, peaks from the top form pairs, with each pair corresponding to a single spatial state with two spin states. Peaks within a pair move apart with increasing magnetic field, due to increasing Zeeman splitting. See text for details. These data were taken on the same SET and same cooldown as those shown in Figures 4-6, 4-7, but with slightly different voltages on the non-plunger gates.

is a pair (5-6) which displays a Kondo valley. This valley occurs for odd electron number as expected. It is expected that neighboring pairs, with comparable or larger tunnel coupling in high field, should show the Kondo effect as well, but confirmation of this was hindered by multiple "switches", which distorted the observed peak shapes and even prevented the identification of particular peaks in the sequence.

Figure 4-8 shows the dependence of peak positions on B-field applied parallel to the plane of the 2DEG, from $B = 0$ to $B = 16$T. These peak positions have been converted from gate voltage to energy with the measured capacitive conversion factor $\alpha \equiv C_g/C_\sigma = 0.099$. The second and third, and fourth and fifth, peaks from the top form pairs, with each pair corresponding to a single spatial state with two spin states. This identification is made based on several properties: 1. similar peak attributes within each pair; 2. relatively small spacing between paired peaks at B=0; 3. observation of a Kondo resonance in differential conductance, in the valleys between paired peaks at B=0 (see Section 5.2). Though the combined weight of all these properties suggests that the identification of pairs is correct, the observed behavior of properties 1 and 2 does not perfectly match expectations. For example, the spacing between the first and second peaks is even smaller than that between the "paired" second and third peaks. This discrepancy might be caused by a "switch" (see Appendix C): the motion of a charge near the AA, capacitively shifting the energies of all the states in the AA.

Paired peaks move apart with increasing B due to increasing Zeeman splitting between the two spin states in the pair. All the peaks drift upward in energy with field, presumably due to a small accidental normal component of the field caused by misorientation of the sample by 1–2°. A normal magnetic field couples strongly to the spatial states, so even a small normal component can produce effects rivaling or exceeding those caused by a much larger parallel field. Each state has a different slope with field, but within a peak pair (representing two electrons entering the same spatial state) the two peaks move with almost the same slope. However, they move slightly apart with field, due to the different Zeeman couplings to the two spin states. For the two pairs seen here, rough values of the Zeeman splittings deduced from the measured slopes are 8μeV/T and 17μeV/T, corresponding to g-factors of 0.14 and 0.29, respectively. More precise measurements will be necessary to determine whether Zeeman splittings for different spatial states are really quantitatively different. This outcome might be understandable in a more complex model for the AA, with finite total spin polarization. Coulomb exchange energies would then be different for spin up electrons than for spin down electrons entering the same spatial state. If we take the

values for Zeeman splitting seriously, they are lower than the 25μeV/T ($|g| = 0.44$) expected for bulk GaAs. As explained in Section 5.4, this suppression of Zeeman splitting is not only expected in a confined geometry but is also consistent with splittings observed in the same batch of SETs in the context of the Kondo effect.

Given the typical level spacing of 400–500 μeV in these AAs, we should expect the increasing Zeeman energy to drive level crossings, changing the spin polarization of the ground state, though at the accessible fields they would only be expected if an excited state were unusually close to the ground state in energy, so that $E_{Z,max} \approx 270\mu\text{eV} > \Delta\varepsilon$. This phenomenon might be manifested by a kink in the position vs. field of two consecutive peaks (due to a swapping of spin state), combined with an exchange of shape between those two peaks (due to a swapping of spatial state). So far, evidence for such Zeeman-driven level crossings in these AAs is inconclusive. Nor, to my knowledge, have they been observed in other AAs.

Chapter 5

Basic Experiments on Kondo in an SET

In Chapter 4, I showed evidence that for odd occupancy my AAs have an unpaired electron with net spin, and hence may be considered magnetic. We also saw that when they are strongly coupled by tunneling to nearby leads, these magnetic AAs display the Kondo effect at low temperature. Sometimes the best way to learn about a phenomenon is to investigate the conditions for its occurrence. Equivalently, we can examine what it takes to *destroy* the Kondo effect in these AAs. Fortunately, as mentioned in Chapter 2, there are many ways to break the Kondo singlet, and we can easily identify this destruction by a decrease in conductance through the SET. We've already seen the effect of increasing temperature in Figure 4-2, and this effect will be examined much more quantitatively in Chapter 6, so in this chapter we will touch on it only briefly, focusing mostly on the effects of tuning other parameters.

5.1 Temperature (recap)

When $\Gamma \leq kT$, the Kondo effect is not a major factor. The peaks in conductance versus gate voltage become narrower and larger with decreasing T, as illustrated in Figure 4-2(b), saturating at low T to a width and height determined by Γ. As noted in Chapter 3, this behavior results from the sharpening of the Fermi distribution [40, 74]. Figure 4-2(a) illustrate that this pattern is followed for large Γ, as well, on the outside edges of paired peaks at all T. However, inside of pairs the peaks become narrower as T is reduced from 800 mK to 400 mK, but then broaden again at low temperatures, resulting in increased conductance in the intra-pair valley. Thus, not only the peak

spacing but also the mechanism of conduction itself is different intra-pair from inter-pair. The enhancement of linear conductance at low temperature for odd but not even N is a manifestation of Kondo physics. If N is odd there is an unpaired electron with a free spin which can form a singlet with electrons at the Fermi level in the leads. This coupling results in an enhanced density of states at the Fermi level in the leads, and hence an enhanced conductance [64, 65]. Raising the temperature destroys the singlet and attenuates the conductance.

5.2 Nonequilibrium bias and differential conductance

So far, all the experiments shown have measured linear conductance, determined from current flowing due to the presence of a bias applied between the two leads, where the applied bias is smaller than all other energy scales and simply defines a direction for current flow. Experimentally, one has the flexibility to apply a larger bias between the two leads (see Figure 3-4(c)), driving the system out of equilibrium. The extra conductance carried by the Kondo bond is sensitive to even small applied biases, of order $eV_{\mathrm{LR}} = kT_{\mathrm{K}}$. This is because the unpaired electron in the AA couples to electrons in both leads, giving an enhanced density of states at both Fermi levels [50, 75, 76]. This enhancement can be thought of as a manifestation of the Kondo bond. The electrons participating in the bond are those near the Fermi level, since above the Fermi level no electrons are present and below the Fermi level all states are filled, so electrons cannot choose to have their spins anti-aligned with the spin on the impurity. When the applied voltage is large, separating the Fermi levels in the two leads, the electrons at the Fermi level in the higher energy lead can no longer resonantly tunnel into the enhanced density of states associated with the lower energy lead, so the extra conductance is suppressed. This can be seen in Figure 5-1(a), a plot of differential conductance dI/dV_{LR} versus V_{LR} for a magnetic configuration of the AA (achieved using a gate voltage midway between the lefthand pair of peaks in Figure 4-2(a)). Figure 5-1(b–c) illustrates how this nonlinear conductance measurement also offers a complementary way of seeing the suppression of the zero-bias conductance with temperature. By 600 mK, the Kondo resonance has almost disappeared completely.

This type of nonequilibrium experiment is impossible in a bulk metal with magnetic impurities, since only a minute proportion of the bias applied across the sample falls across any individual impurity. However, results similar to mine have been ob-

tained in previous experiments involving tunneling through many [77] magnetic impurities in parallel, and even in a beautiful experiment on a single magnetic impurity trapped in a metallic point contact [51]. Semiconductor SETs offer the additional flexibility to tune system parameters other than the bias across the impurity. For example, the impurity can be changed from magnetic to non-magnetic by adding a single electron, a capability which I have exploited to demonstrate that this zero-bias feature occurs only when the impurity is magnetic (see Figure 5-2).

5.3 Magnetic field

A magnetic field also alters the Kondo physics. Applying a magnetic field splits the unpaired localized electron state into a Zeeman doublet separated by the energy $g\mu_B B$. This also splits the enhanced density of states at the Fermi level into two peaks with energies $g\mu_B B$ above and below the Fermi level [50] (see Figure 3-6(b) for $B = 0$, Figure 5-4 for $B \neq 0$). At the Fermi level, the density of states is no longer enhanced, so linear conductance is suppressed.

5.4 Kondo lost and Kondo restored: Combining finite bias with a magnetic field

When a bias $V_{\mathrm{LR}} = g\mu_B B/e$ is applied with either polarity between the two leads, electrons can tunnel from one lead into the Kondo-enhanced density of states associated with the other lead, restoring enhanced conductance. In differential conductance at high magnetic field, we thus see peaks at $V_{\mathrm{LR}} = \pm g\mu_B B/e$ (see Figure 5-1(d–f)). This behavior is seen even more dramatically in Figure 5-6, in which the sharp Kondo resonance that appeared at zero bias in zero field (Figure 5-2) splits into two resonances at positive and negative bias. These resonances still only appear for odd and not for even electron occupancy. The splitting of peaks in differential conductance by *twice* $g\mu_B B$ (compared to the spin splitting of the localized state, $g\mu_B B$) provides a distinctive signature of Kondo physics. Since the peaks are broad and overlapping, the distance between their maxima may underestimate their splitting at lower magnetic fields. At 7.5 T, when the peaks no longer overlap, their splitting is $0.033 \pm .002$ meV/Tesla. In comparison to measurements on bulk GaAs, this is significantly smaller than $2g\mu_B B$ yet larger than $g\mu_B B = 0.025$ meV/Tesla. Electron spin resonance measurements have found that spin splittings in a two-dimensional

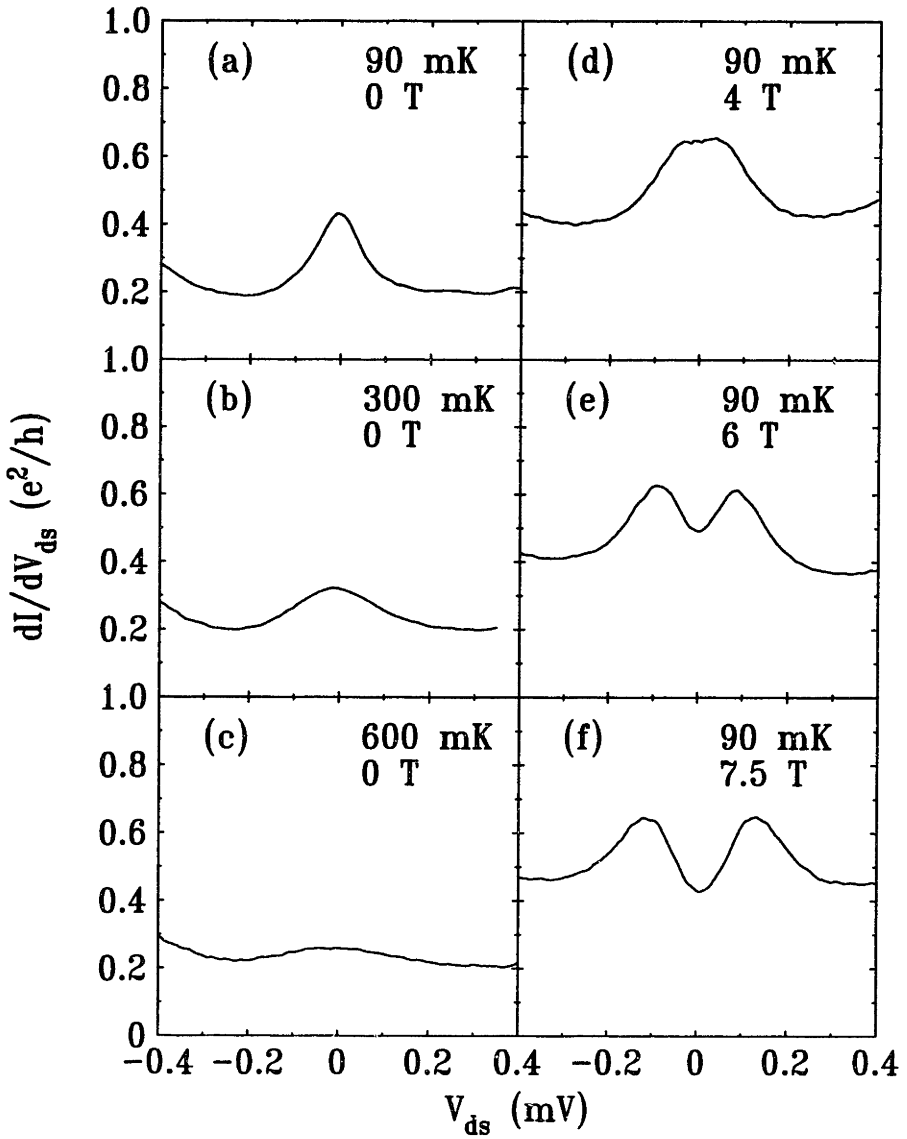

Figure 5-1: Differential conductance versus bias of an SET for a magnetic configuration of its central AA. (a) At the base temperature of the dilution refrigerator differential conductance shows a strong enhancement at zero bias due to the Kondo effect. The width of this zero-bias peak is expected to be determined by kT or kT_K, whichever is greater. (b,c) As temperature is increased, the peak becomes lower and broader as expected, almost disappearing by around 600 mK. Note that this is a much lower tempererature than that required to add an electron to the AA, "ionizing" it, so the electron occupancy is still well-quantized. (d–f) With increasing magnetic field, the Kondo singlet is destroyed, lowering the zero-bias conductance. However, applying a bias can compensate the magnetic-field-induced Zeeman splitting, restoring extra conductance. See text for details.

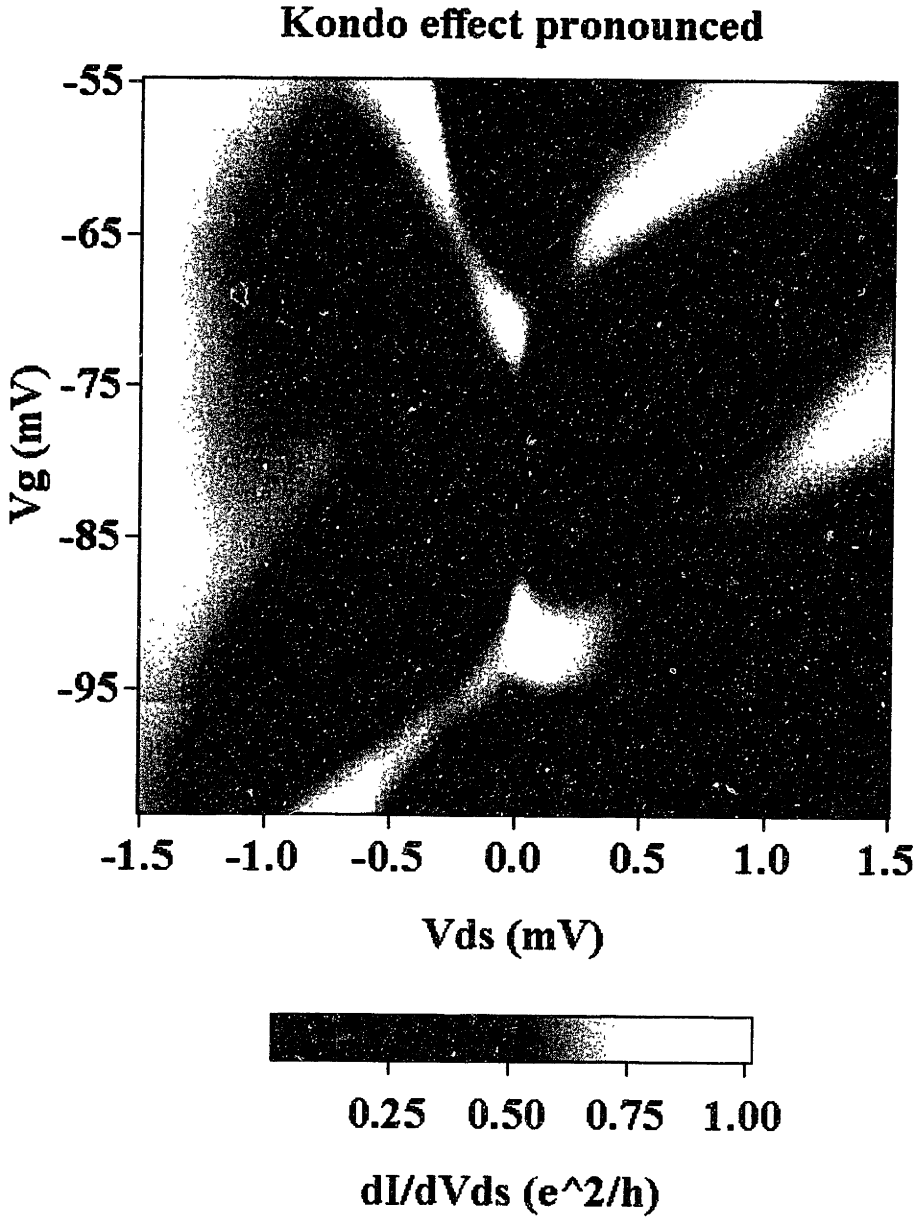

Figure 5-2: Differential conductance on a gray scale as a function of both gate voltage V_g on the vertical axis and source-drain bias V_{LR} on the horizontal axis. A line drawn down the center from top to bottom corresponds to equilibrium or zero source-drain bias. At the top and bottom of the figure, the equilibrium occupancy N of the artificial atom is even, so almost no current flows. The thin white vertical line in the middle indicates that for odd N current can flow through the artificial atom even though its occupancy cannot fluctuate. This is a manifestation of the Kondo effect, which occurs only when N is odd so that the unpaired electron can bond with an electron in the nearby leads. The Kondo-related feature occurs only at zero bias since the bond can occur only with electrons near the Fermi level in each lead (see text for more details). Notice that the vertical line is very narrow, much narrower than the diagonal features which correspond to addition or removal of an electron from the artificial atom, and which hence have width Γ. Relating width to inverse lifetime, we must conclude that the many-body "Kondo bond" state remains coherent much longer than the lifetime of an individual electron on the artificial atom.

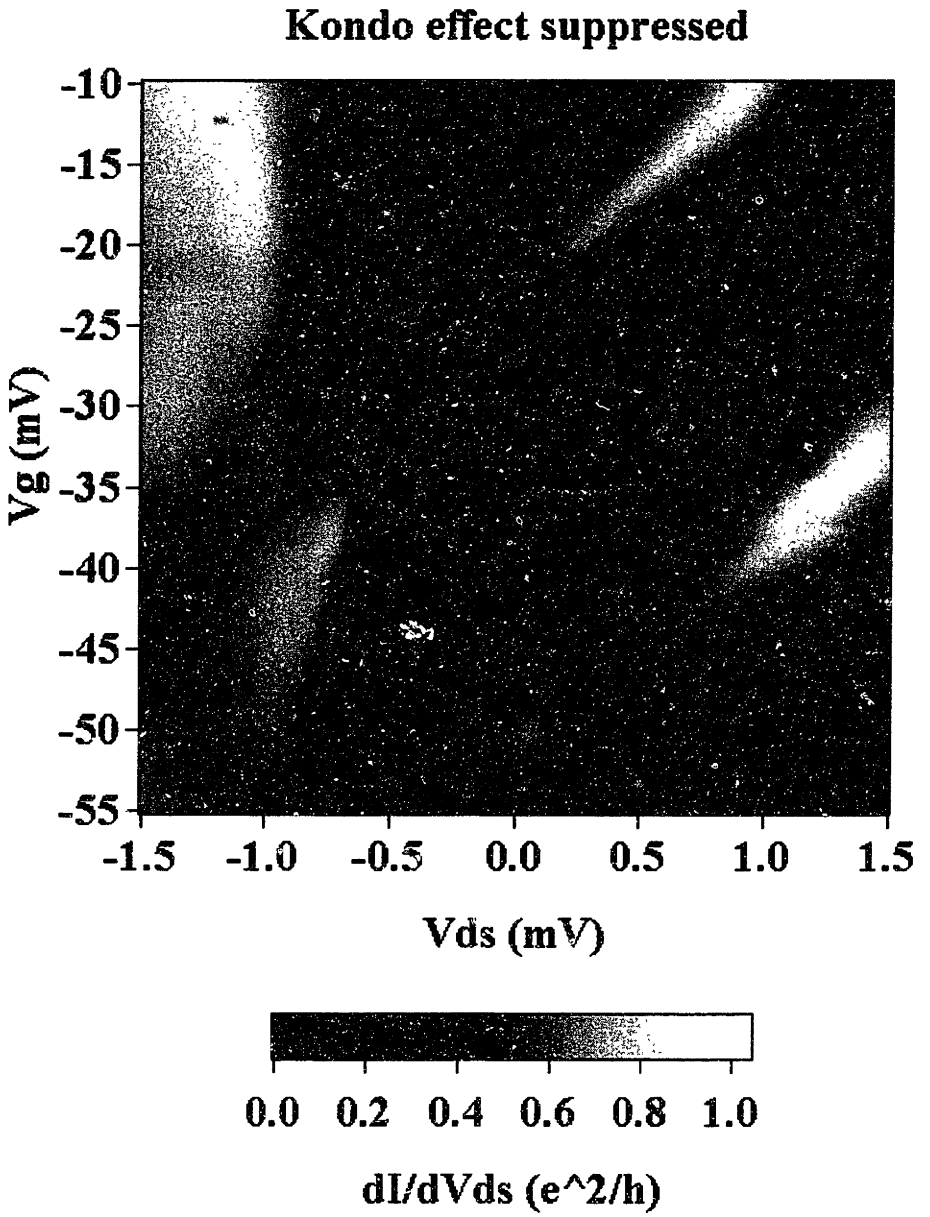

Figure 5-3: Differential conductance on a gray scale as a function of both V_g and V_{LR}. Parameters are the same as for Figure 5-2, except that Γ has been reduced by approximately 30%. The picture is mostly unchanged, except that the white vertical line between the two maxima, the signature of the Kondo effect is now absent. A small reduction in Γ has driven the Kondo effect from prominent to invisible at accessible temperatures, a dramatic demonstration of the sensitivity of the Kondo bond's strength to the coupling Γ between artificial atom and leads.

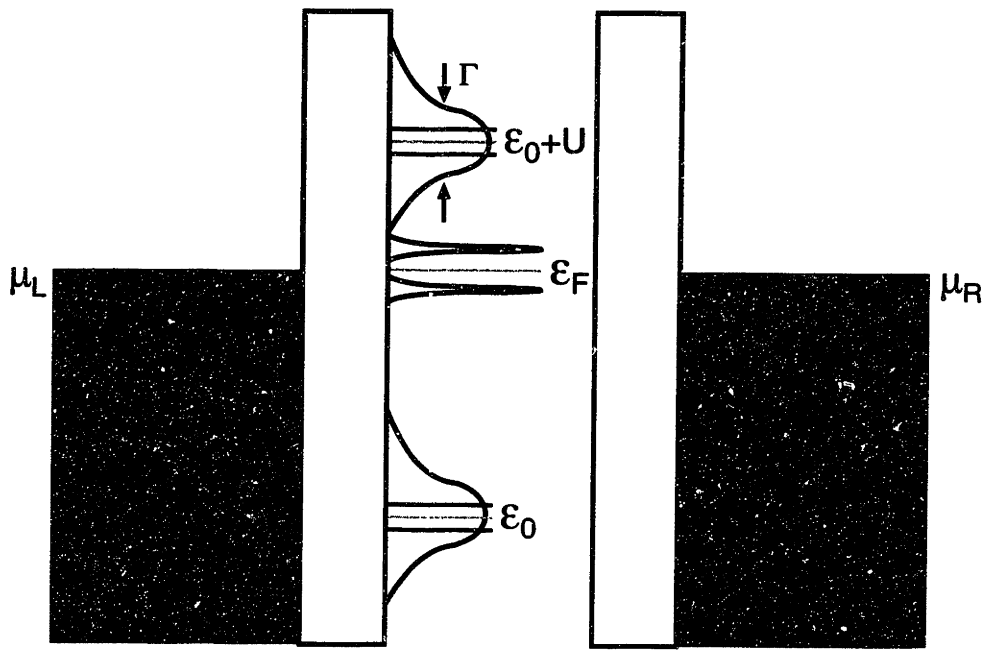

Figure 5-4: Local density of states of an SET in finite magnetic field (see Figure 3-6(b) for the zero-field version). The localized state is split into a Zeeman doublet with separation $g\mu_B B$, breaking the Kondo bond — Kondo-related features move away from the Fermi level to energy $\pm g\mu_B B$, spaced twice as widely as the single-electron spin states. See text for details.

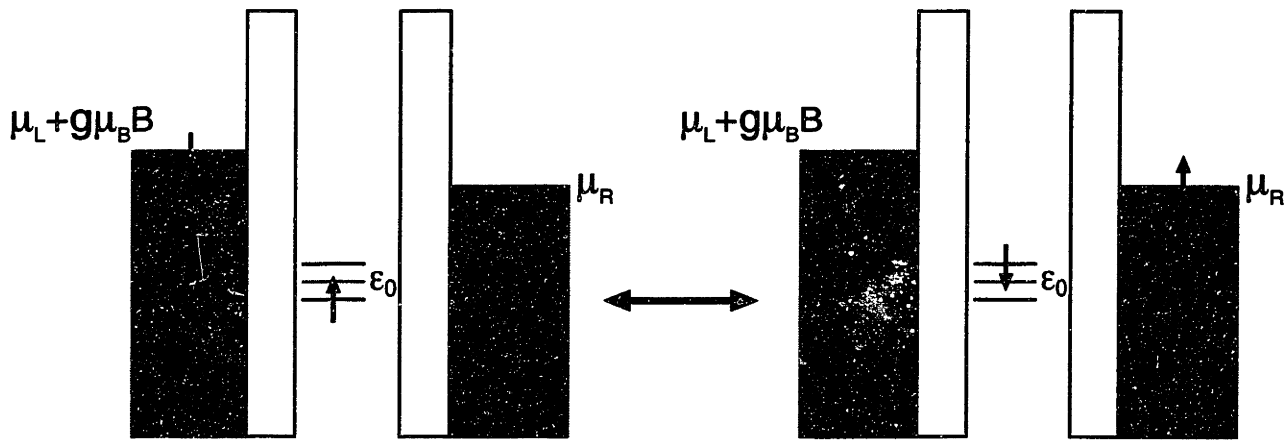

Figure 5-5: Explanation of displaced peaks in local density of states of an SET in finite magnetic field (as shown in Figure 5-4). The localized state is split into a Zeeman doublet with separation $g\mu_B B$, breaking the Kondo bond, and preventing electron pairs from "sloshing" across the SET resonantly without changing AA occupancy. To restore degeneracy of the initial and final states, one can compensate the magnetically-induced spin-splitting on the localized site with a bias $eV_{\mathrm{LR}} = g\mu_B B$ applied across the SET. Now as electrons "slosh" across, the energy of the localized electron increases but that of the delocalized electron decreases by the same amount. Compare Figure 3-7.

electron gas are suppressed compared with values for bulk samples, sometimes by as much as 35% [78]. Independent determination of the g-factor in these SETs with B in the plane of the 2DEG shows just such a suppression (Fig. 4-8). Thus, this measurement is consistent with a splitting of $2g\mu_B B$.

Understanding of the exact amplitude of the splitting is complicated by the fact that the magnetic field was applied normal to the heterostructure. In this geometry, the field couples not only to spins but also to spatial states of electrons in the leads. In fact, in high enough magnetic field electrons fill only one or two Landau levels, and must tunnel into the AA from a single, spin-polarized quantum Hall edge state, preventing electrons with opposite spin from participating in transport. In the experiment under discussion, this extreme limit was not reached: even at 7.5 T six Landau levels were filled, due to the unusually high density of the 2DEG. The persistence of the Kondo effect in this regime indicates that at least two edge states could participate in transport.

A more recent experiment by the Delft group on an SET in parallel magnetic field (which couples only to spin) observed similar split peaks in differential conductance [79]. The splittings were linear with field, and the magnitude of the splitting was precisely as one would naïvely predict: $V_{\rm LR} = \pm g\mu_B B/e$, where $|g| = 0.44$, the value for bulk GaAs. I have also since measured one of my SETs in parallel field, with qualitatively similar results.

5.5 AC excitation

The Kondo bond can also be destroyed by shining light on the SET. Due to the lower energy scales for AAs as compared to ordinary atoms, the appropriate frequencies for spectroscopy are in the microwave rather than the visible range. We saw that temperature need not be raised high enough to ionize the artificial atom in order to suppress the Kondo effect; similarly, microwaves need not be of high enough frequency to ionize the AA to suppress the Kondo effect. Lower frequency microwaves should suppress the Kondo effect by a process termed spin-flip cotunneling [80]: an electron in one of the leads, coupled to the unpaired electron in the AA, absorbs a photon and jumps to an energy above the Fermi level. At this energy both spin states are available, so half the time the electron will flip its spin, in which case the localized electron flips its spin as well. This random process causes dephasing of the singlet state, shortening its lifetime. Translated to the local density of states, this means that the Kondo resonance at the Fermi level becomes lower and broader, so linear

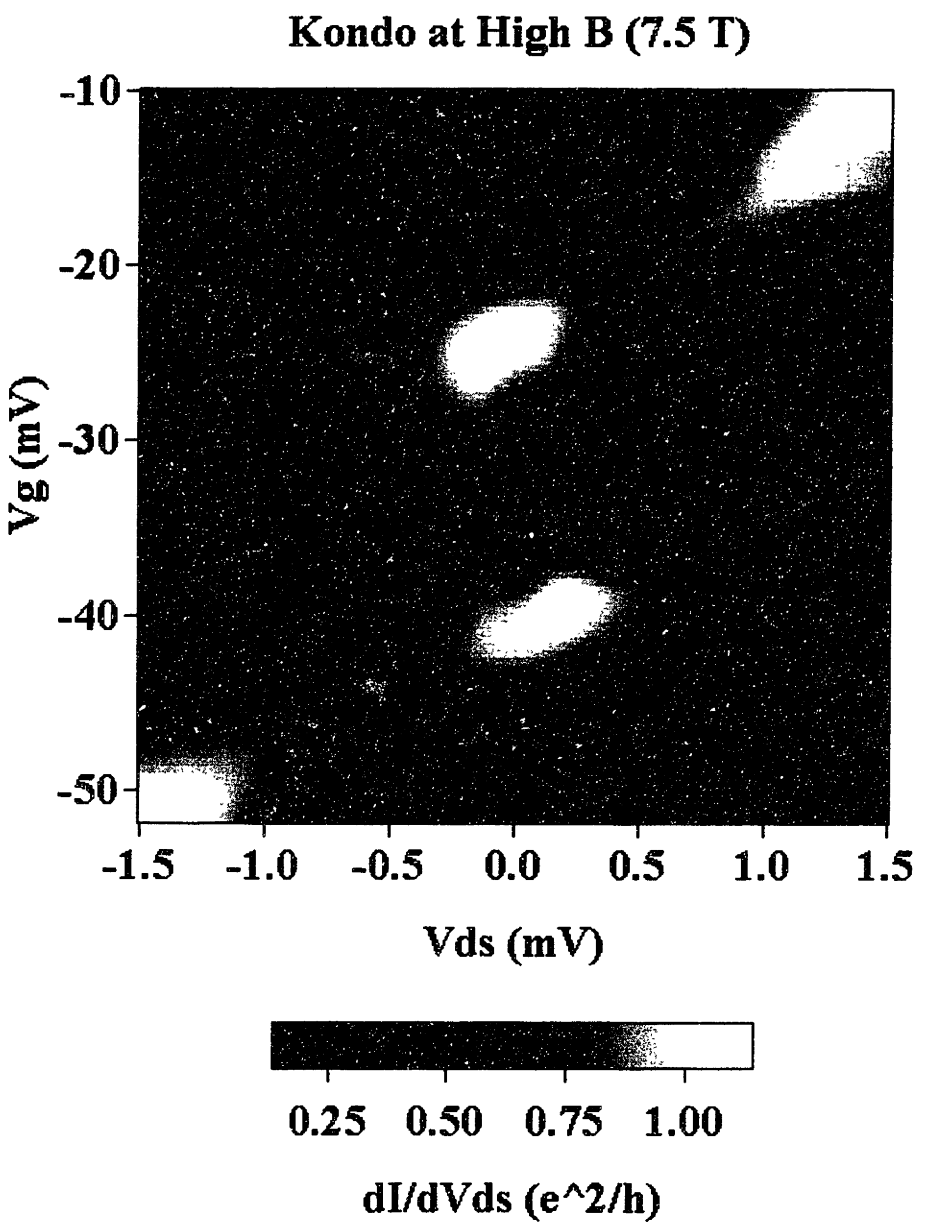

Figure 5-6: Differential conductance on a gray scale as a function of both V_g and V_{LR}. The high magnetic field has broken the energy of the localized electron into a Zeeman doublet. The white vertical line from Figure 5-2 splits into two lines at positive and negative bias, showing that (i) in equilibrium, the Zeeman splitting destroys the Kondo bond with its associated conductance, and (ii) application of an appropriate non-equilibrium bias across the artificial atom can compensate the Zeeman splitting and restore enhanced conductance. See Figures 5-4 and 5-5 for a schematic explanation of this remarkable phenomenon.

conductance is suppressed. Stray microwaves may be the cause for the unexpected finding in Chapter 6 that the width of the Kondo resonance is larger than either kT_K or kT.

Now that we've reviewed the excellent qualitative match between experiments and theory for the Kondo effect in an SET, the next chapter will examine in quantitative detail how the Kondo bond is suppressed by raising the temperature.

Chapter 6

Quantitative Analysis: Kondo Temperature and Occupancy

6.1 Qualitative temperature-dependence (recap)

When $\Gamma \leq kT$, the Kondo effect is not a major factor. The peaks in conductance versus gate voltage become narrower and larger with decreasing T, as illustrated in Figure 4-2(b), saturating at low T to a width and height determined by Γ. As noted in Chapter 3, this behavior results from the sharpening of the Fermi distribution [40, 74]. Figure 4-2(a) illustrates that this pattern is followed for large Γ, as well, on the outside edges of paired peaks at all T. However, inside of pairs the peaks become narrower as T is reduced from 800 mK to 400 mK, but then broaden again at low temperatures, resulting in increased conductance in the intra-pair valley. Thus, not only the peak spacing but also the mechanism of conduction itself is different intra-pair from inter-pair. The enhancement of linear conductance at low temperature for odd but not even N is a manifestation of Kondo physics. If N is odd there is an unpaired electron with a free spin which can form a singlet with electrons at the Fermi level in the leads. This coupling results in an enhanced density of states at the Fermi level in the leads, and hence an enhanced conductance [64, 65]. Raising the temperature destroys the singlet and attenuates the conductance.

6.2 Quantitative analysis of $G(T)$, T_K, and state occupancy

Now I will examine how to extract quantitative information on the Kondo effect from measurements on an SET. As discussed in Chapter 3, the AA in an SET can be thought of as a realization of an Anderson impurity, with the parameters U, ϵ_0, and Γ determined by the lithographically-defined size of the AA and by the voltages on nearby gate electrodes: the plunger gate voltage V_g tunes ϵ_0, and the point contact voltages tune Γ. Depending on the values of these voltages, the artificial Anderson impurity can be in one of the several regimes of the Anderson model, parametrized by $\tilde{\epsilon}_0 \equiv \epsilon_0/\Gamma$: the Kondo regime $\tilde{\epsilon}_0 \ll -0.5$ (in which the spatial state is singly-occupied), the mixed-valence regime $-0.5 \lesssim \tilde{\epsilon}_0 \lesssim 0$ (in which the spatial state is occupied by *less* than a full electron), and the empty orbital regime $\tilde{\epsilon}_0 \gtrsim 0$ (in which the spatial state is, as might be expected, empty). Each of these regimes has different transport properties. In bulk materials, the Kondo regime describes many systems of dilute magnetic impurities in metals, while the mixed-valence regime provides some understanding of heavy-fermion compounds [6, 81, 82]. I am unaware of any material described by the empty orbital regime. Though, by analogy to resistivity of bulk Kondo systems (see Chapter 3), conductance through an SET normalized to its zero-temperature value $\tilde{G}(\tilde{T}) \equiv G(T/T_K)/G_0$ is expected to be universal in the Kondo regime, where the only small energy scale is T_K, it should change as $\tilde{\epsilon}_0 \to 0$ (the mixed-valence regime), where T_K and Γ become comparable [39, 75, 54]. The great advantage of the SET is that ϵ_0 can be tuned by varying V_g to test the predictions for all regimes in one and the same system.

To recap the discussion of Chapter 3, as V_g is varied[1], the conductance of an SET undergoes oscillations caused by Coulomb blockade. Current flow is possible in this picture only when two charge states of the droplet are degenerate, i.e. $\epsilon_0 = 0$ or $\epsilon_0 + U = 0$, marked by vertical dashed lines in Fig. 6-1 as determined by the analysis of Fig. 6-4.[2] The conductance between these dashed lines is expected to be very small.

[1] We focus here on zero-bias (linear) conductance, for which a quantitative comparison with theory is possible. As noted in Section 5.2, striking features caused by the Kondo effect are also observed in finite-bias measurements. These features, and their dependence on magnetic field, are perhaps the clearest qualitative signatures of the Kondo effect, but the resultant nonequilibrium effects are not as amenable to quantitative theoretical study. Measurements of similar features have now been reproduced by other groups [79, 83, 84].

[2] All the discussion in this chapter is based on measurements on a single SET, nominally identical to that discussed in Chapter 5

However, in this range the charge state of the site is odd, as portrayed in Fig. 3-6(b), and the Kondo effect allows additional current flow. Strikingly, at low temperature (dots, 100 mK and triangles, 800 mK), the conductance maxima do not even occur at $\epsilon_0 = 0$ and $\epsilon_0 + U = 0$ — the Kondo effect makes the off-resonant conductance even larger than the conductance at the charge-degeneracy point [50]. Raising the temperature suppresses the Kondo effect, causing the peaks to approach the positions of the bare resonances.

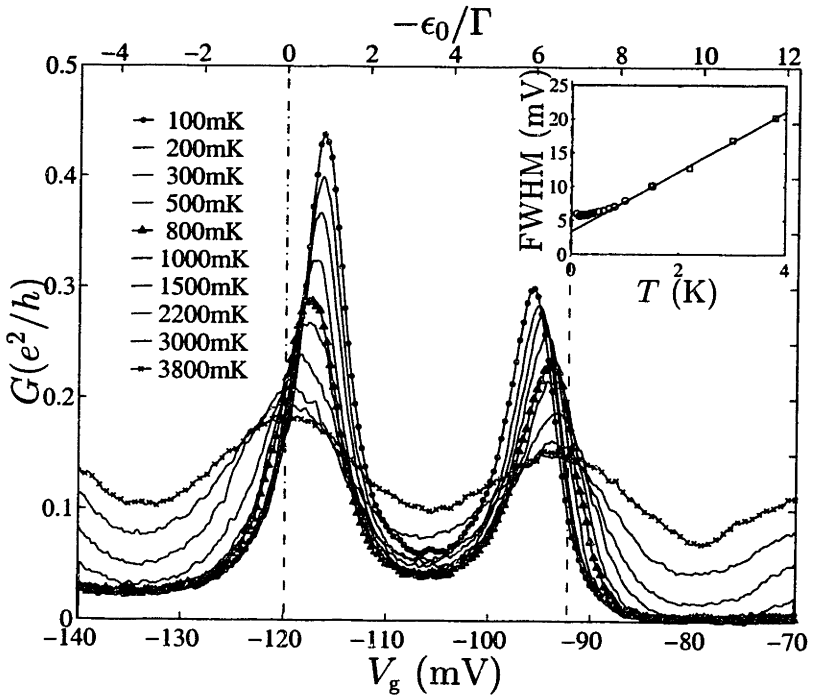

Figure 6-1: Conductance versus plunger gate voltage V_g at various temperatures. The localized-state energy $\epsilon_0 = \alpha V_g$ + constant. The vertical dashed lines mark gate voltages at which two charge states are degenerate (i.e. $\epsilon_0 = 0$ or $\epsilon_0 + U = 0$) based on the analysis in Figs. 6-4 (a),(b). Between the dashed lines the charge state of the site is odd, as portrayed in Fig. 3-6(b), and the Kondo effect enhances conductance. Inset: Linear temperature dependence of peak width extrapolated back to $T = 0$ to extract $\Gamma = 295 \pm 20\,\mu$eV. The slope of the same temperature-dependence gives the constant of proportionality $\alpha = 0.069 \pm 0.0015$ between ϵ_0 and V_g.

The inset of Fig. 6-1 shows how Γ is determined: For $T \geq \Gamma/2$, the Kondo effect plays only a small role, so the conductance peak should be (and empirically is) well-described by the convolution of a Lorentzian of FWHM Γ with the derivative of a Fermi-Dirac function (FWHM $3.52kT$). This convolution has a FWHM $0.78\Gamma + 3.52kT$, and extrapolating the experimentally-measured linear dependence back to $T = 0$ gives $\Gamma = 295 \pm 20\,\mu$eV.

When the energy of the localized state is far below the Fermi level ($\tilde{\epsilon}_0 \ll -1$), scaling theory predicts that T_K depends exponentially on the depth of that level [85]:

$$T_K = \frac{\sqrt{\Gamma U}}{2} e^{\pi\epsilon_0(\epsilon_0+U)/\Gamma U}. \tag{6.1}$$

Note that, because U is finite, $\log T_K$ is quadratic in ϵ_0. This strong dependence on ϵ_0 causes the Kondo-enhanced conductance to persist to higher temperatures near $\epsilon_0 = 0$ (and near $\epsilon_0 = -U$, by particle-hole symmetry) than in-between. In fact, at $T = 0$ the conductance should sustain its maximum value all the way between the two observed peaks in Fig. 6-1 [64, 65, 18] (see Fig. 6-4(b) for expected $G(\tilde{\epsilon}_0)$ at $T = 0$), but in the valley even our $T_{base} \simeq 100$ mK $> T_K \approx 40$ mK.

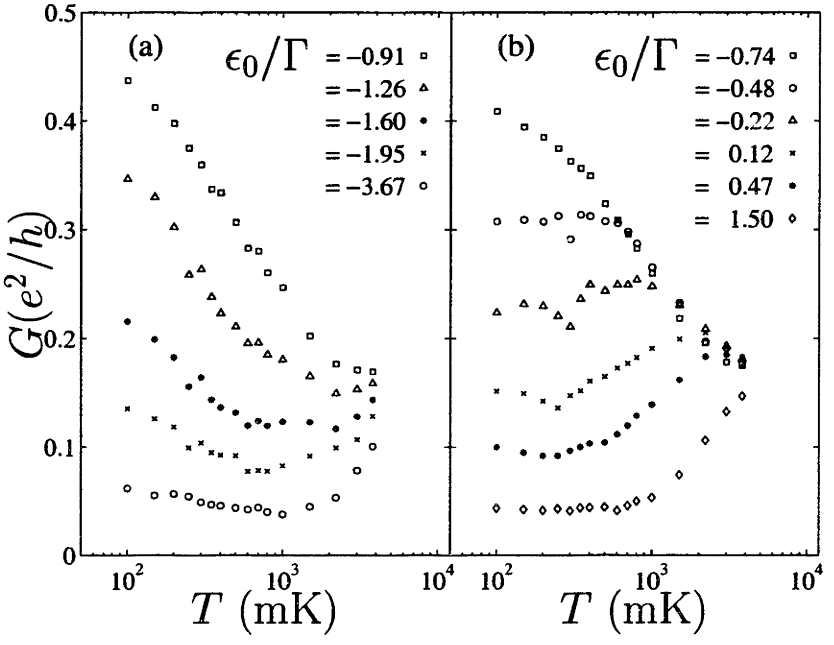

Figure 6-2: Conductance versus temperature for various values of ϵ_0 on the right side (a) and left side (b) of the left-hand peak in Fig. 6-1.

Figure 6-2(a) shows that, for fixed $\tilde{\epsilon}_0$ in the Kondo regime, $G \sim -\log(T)$ over as much as an order of magnitude in temperature, beginning at T_{base}. Thermal fluctuations in localized state occupancy cut off the $\log(T)$ conductance for $kT \gtrsim |\epsilon_0|/4$, consistent with simulations I've made of thermally-broadened Lorentzian resonances. As $\tilde{\epsilon}_0 \to 0$ (Fig. 6-2(b)), T_K increases, as evinced by the saturation of the conductance at low temperature.

To fit the experimental data for each ϵ_0 we use the empirical form

$$G(T) = G_0\Big(\frac{T_K'^2}{T^2 + T_K'^2}\Big)^s, \tag{6.2}$$

where T_K' is taken to equal $T_K/\sqrt{2^{1/s}-1}$ so that $G(T_K) = G_0/2$.[3] For the appropriate choice of s, which determines the steepness of the conductance drop with increasing temperature, this form provides a good fit to numerical renormalization group results [39] for the Kondo, mixed-valence, and empty orbital regimes, giving the correct Kondo temperature in each case. The parameter s is left unconstrained in the fit to our data, but its fit value is nearly constant at 0.20 ± 0.01 in the Kondo regime, while as expected it varies rapidly as we approach the mixed-valence regime (Figure 6-2(b)). Based on fitting to a perturbation theory result valid above T_K ([63], cited in [3, Eq. 3.12]), the expected value of s in the Kondo regime depends on the spin of the impurity: $s = 0.22 \pm 0.01$ for $\sigma = 1/2$.

Using the values of G_0 and T_K extracted in this way we confirm that $\tilde{G}$ is universal in the Kondo regime. Figure 6-3 shows $\tilde{G}(\tilde{T})$ for data like those of Figure 6-2 for various values of $\tilde{\epsilon}_0 \approx -1$ (on the left peaks of Fig. 6-1). We have also included data from the same SET, but with Γ reduced by 25% by adjusting the point-contact voltages. The data agree well with numerical renormalization group calculations by Costi and Hewson (solid line) [39]. In the mixed-valence regime it is difficult to make a quantitative comparison between theoretical predictions and our experiment. Qualitatively, in both calculation and experiment, $\tilde{G}(\tilde{T})$ exhibits a sharper crossover between constant conductance at low temperature and logarithmic dependence at higher temperature in the mixed-valence regime than in the Kondo regime (see Fig. 6-3) [39].

In Figure 6-4(a), we plot $T_K(\tilde{\epsilon}_0)$ extracted from our fits, along with the theoretical prediction (Eq. 6.1) for the Kondo regime. The value of $\Gamma = 280 \pm 10\,\mu$eV extracted is in good agreement with the value $\Gamma = 295 \pm 20\,\mu$eV determined as illustrated in Fig. 6-1 (inset). The prefactor is approximately three times larger than $\sqrt{\Gamma U}/2$, which must be considered good agreement given the simplifying assumptions in the calculations and the sensitivity to the value of the exponent.

G_0 is predicted to vary with the site occupancy n_d, and hence also with $\tilde{\epsilon}_0$, ac-

[3] It is easier in practice to fit experimental data to an approximate analytical form than to exact numerical calculations, but the resulting fits provide a good match between the data and the numerical calculations as well.

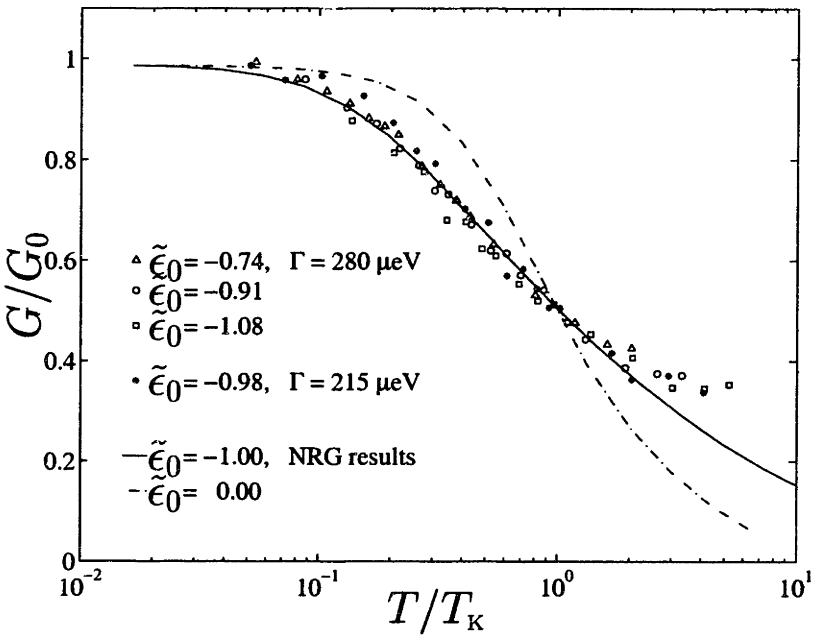

Figure 6-3: The normalized conductance $\tilde{G} \equiv G/G_0$ is a universal function of $\tilde{T} \equiv T/T_K$, independent of both $\tilde{\epsilon}_0 \equiv \epsilon/\Gamma$ and Γ, in the Kondo regime, but depends on $\tilde{\epsilon}_0$ in the mixed-valence regime. Scaled conductance data for $\tilde{\epsilon}_0 \approx -1$ are compared with NRG calculations [T. Costi et al.] for Kondo (solid line) and mixed-valence (dashed line) regimes. The stronger temperature dependence in the mixed-valence regime is qualitatively similar to the behavior for $\tilde{\epsilon}_0 = -0.48$ in Fig. 6-2(b).

cording to the Friedel sum rule

$$G_0(n_d) = G_{max} \sin^2\left(\frac{\pi}{2} n_d\right), \tag{6.3}$$

where G_{max} is the unitary limit of transmission: $2e^2/h$ if the two barriers are symmetric, less if they are asymmetric. For small $|\tilde{\epsilon}_0|$, $T_K \gg T_{base}$, so we can directly measure the value of G_0. Even when T_K is not $\gg T_{base}$, we can still extract the value of G_0 from our fit. In Figure 6-4(b), we compare the combined results of both these methods with $G_0(\tilde{\epsilon}_0)$ inferred from a non-crossing approximation (NCA) calculation [50] of $n_d(\tilde{\epsilon}_0)$ according to Equation 6.3. The agreement is excellent except outside the left peak, where experimentally the conductance does not go to zero even at zero temperature (see Fig. 6-1).

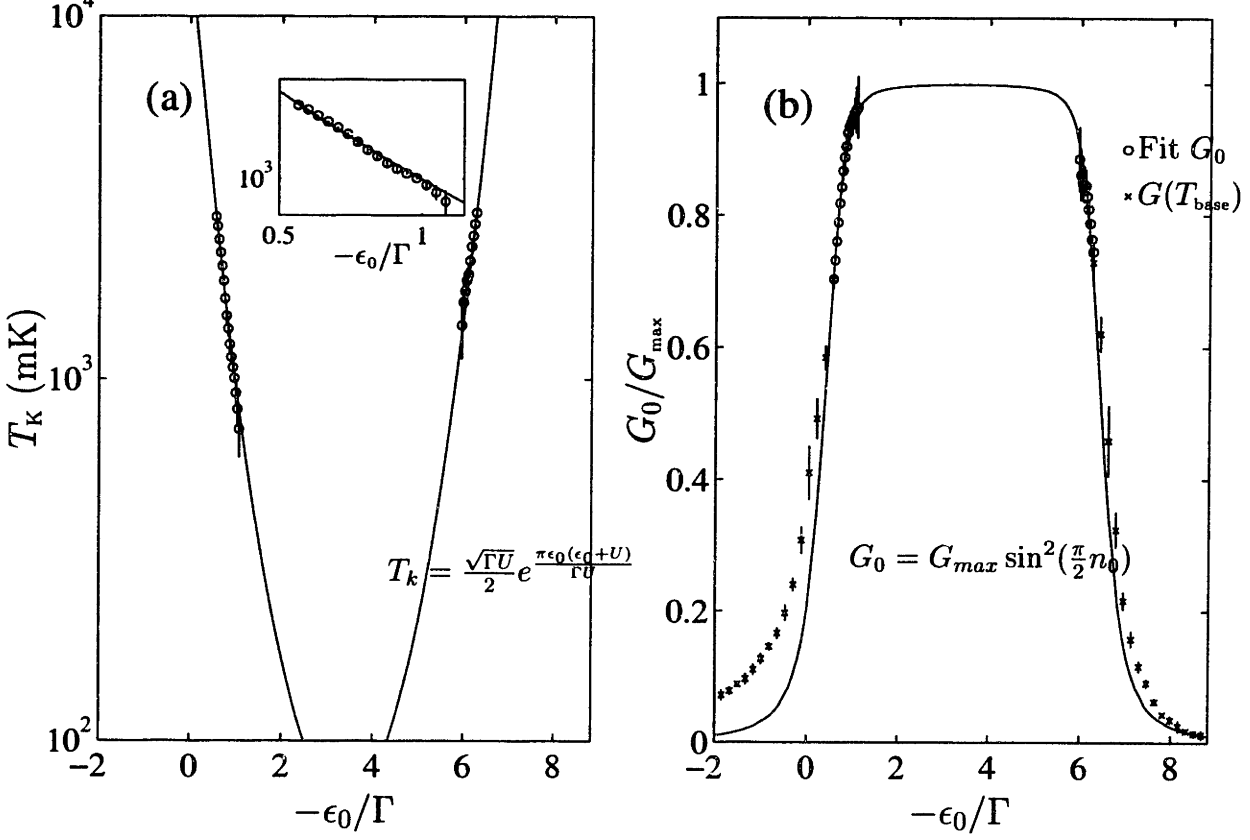

Figure 6-4: (a) Fit values of T_K for data like those in Fig. 6-2 for a range of values of ϵ_0. The dependence of T_K on ϵ_0 is well-described by a prediction from scaling theory (solid line). Inset: Expanded view of the left side of the figure, showing the quality of the fit. (b) Values of G_0 extracted from data like those in Fig. 6-2 at a range of ϵ_0. Solid line: $G_0(\epsilon_0)$ predicted by N. Wingreen and Y. Meir from a noncrossing approximation (NCA) calculation of the level occupancy n_0. $G_{\max} = 0.49e^2/h$ for the left peak, and $0.37e^2/h$ for the right peak.

We have demonstrated quantitative agreement between transport measurements on an SET and calculations for a spin-1/2 Anderson impurity. The SET allows us to both accurately measure and vary Γ and ϵ_0, and to observe their effect on T_K and G_0. We have also observed the cross-over between the Kondo and mixed-valence regimes.

Chapter 7

Other interesting results, and ideas for further work

I think that artificial atoms strongly coupled to their environments will continue to be an exciting area of study for years to come. In this concluding chapter, I hope to give a flavor of the possibilities, by presenting a few surprises and mysteries that have come up in the process of studying the Kondo effect, as well as some possible directions in which this research may grow in the future.

7.1 Higher-spin Kondo

As noted earlier in Chapter 2, a magnetic impurity with spin $S = 1/2$ is only the simplest possible basis for the Kondo effect. The physics is almost unchanged if multiple half-filled states combine to form a net spin on the impurity of 1 or more. Indeed, we should expect such an $S > 1/2$ state to occur if our simple state-filling model of Chapter 4 breaks down. In consequence, Kondo valleys would not simply alternate with non-Kondo valleys in linear conductance versus gate voltage. Instead, two or more Kondo valleys would appear in succession.

A tantalizing suggestion of this behavior appears in Figure 6-1, where in the valley to the left of the central Kondo valley the conductance $G \not\to 0$ even as $T \to 0$, as for a Kondo valley. But the other phenomenology of the valley doesn't match the Kondo effect at all:

1. $G \uparrow$ as $T \uparrow$, indicating thermally-activated breakdown of Coulomb blockade rather than breaking of a Kondo bond.

2. Differential conductance dI/dV_{LR} has a dip rather than a peak at zero bias.

So, while I can't yet explain the strange behavior, it's not spin-1 Kondo.[1] Further, the behavior in the middle valley *is* demonstrably spin-1/2 Kondo since the conductance rise $G(T)$ due to bond formation at low temperature matches $S = 1/2$ calculations [39] beautifully (see Figure 6-2), whereas for higher spin the conductance rise is expected to occur over a narrower range in temperature [63].

7.2 Excited states and Kondo

Existence of low-lying excited states is predicted both to strengthen the Kondo effect (increasing T_K by up to orders of magnitude [86]) and to create interesting structure in differential conductance at finite bias [86]. While in my experiments T_K is in reasonable agreement with calculations based on a single level (see Chapter 6), I do sometimes see satellites of the main Kondo peak in dI/dV_{LR} in remarkable agreement with multi-level predictions. In particular, for gate voltages between the two peaks of Figure 6-1, finite bias measurements show peaks at values of bias including $eV_{LR} = -180\,\mu$eV, $+200\ \mu$eV, and $+300\ \mu\text{eV} \approx \pm\Delta\varepsilon/2$. The positions are roughly as predicted [86], though the doubling on the right is not expected and could reveal interesting structure in the excitation spectrum. As seen in Figure 7-1 (and as predicted), these peaks do not move as a function of gate voltage within this valley. They also disappear outside the Kondo valley, as expected. More investigation will be needed to determine whether the observed structure is indeed caused by Kondo transport through excited states.

On a handwaving level, the satellite peaks have the same origin as the peaks at finite bias in high magnetic field (Section 5.4) — see Figures 5-5, 5-6. In the high magnetic field case, at finite bias a "sloshing" transition can occur from a state with (for example) a spin down electron in the left lead and a spin up electron on the artificial atom to one with a spin down electron on the artificial atom and a spin up electron on the right lead, so long as the bias is chosen to compensate the Zeeman splitting on the artificial atom, making the initial and final states degenerate. The same situation holds true here, except that the energetic splitting on the artificial atom arises not from Zeeman splitting of spin states but rather from the energy difference $\Delta\varepsilon$ between two quantized spatial states.[2]

[1] The behavior in the left-hand valley might possibly be explained by a combination of Kondo physics and interference with another conduction process. The existence of such interference effects in these devices is documented in section 7.3.

[2] This analogy explains the presence in the density of states of satellites of the Kondo peak at

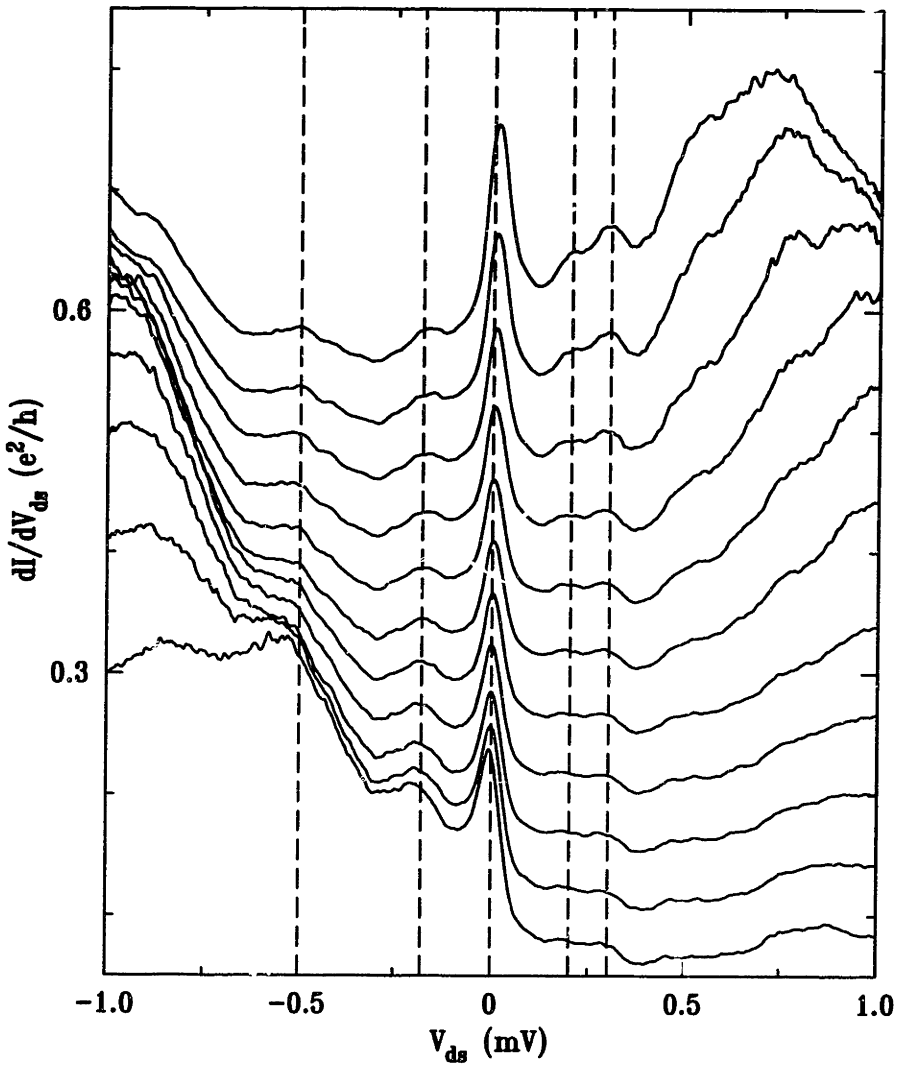

Figure 7-1: Differential conductance as a function of bias at a range of gate voltages spanning the central Kondo valley of Figure 6-1, from slightly to the left of the low point to near the top of the righthand peak. Except for the first (lowest) curve, the curves are offset vertically in steps of 0.05 e^2/h for clarity. Several features remain at the same bias over the whole gate-voltage range, and those at finite bias may be considered satellites of the Kondo resonance at zero bias. Some of the more prominent features of this type are marked with vertical, dashed guides for the eye (at -500 μV, -180 μV, +200 μV, and +300 μV). Such stationary features are absent for gate voltages outside the Kondo valley. More typical peak motion is exemplified by the broad peak on the right, which moves capacitively to lower bias as the Coulomb blockade peak is approached.

7.3 Fano lineshapes and interference

When coupling to the reservoirs is tuned to be even stronger than that used to observe the Kondo effect, Coulomb blockade peaks evolve into interesting interference patterns (see Figure 7-2). A background conductance emerges, with which resonant features (the former Coulomb blockade peaks) appear to interfere coherently, often varying from destructive to constructive interference across a single resonance. This behavior may be understandable as the interplay of both resonant and non-resonant transmission through the SET, possibly with two subbands playing a role in at least one point contact.[3] Similar resonances, explained by Ugo Fano in 1961 [87], have long been observed in atomic and nuclear physics, as well as in optical studies of semiconductors. In contrast, they were first seen only recently in electronic transport [52] despite numerous theoretical predictions [88, 89]. The phenomenology and possible origins of the Fano resonances seen in these SETs will be described in detail in a forthcoming paper [90].

7.4 Future prospects

Even with a single artificial atom, there is still more to study beyond the basic Kondo effect. For example, the mixed-valence regime of the Anderson model, touched on in Chapter 6, is less well-understood both experimentally and theoretically than the Kondo regime. The excellent quantitative match between artificial atom experiments and theory in the Kondo regime establishes a basis for trusting that measurements in the mixed-valence regime describe the behavior of an idealized Anderson impurity even if they do not fully match theoretical expectations.

With more complex nanofabricated systems, it will be especially important to ask how experiments on them should be interpreted. I like the idea of building a structure to manifest a particular Hamiltonian whose behavior is expected to be interesting, with the advantage that most parameters of said Hamiltonian are measureable and even tunable *in situ*. This philosophy is manifested in this thesis. You could even

energies $\pm\Delta\varepsilon$ relative to the Fermi level. One would then expect peaks in differential conductance at $eV_{\rm LR} = \pm\Delta\varepsilon$. Their actual position shifts in both calculation [86] and experiment to roughly half this bias, because the peaks in density of states change with bias, becoming rapidly weaker with increasing bias. So $dI/dV_{\rm LR}$ reaches its maximum well before $eV_{\rm LR}$ reaches $\pm\Delta\varepsilon$. A weaker feature is observed at $eV_{\rm LR} = -500\mu{\rm eV} \approx -\Delta\varepsilon$.

[3] These would be 1D subbands formed in the point contact itself rather than 2D subbands, of which only one is filled in my heterostructures (see Appendix B).

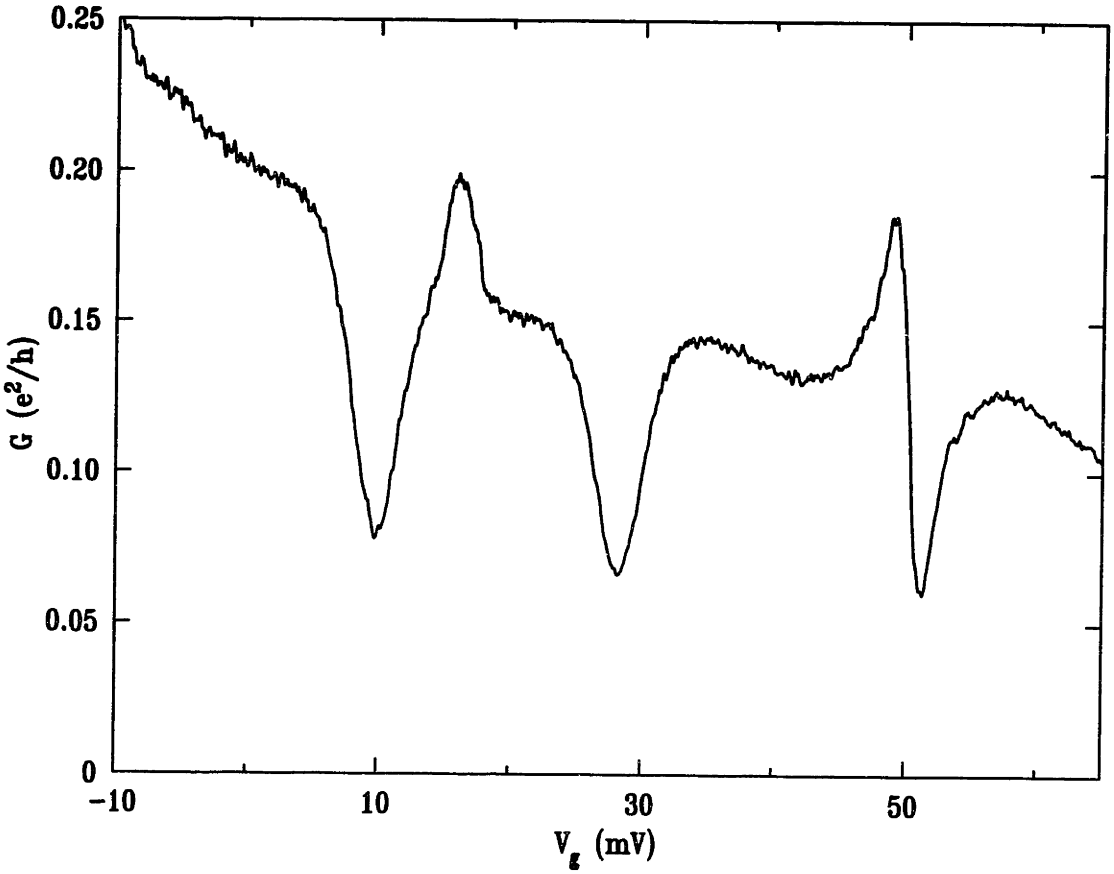

Figure 7-2: A smooth background conductance slowly varies from 0.1 to 0.2 e^2/h as a function of gate voltage. On top of this background are overlaid three striking resonances, with their minima at approximately 10, 28, and 51 mV, respectively. In the absence of background conductance, these resonances would appear as ordinary Coulomb blockade peaks. However, instead of simply adding incoherently to the non-resonant background, the resonances add as complex amplitudes, interfering both constructively and destructively as the phase of transmission changes across a single resonance. The shapes of all three resonances belong to the family of Fano lineshapes [87] $F(\epsilon) = (\epsilon+q)^2/(\epsilon^2+q)$, where ϵ is a normalized energy distance from resonance and q is the ratio of resonant to nonresonant transmission amplitudes. The failure of the resonances to dip all the way to zero may be due to the presence of two non-resonant paths, or to partly incoherent transmission through the SET [91]. The origin of the background conductance itself is not yet certain, but its coherent interference with the resonant transmission indicates that it too must pass through the SET.

consider this approach as building an analog computer to exhibit the properties of a particular Hamiltonian. But for such a program to be really interesting, it must be feasible to be surprised by the results yet still take them seriously. In turn, this means we must be able to evaluate whether the surprises come because we didn't build the Hamiltonian we expected or because the desired Hamiltonian itself shows unexpected behavior. I won't try to address this issue in individual scenarios below, but it is important to consider in planning any experiment which treats nanostructures as model systems.[4]

Since the Kondo impurity is such a beautifully simple system, there are many interesting extensions to study using artificial nanostructures. For example, consider two artificial atoms coupled by tunneling to form an "artificial molecule" [92, 93] (but so far isolated from the external world). If each artificial atom in the molecule has a singly-occupied state, and the energies of these two states are tuned to be the same, the ground state of the system will be a singlet or bonding state built from the spatial ground states in the two artificial atoms [94]. If we choose the limit opposite to this one (i.e. no coupling between atoms, strong coupling to reservoirs) we should simply get two non-interacting Kondo impurities of the type discussed in this thesis. This ground state also involves singlets, but here they are singlets between localized and delocalized electrons. Finally, if the intramolecular coupling and that to the external reservoir are of comparable strength, we have a conflict between the two distinct choices for ground state mentioned above. As the relative coupling strengths are tuned, a quantum phase transition between these two states should occur [95]. It may even be observable in transport measurements in the appropriate geometry [96]: unlike the Kondo state, the simple molecular singlet state has no density-of-states resonance at the Fermi level, so it should show much smaller linear conductance at low temperature.

This system could be made even more exciting by coupling the two artificial atoms only indirectly, through their mutual coupling to an electron reservoir. This type of indirect coupling between two magnetic impurities through a Fermi sea may be ferromagnetic or antiferromagnetic depending on the spacing between the impurities, and is known as RKKY coupling after its theoretical discoverers (Ruderman, Kit-

[4] A complementary philosophy is to build something interesting in its own right and see how it behaves. This has been the way most artificial atom experiments were conceived of until recently, and indeed there have been many interesting surprises which could be modelled after the fact. I feel that this philosophy becomes less tenable when the complexity is increased beyond that of a single artificial atom. There are too many parameters and uncontrolled influences if one doesn't have a sense of what one's looking for at the start.

tel, Kasuya and Yosida) [97]. When magnetic impurities are not so dilute as in an ideal Kondo system, they cannot be considered to act independently. The competition between Kondo and RKKY ground states in this situation is an active area of theoretical enquiry today, an area in which experiments on simple, tunable artificial systems might shed much light.

A final enticing prospect for fabrication and study would be the extension of the above ideas to the many-impurity system known as a Kondo lattice, which may be a good model for heavy-fermion compounds found in nature.

7.5 Closing

The field of artificially-fabricated nanostructures continues to get more exciting by the year. From satisfying confirmations of the theory of the Kondo effect to surprises like Fano resonances, my work on artificial atoms strongly coupled to their environment has just begun to show their potential as model systems. Other researchers around the world have also recognized that artificial atoms are excellent tools for exploring the coupling of a simple electronic system to its environment, whether that environment be an electron sea [14, 15, 18, 55, 79, 83, 84, 98, 99], a phonon bath [17], or a coherent source of photons [16, 94, 100]. I hope to continue exploring these fascinating frontiers in the years to come.

Appendix A

Fabrication

The basic techniques I used to fabricate my SETs were invented more than a decade ago, and were well-established by the time I set out on my project [101]. They are admirably described in Ethan Foxman's thesis [19], and I will present the detailed steps of one of my typical fabrications below, so I shall only summarize here. I started with a GaAs/AlGaAs heterostructure hosting a 2DEG at an interface beneath its surface. Then I used conventional photolithography coupled with wet etching to deplete the 2DEG except in a desired active area or mesa; more photolithography followed by metal deposition, liftoff, and annealing served to make ohmic contacts from the surface to the buried 2DEG, allowing transport measurements. Next, I defined the fine gate structures of the SET (see Figures 3-1, 3-5) by electron-beam (e-beam) lithography and metal deposition. Finally, I deposited thick metal pads to ease wire bonding to both gates and ohmic contacts.

However, this is where the similarity to previous work ended. As explained in Chapter 3, observation of the Kondo effect in an SET at accessible temperatures requires that the SET have a very small central artificial atom. During my year at the Weizmann Institute, I set out to fabricate such SETs, in the face of two main challenges. First, and most obvious, making an AA dramatically smaller than the half-micron size typical of prior work required very fine lithographic patterning. I aimed for 20 nm lines and spaces, beyond what had been previously achieved at Weizmann, and near the state of the art. Diana Mahalu, e-beam lithographer extraordinaire, took up this challenge and met it brilliantly. Less obvious, but even more challenging, I needed my starting heterostructure to be very shallow, with its electron gas only 20 nm from the surface, as compared to 50 to 100 nm in typical extant structures. The potential produced by even a very fine wire blurs as one recedes from the wire, so the potential landscape felt by a 2DEG has no gate-induced

features with length scale smaller than the depth of the 2DEG. When making a small SET, it's also important to ensure that the underlying 2DEG's density is high enough to leave a few electrons in the AA. Fortunately, this property emerges naturally in shallow heterostructures, as I will explain below.

Only a few labs in the world had fabricated heterostructures approaching the shallowness I needed, and none had successfully used them to create interesting nanostructures, so I realized that the heterostructure would be my first major hurdle. Udi Meirav advised me to aggressively aim for below 20 nm depth, and so in collaboration with Hadas Shtrikman I designed a series of heterostructures supposed to host 2DEGs from 16–20 nm below the surface. Remarkably, most of them worked: they contained 2DEGs with high density (about 10^{12} cm^{-2}, reasonable mobility (about 10^5 cm^{2}V^{-1}s^{-1}), no parallel conduction and, remarkably, only a single filled subband. For more details, see Appendix B. Unlike with many heterostructures, making good ohmic contacts to these 2DEGs was trivial due to the extremely thin AlGaAs or AlAs barrier between surface and 2DEG. But here the problems started, since gate electrodes too showed (now undesirable) conduction to the 2DEG. The threshold for leakage, 200–300 mV of either polarity, was too low to allow full depletion of the electrons below the gates, hence preventing formation of an AA in the 2DEG layer.

These initial experiments had been conducted with large-area $(100\mu m)^2$ gates, and I hoped the leakage was due to a known class of sparse growth defects (elliptical defects), so that the much slimmer gates of an SET would not leak. So I set out to design and fabricate the SET gate structures. With input from Udi Meirav and Diana Mahalu, I designed two sizes of SETs with AAs lithographically 80 nm and 150 nm across, respectively. This should be compared with the half-micron structures typical at the time. After several exposure tests and iterations, we got both size structures working, each with a range of linewidths from 20 to 30 nm. Unfortunately, when I set out to make transport measurements of the SETs I had made, my earlier hopes proved unfounded. Even a narrow line gate laid across the 2DEG mesa, 0.02–0.1 by $10\mu m$, could not cut off the flow of electrons beneath it before leaking.

After dismissing the possibility of laying down an extra insulating layer before depositing the gates, since I would thereby throw away the hard-won advantage of the shallow heterostructures, I recalled one of the central issues that arises in designing 2DEG heterostructures, especially shallow ones. At a free GaAs surface, there are many electron states corresponding to unsatisfied bonds. Since the energies of these states fall in the middle of the gap between valence and conduction bands, the Fermi energy is pinned in the gap, typically 0.7 V below the conduction band edge (see

Figure B-2). This means that no electrons can accumulate in the conduction band at the top surface. Accumulating electrons below the surface is achieved by placing donor impurities between the surface and the desired accumulation region, bending the conduction band below the Fermi level (see Figures B-1,B-2). Even so, if the surface is made close enough to the 2DEG, the proximity of the surface states will be enough to partially or fully deplete the 2DEG despite the presence of the donors. So I decided to try a shallow etch under the gates (before gate deposition) to bring the surface closer to the 2DEG in these regions.

I wanted to keep the etch both shallow and uniform, to deplete the 2DEG everywhere beneath the gates but not to reach deep enough to damage the surrounding 2DEG. Simulations showed that my aims could be achieved simply by removing the 4 or 5 nm GaAs cap layer on the heterostructures. Wet etches have strong advantages over dry etches in this context, including strong selectivity between different materials (e.g. GaAs and AlGaAs) and minimal damage to the underlying heterostructure. However, after experimenting with wet, acid-based etches, I found that they were slow, unpredictable, and nonuniform in their rate. Possible problems were the extremely small lateral dimensions of the features to be etched (20–40 nm at their narrowest) and unintentional traces of PMMA e-beam resist left on the surface, which might be resistant to the acid mixture. Instead I adopted a dry etching method based on a reactive ion etch. I began with an oxygen plasma to clean any traces of PMMA from the nominally bare parts of the GaAs surface, then switched to $SiCl_4$ in an *Ar* buffer gas. Under appropriate conditions, $SiCl_4$ etches GaAs more than ten times as rapidly as the underlying $Al_{.3}Ga_{.7}As$, so I could get it to etch off the cap uniformly without going significantly deeper anywhere. After the etch, I moved the sample quickly through air to the evacuated metal evaporator to limit further depletion of 2DEG due to oxidation. After depositing gate metal, and performing liftoff to remove metal from everywhere except on top of the etched regions, I coated the samples in either photoresist or polyimide to prevent further oxidation during storage.

Unfortunately, the best time and power parameters for the dry etching varied seemingly randomly between sessions, despite Grisha Bunin's knowledgeable assistance, but a few parts of the protocol remained consistent. RF-excited plasmas produced more directional etching and hence finer features than microwave-excited (cyclotron resonance) plasmas, and so I used them even though they probably cause more damage to the sample. The initial oxygen plasma cleaning lasted 30–60 seconds: shorter, and the subsequent etch was not uniform; longer, and the e-beam written features in the PMMA were seriously degraded. For similar reasons, the $SiCl_4$ etch

lasted 20–60 seconds. In any case, 20 nm gate lines became 30 nm after etching since both the cleaning step and the $SiCl_4$ etch slowly attack the PMMA.

After etching, with or without subsequent deposition of gate metal, the 2DEG below the gates was depleted to between 0 and 10% of its original density (at low temperature), allowing definition of an artificial atom with grounded gates or with only slight negative bias. The threshold for leakage moved to higher voltages after etching, but even so I have made most of my measurements with gates biased around -100 mV, reaching -300 mV only in a few cases (see Appendix C).

WIS - Sub 1000 Å Quantum Dot on 150- 200 Å Deep 2DEG

Process Follower

_____ Substrate Name _____ Sample Number (starting March 1996)
_____ File, datatypes for ebeam features
_____ What is written? (Point contacts? Dots?)

Mesa Isolation

_____ Sample Clean: ACE, IPA/METH
_____ Coat resist: S1805, 4 krpm, 40 sec
_____ Bake: 80° C hot plate, 5 min
_____ Exposure: 9 sec (I = 10 mW/cm^2)
_____ Develop: 1:1 MF312 : DI H_2O, ~~45 sec?~~ 25 sec (20s is better)
_____ Rinse: DI H_2O
_____ N_2 dry
_____ Mesa etch: 1:1:50 H_3PO_4 : H_2O_2 : DI H_2O, 20 sec (300 Å) (~800 Å /min)
_____ Rinse: DI H_2O
_____ Sample Clean: ACE, IPA/METH

Ohmic Contacts (image reversal process)

_____ Sample Clean: ACE, IPA/METH
_____ Coat resist: AZ5214E, 5 krpm, 40 sec
_____ Bake: 100° C hot plate, 1:15 min (more than 45 sec to harden)
_____ Exposure: 9 sec (I = 10 mW/cm^2)
_____ Post-bake: 120° C vacuum hot plate, 45 sec
_____ Flood Exposure (no glass): 2.1 min (I = 10 mW/cm2)
_____ Develop: AZ 524 MIF, 25 sec
_____ Rinse: DI H_2O
_____ N_2 dry
_____ Evaporate (1-2 Å/sec)
  _____ 50 Å Ni
  _____ 300 Å Ge
  _____ 600 Å Au
  _____ 150 Å Ni
  _____ 1000 Å Au
_____ Lift off in ACE, using heat then ultrasonic if necessary
_____ Sample Clean: ACE, IPA/METH

_____ Anneal: Small annealer 420° C, 30 sec; then turn sample 180 degrees, do another 30 sec (heating is nonuniform)

Figure A-1: This is an example of a "follower" or checklist I used during processing of my SETs. During the last batches, as explained in the main text, I ad led a dry etch to the fine gate pattern definition procedure, after development of the PMMA and immediately before metal evaporation.

Schottky Contact (Submicron Gates)

_____ Sample Clean: ACE, IPA/METH
_____ Coat resist: ?? K PMMA ? %, 4 krpm, 60 sec
_____ Bake: 180° C, 60 min
_____ Coat resist: ?? K PMMA ? %, 4 krpm, 60 sec
(spin immediately after dripping on PMMA)
_____ Bake: 180° C, 60 min
_____ Evaporate
_____ 200 Å PdAu
(400 Å according to monitor because of larger distance to sample)
_____ Lift-off in ACE, using heat then ultrasonic if necessary
_____ Sample Clean: ACE, IPA/METH

Gate Pads (image reversal process)

_____ Sample Clean: ACE, IPA/METH
_____ Coat resist: AZ5214E, 5 krpm, 40 sec
_____ Bake: 100° C hot plate, 1:15 min (more than 45 sec to harden)
_____ Exposure: 9 sec (I = 10 mW/cm^2)
_____ Post-bake: 120° C vacuum hot plate, 45 sec
_____ Flood Exposure (no glass): 2.1 min (I = 10 mW/cm2)
_____ Develop: AZ 524 MIF, 35 sec (longer than ohmics -- no fear of etching)
_____ Rinse: DI H_2O
_____ N_2 dry
_____ Evaporate (1-2 Å/sec)
_____ 200 Å Ti
_____ 1000 Å Au
_____ Lift off in ACE, using heat then ultrasonic if necessary
_____ Sample Clean: ACE, IPA/METH

Variants

_____ Use Nb in contacts to avoid shorting to conducting substrate

Appendix B

Details of heterostructure design, growth and characterization

B.1 Introduction

We have grown and characterized four extremely shallow two-dimensional electron gases (2DEGs), ranging from 16 to 20 nm below the surface of GaAs/AlGaAs heterostructures. These are among the shallowest 2DEGs so far achieved in this material system. Mobilities measured at 4.2 K range from 70,000 to 130,000 cm^2/ V s, and densities range from 0.7 to 1.1 x10^{12}/cm^2. These 2DEGs have proven essential for making the extremely small electronic nanostructures described in the main body of this thesis, whose minimum lateral dimension is generally limited by the depth of the 2DEG.

B.2 Shallow 2DEGs

Making small or precisely-shaped features in a 2-dimensional electron gas (2DEG) is important for advancing both technology and basic science. For example, such features are needed for making fast amplifiers or dense computer memories, and for studying the fundamental physics of low-dimensional electronic systems such as dots, wires, or 2D billiards with controlled shapes [102, 103]. Since 2DEGs cannot be patterned on length scales much smaller than their depth below the heterostructure surface, very shallow 2DEGs should find many uses. We have grown GaAs/AlGaAs heterostructures containing 2DEGs as close as 16 nm to their surface. Quantum dots of 80 nm and 150 nm diameter patterned in these 2DEGs are amongst the smallest

fabricated to date [18] (see [102] for related work). This small size has enabled us to observe the Kondo effect in a quantum dot, a phenomenon predicted and widely sought for the past decade [64, 65].

The two most common methods of patterning 2DEGs in GaAs-type heterostructures are shallow etching [104] and depositing metal electrodes which are then negatively biased [105]. Electrons are driven away from beneath the etched regions or the electrodes, respectively. But the depletion regions extend beyond the region directly under the etched surface or electrodes [60, 104, 105]. The width of these depletion regions depends on geometry and electron density but roughly scales with the depth of the 2DEG [60]. This is why 2DEGs cannot be patterned on length scales much smaller than their depth. In addition, GaAs/AlGaAs 2DEGs with typical densities ($1\text{–}2 \times 10^{11}/\text{cm}^2$) could not be used to make conducting sub-100 nm nanostructures, since few or no electrons would remain in the patterned region.

The Si/SiO_2 material system features a good-quality oxide insulator at thicknesses down to a few nanometers, allowing production of very shallow 2DEGs. However, even excellent Si/SiO_2 2DEGs have low temperature mobilities of only 30,000 $\text{cm}^2/\text{V s}$ [106, 107], well below what is achievable in GaAs/AlGaAs heterostructures. Previous work has confirmed that extremely shallow 2DEGs can be achieved in GaAs/AlGaAs heterostructures without completely sacrificing the characteristic high mobility of that material system [108, 109, 110, 111, 112]. However, the shallowest 2DEGs have proved of limited use for making gated nanostructures because of leakage currents between the electrodes on the surface and the 2DEG beneath them [109]. The present study was aimed at matching the shallowest depth previously achieved, then exploring how to fully deplete such shallow 2DEGs with surface gates.

B.3 Growth of Samples

The samples were grown in a solid source Riber 32 Molecular Beam Epitaxy (MBE) system, which provides samples with a low unintentional p-type background of about 1×10^{14} cm^{-3} in high purity GaAs, and between 1×10^{15} and 1×10^{16} cm^{-3} in AlGaAs. The samples were grown on accurately oriented (100), undoped, semi-insulating GaAs. The buffer layer, grown at 635 °C as measured by infrared pyrometer, consisted of 250 nm of GaAs, 300 nm of AlAs/GaAs superlattice, and 600 nm of GaAs. After growth of an AlGaAs spacer of 5 nm the substrate temperature was lowered to 500 °C, to ensure minimal Si diffusion and segregation during the growth of the rest of the structure. The growth rates for GaAs and AlAs were 10 and 6.6 nm/s, respectively.

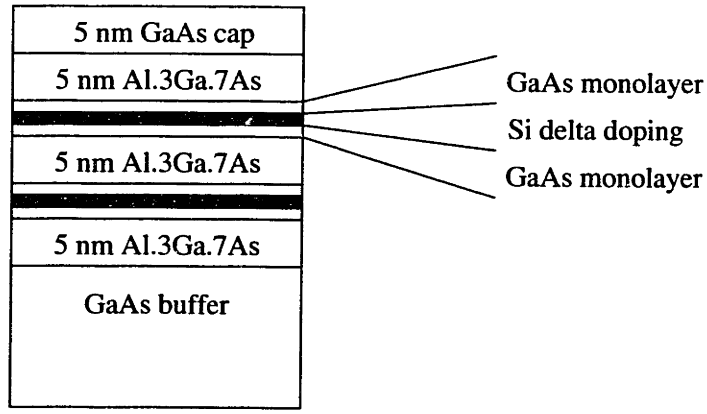

Figure B-1: Layer sequence of heterostructure cbe516–the slightly different parameters for the other heterostructures are given in Table B.1.

These rates were measured by the periodicity of the RHEED intensity oscillations, and verified in other samples by photoluminescence of thin quantum wells. The As to group III flux ratio was about 10. The entire structure is schematically presented in Figure B-1. The total areal doping density of $1x10^{13}$ cm^{-2} was separated into two or three layers of Si δ-doping. In order to maximize the number of activated donors for a given areal doping density, each doping layer contained no more than $5x10^{12}$ dopants cm^{-2}. This relatively high areal doping density was required in order to bend the conduction band down to the Fermi level and produce a 2DEG so close to the surface. Each doping layer was embedded between two monolayers of GaAs in order to enhance the Si activation and to minimize impurity incorporation during the deposition of Si. A 5 nm GaAs cap layer was grown for protection on top of the structure. Figure B-2 shows the band diagram derived from a solution of Poisson's equation. Details of the individual growths are listed in Table B.1.

B.4 Characterization

We used cross-sectional scanning tunneling microscopy (XSTM) to measure layer thicknesses in our structures. For this purpose, we grew an additional GaAs-AlGaAs test structure under conditions almost identical to those of the earlier growths, including growth stops. However, several modifications were necessary to enable XSTM of this test structure. First, the substrate was n^+ doped rather than SI, and the entire structure was grown with uniform $2x10^{18}$ cm^{-3} n^+ doping instead of delta-doping. In addition, the thin layers were located well beneath the sample surface, and thick

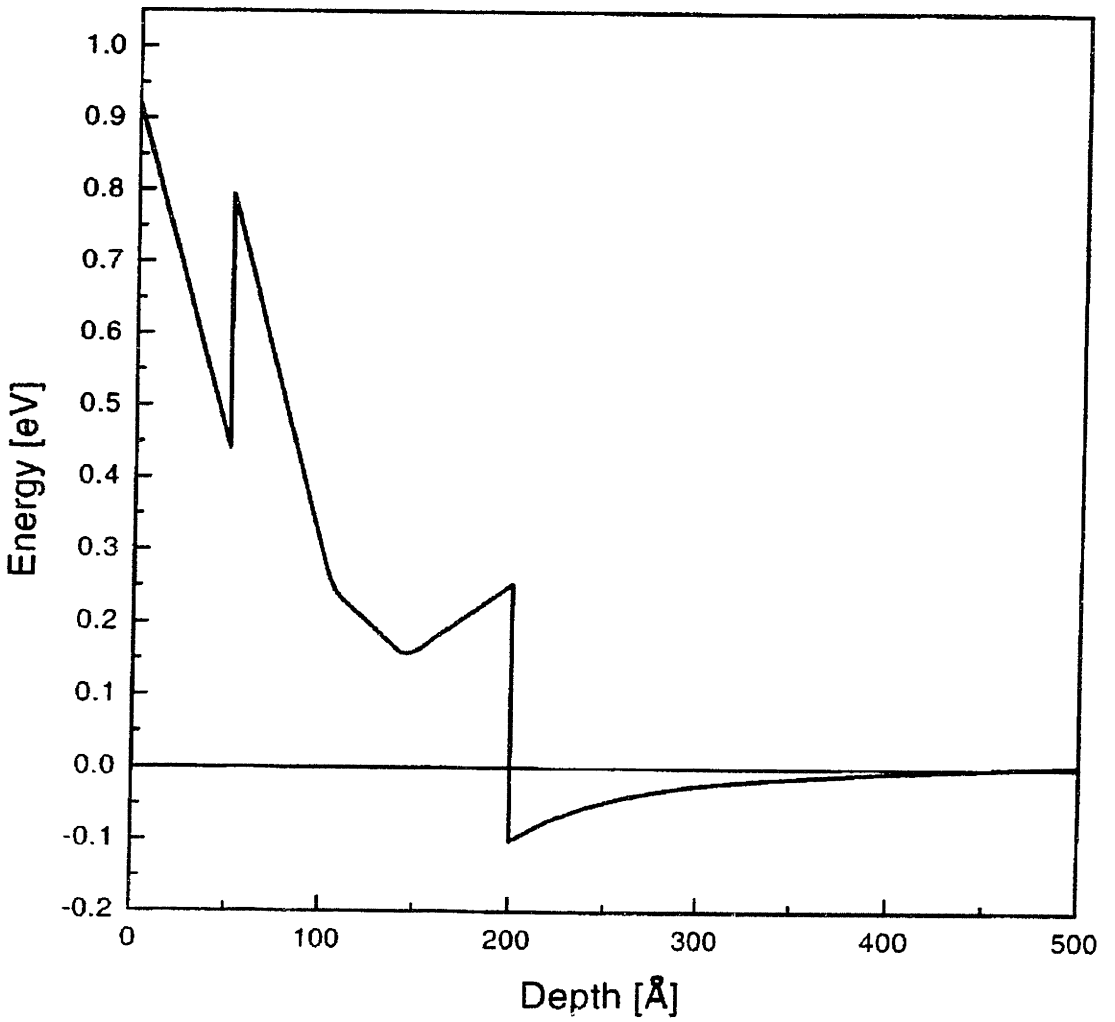

Figure B-2: Solution of the Poisson equation in the direction normal to the plane of the 2DEG in heterostructure cbe516, showing that the conduction band edge dips below the Fermi level to form a 2DEG only 20 nm below the heterostructure surface. Bending the conduction band so sharply requires doping densities of 10^{13} cm^{-3}, or even higher for our 15 nm deep 2DEGs. The predicted density of the electron gas is 1.15×10^{12} cm^{-2}, in good agreement with our measured value of 1.1×10^{12} cm^{-2}.

marker layers of AlGaAs and GaAs were grown to aid in locating the thin layers of interest. For XSTM studies, the wafer was cleaved in ultra-high-vacuum to expose a (110) surface, and the cleaved edge was examined *in-situ*, using constant current STM. The test structure consisted of the following: 40Å GaAs, 40Å AlGaAs, 2.8Å GaAs, 10ÅAlGaAs, 2.8Å GaAs, 10Å AlGaAs, 5.6Å GaAs, and 50Å AlAs, with a total thickness of 16 nm. These desired thicknesses were verified by our XSTM measurements, which were calibrated by the observed corrugations associated with (001) lattice planes.

Figures B-3 and B-4 show STM topographic images of the GaAs-AlGaAs test structure, displayed with the growth direction from right to left. In these empty-state images, the Al-containing compounds appear as depressions (dark regions) compared with the GaAs layers (brighter regions). The large-scale image in Fig. B-3, acquired at a sample bias voltage of +2.5V, shows one set of thin layers sandwiched between thick GaAs and AlGaAs marker layers. In addition, on the far left side of the image, a portion of another set of thin layers is observed. In Fig. B-4, we present a closeup view of the thin layers, acquired at a sample bias voltage of +2.5V. Fringes with a spacing of 5.66 Å, corresponding to the (001) lattice planes of AlAs, are observed in the darkest portion of the image. These fringes, along with GaAs fringes observed in other parts of the sample (not shown), provide an internal calibration of layer thicknesses, such that the total thickness of these thin layers is 16 ± 0.5 nm, as expected.

For transport measurements, we produced standard six-contact Hall bars from the four shallow 2DEG wafers, defining the mesa with a $300\mathring{A}$ wet etch. We made ohmic contacts with standard NiAuGeNiAu layers, annealed at 420 °C for 30-60 seconds. We then measured longitudinal and Hall resistivities ρ_{xx} and $\rho_{xy}(B)$ using a standard four-terminal lockin measurement with $0.1\mu A$ current at 10-30 Hz, to determine density and mobility for the 2DEG in each of the four heterostructures. The densities ranged from 0.62 to 1.1x10^{12} cm^{-2}, and mobilities ranged from 70,000 to 130,000 cm^2/V s at 4.2 K, without illumination. Table B.1 lists the exact density and mobility of each 2DEG. We also observed Shubnikov-deHaas oscillations in $\rho_{xx}(B)$, which give information on 2-dimensional carrier concentration (see Figure B-5). The high doping densities used to produce such shallow 2DEGs prompted us to worry that charges in the dopant layers might be mobile even at low temperatures. This concern proved unfounded, as documented below. For each 2DEG, a Shubnikov-deHaas measurement showed only one period in B^{-1}, suggesting that only one subband of the 2DEG potential well was occupied. Further, the density determined from the period of the

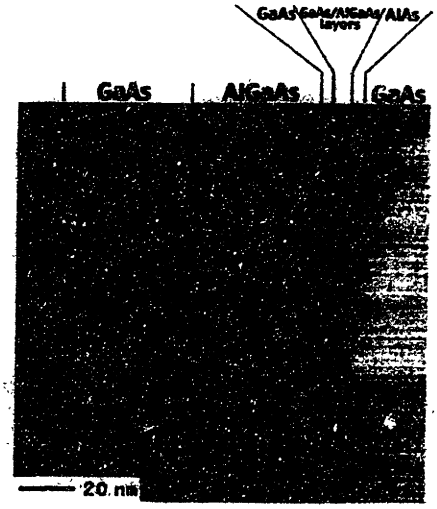

Figure B-3: XSTM image of a GaAs-AlGaAs test structure grown under the same conditions as cbe528, except that these thin layers were uniformly n^+ doped rather than delta-doped and were buried more than 1 μm beneath the heterostructure surface. The 16 nm layer sequence is sandwiched between thick GaAs and AlGaAs marker layers.

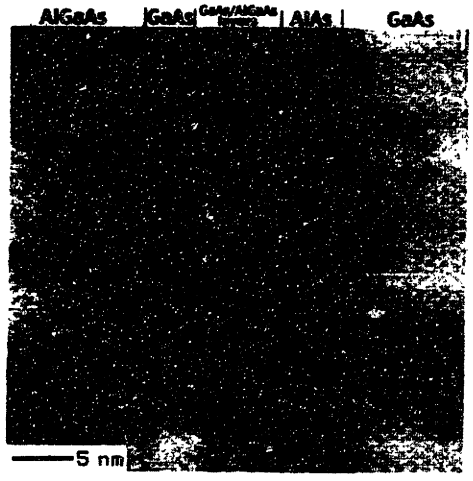

Figure B-4: A closeup view of the thin layers from Figure B-3, showing fringes associated with the (001) lattice planes of AlAs. These fringes provide an internal calibration of layer thicknesses, such that the total thickness of the thin layers is 16 ± 0.5 nm, as expected.

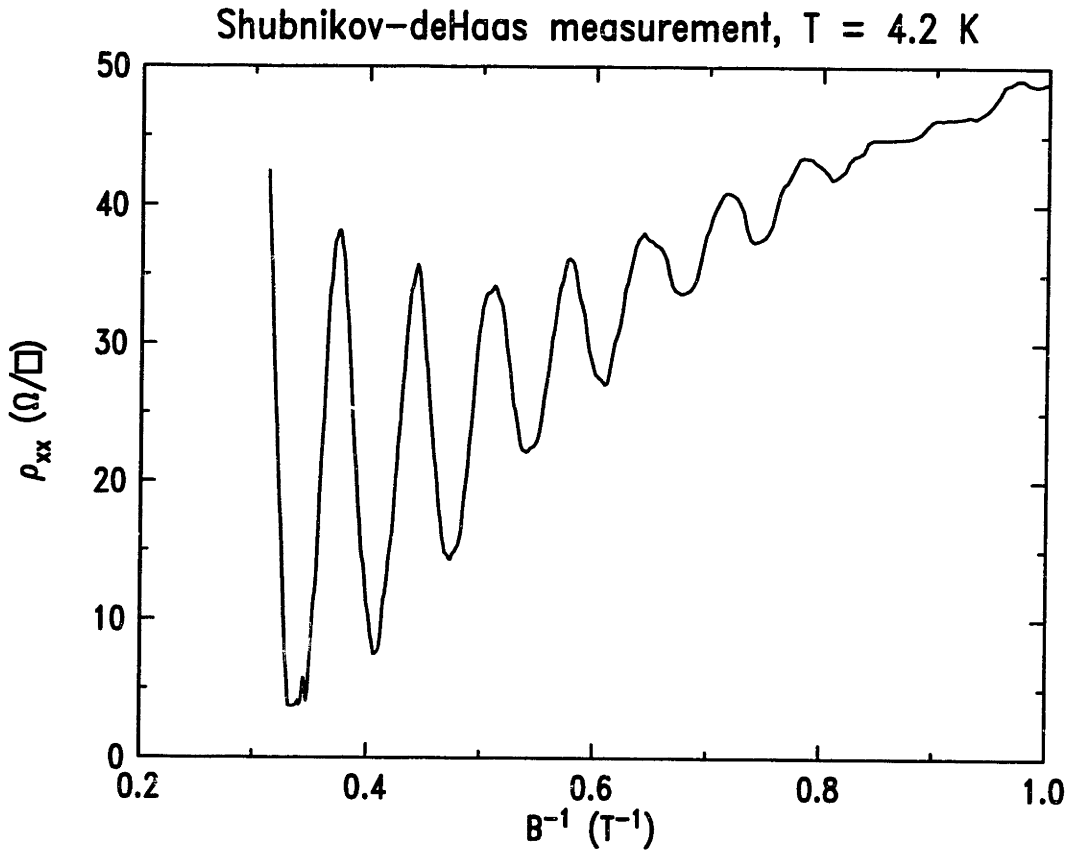

Figure B-5: Shubnikov-deHaas measurement on cbe527. The period of oscillations in ρ_{xx} vs. B^{-1} is 0.066 T^{-1}, corresponding to an electron density of 7.3 x 10^{11} cm^{-2}. Only a single subband is occupied, as evidenced by the absence of a second periodicity in the oscillations. Similar singly-periodic oscillations are seen for all four heterostructures in this study.

oscillations was always identical to that determined from $\rho_{xy}(B)$ Hall measurements, and $\rho_{xx}(B)$ vanished fully in the regime of the quantum Hall effect. Finally, at low B, the Hall voltage was linear in B. None of these transport measurements could detect a parallel layer with mobility much lower than that of the 2DEG, however any layer would screen the 2DEG from effects of an applied top-gate voltage until the extra layer had been depleted. By contrast, we observed a steady linear variation of 2DEG density with gate voltage, as discussed in more detail below. Together, these observations indicate that conduction was through a single 2-dimensional layer in these samples, probably through a single subband.

Next, we evaporated large-area TiAu gates on Hall bars from each growth and measured mobility and density as a function of gate voltage. Due to the thin barrier and heavy doping, the possibility of gate leakage was a major concern in evaluating

the usefulness of these 2DEGs. Leakage of the gate to the 2DEG was less than 1 nA up to gate biases of ± 0.2 to 0.3 V for the different growths. When the gate was grounded during cool-down, the 2DEG could only be partially depleted before the onset of leakage at the nA level. This situation, which has also occurred in previous studies of ultra-shallow 2DEGs [109], presents a major obstacle to patterning the 2DEGs.

However, when we cooled from room temperature with a gate voltage V_c applied, the 4.2 K n and μ vs. V_g curves shifted by V_c. Thus, if V_c were positive, grounding the gate at low temperature would already partly deplete the 2DEG. Interestingly, the leakage current as a function of gate voltage at 4.2 K was insensitive to V_c until the 2DEG was almost fully depleted. Because of this, V_c did not affect the range of V_g we could safely apply at 4.2 K, but did shift the range of accessible density.

Figure B-6 shows density and mobility $n, \mu(V_g)$ for two different positive values of V_c applied to the same gated cbe516 sample. Cooling with positive V_c enabled us to deplete the electron gas beneath the gates at 4.2 K without significant leakage. The two sets of data are identical except for a 50 mV offset due to the different positive cooling voltages. Further, both mobility and density vary linearly over a wide range of gate voltage. The linear variation of density with gate voltage is to be expected from a simple capacitor model of the system, with the gate as one plate and the 2DEG as the other. The measured capacitance is slightly below the value expected from our simple model, even if we include the finite spread of the electron wavefunction into the GaAs, which makes the 2DEG electrons on average 50Å below the interface. One possible source of the deviation could be a several Å low dielectric constant contaminant on the surface of the sample. Measurements of n versus V_g on cbe528 yielded a maximum capacitance of 5.4 mF/m^2, corresponding to a 2DEG 29Å below the GaAs/AlAs interface, close to the depth expected.

In addition to minimizing gate leakage it is important for nanostructures to eliminate motion of charge near the 2DEG. Studies like the present one, which use large regions of 2DEG, are sensitive only to the problem of leakage between gate and 2DEG. However, local motion of charges can drastically affect the transport of electrons through narrow 2DEG constrictions, and can reduce the stability of devices based on Coulomb blockade. The 2DEGs described here have been used successfully to make quantum dots as small as 80 nm, whose fabrication and behavior are described elsewhere in this thesis. To obviate the need to cool these quantum dots with nonzero voltage on their gates, we added a step to the dot fabrication producedure: immediately before evaporating metal for the gates, we etched off the GaAs cap layer

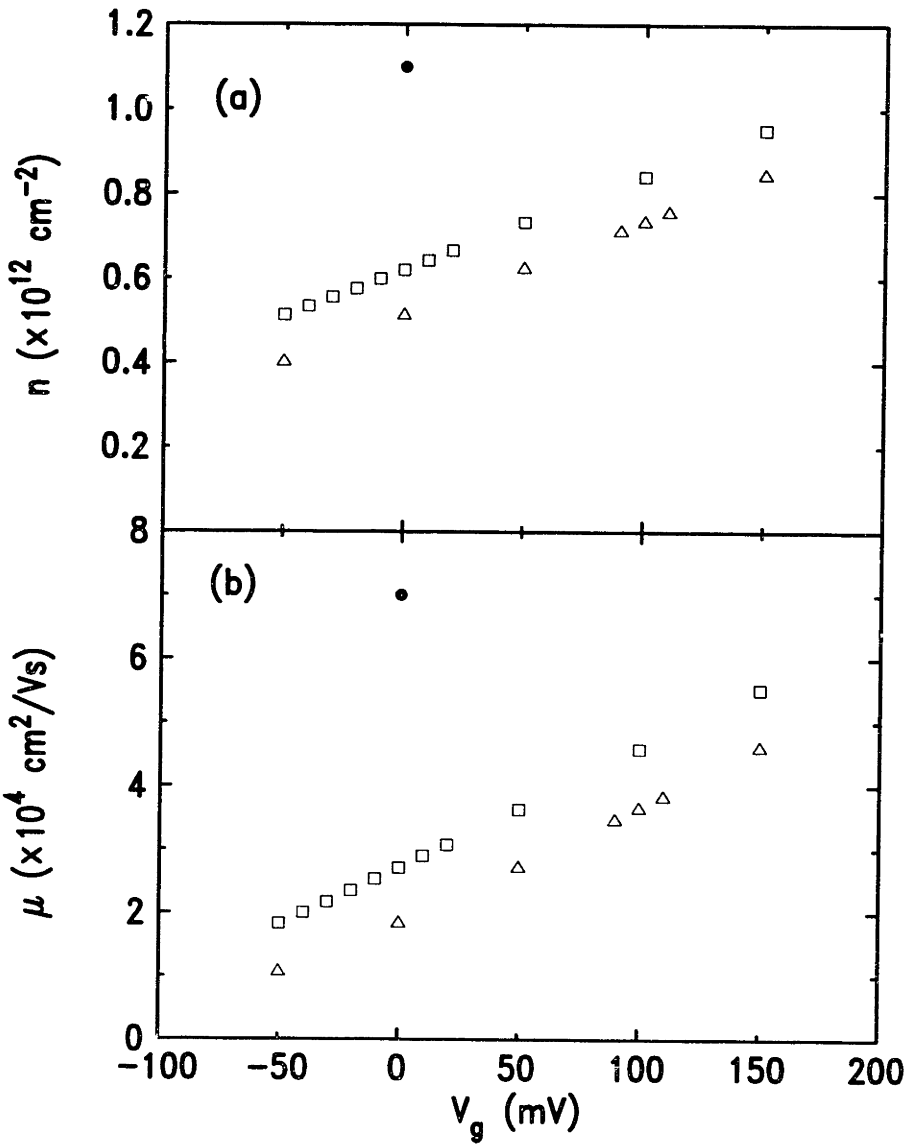

Figure B-6: (a) Density and (b) Mobility versus gate voltage at 4.2 K, for different cooling voltages. Changing the voltage applied to the gate during cooling from +200 mV (squares) to +250 mV (triangles) shifts the voltage required at low temperature to produce a given density and mobility by 50 mV. A measurement with zero cooling voltage is shown for reference (filled circle). A combination of cooling with V_c = +250 mV, and and applying V_g = -50 mV at 4.2 K depletes the 2DEG to 35% of its normal density, $1.1 \times 10^{12} cm^{-2}$. Up to -300 mV can be applied at 4.2 K without significant leakage, probably corresponding to full depletion. However, the mobility is so low by V_g=-100 mV that it is difficult to extract values for mobility and density.

in the same places where the gates were to be. This etch was sufficient to fully deplete the 2DEG beneath the gates, even when the gates were grounded. It also dramatically reduced the leakage from gate to 2DEG for a given gate voltage.

B.5 Conclusions

In conclusion, we have fabricated amongst the shallowest gateable GaAs 2DEGs achieved to date, while retaining relatively high mobilities, in the neighborhood of 10^5 cm^2/V s. The densities of these 2DEGs are high, even exceeding 10^{12} cm^{-2}, but electrons appear to occupy only the lowest 2D subband. These high densities should reduce depletion lengths within the 2DEG, lowering the size of the smallest regions of electron gas which can be lithographically defined by gates or etching while still retaining electrons.

Table B.1: Some properties of the heterostructures studied

Sample Name	Number of δ dopings	Total doping level (cm^{-2})	Cap thickness (nm)	Barrier 1 thickness (nm)	Barrier 2 thickness (nm)	Spacer thickness, material	Total depth of 2DEG (nm)	Carrier density (cm^{-2})	Mobility ($cm^2V^{-1}s^{-1}$)
CBE516	2	10^{13}	5	5	5	5, $Al_{.4}Ga_{.6}As$	20	$1.1\,10^{12}$	$0.7\,10^5$
CBE518	2	10^{13}	5	5	3	7, $Al_{.4}Ga_{.6}As$	20	$0.81\,10^{12}$	$1.0\,10^5$
CBE527	3	$1.5\,10^{13}$	5	5	1	4, $AlAs$	16	0.7310^{12}	$0.91\,10^5$
CBE528	3	$1.5\,10^{13}$	4	4	1	5, $AlAs$	15	$0.62\,10^{12}$	$1.3\,10^5$

Appendix C

Details of experimental methods

As with the fabrication, the measurement setup and techniques are largely as described in Ethan Foxman's thesis [19], and I commend you once again to that excellent document. Here, I will simply outline the basic measurement techniques before presenting a taxonomy of a problem which plagues most measurements on semiconductor SETs, not least mine: charge motion ("switching") near the artificial atom.

C.1 Basic Experimental Methods

In my experiments, I make two types of measurements. In the first, I apply a voltage of a few (2-8) μV between the two leads of the SET, called the source and drain in analogy to conventional transistors, and measure the current that flows through the droplet as a function of the voltage V_g on one of the SET's gates (the middle electrode on the left in Figure 3-5). For such small applied voltage ($< kT/e$), current varies linearly with voltage, and the zero-bias conductance can be measured. I use a 10 Hz ac excitation, and perform lock-in detection of the current using a commercial current amplifier (Keithley 417 or Ithaco 1211). This is effectively just like a dc measurement, except that the use of a lock-in (the PAR 124) helps with noise rejection and allows me to achieve a current resolution of a few fA/$\sqrt{\text{Hz}}$, approaching the rating of the current amps.

In the second class of measurements, I add a variable dc offset V_{LR} (up to several mV) to the ac excitation, and again use lock-in detection of current to obtain differential conductance dI/dV_{LR} versus V_{LR}. Here the lock-in technique is even more important, removing the need for a noisy numerical differentiation of the $I-V$ curve.

The dc gate and source-drain voltages are applied using a motley assortment

of home-made analog voltage sources (for precision, stability, and low noise) and commercial voltage sources made by HP and Yokogawa, for ease of computer control. The output of the commercial voltage sources is heavily divided and filtered with simple resistor and capacitor networks to attenuate noise before the relevant line reaches the dilution refrigerator. Leads also run through LC "pi" filters as they enter the shielded room surrounding the refrigerator and home-built electronics. No digital devices are run inside this room during experiments. At present, there is no careful filtering on the refrigerator itself, either as leads enter or at low temperature. Even unattenuated thermal noise from room-temperature resistors can heat up electrons in an artificial atom, so good filtering at low temperature is quite an advantage.[1] I am in the process of setting up a new fridge and measurement system, and I'm doing the filtering more carefully this time.

C.2 Switching

Single-electron transistors are among the world's best electrometers, turning on or off when a fraction of an electron's charge is added to a nearby gate. Unfortunately, not all the electrons in an SET's environment are on its gates, and some of these other electrons can move around. For example, if donor impurities are spaced sufficiently closely, an electron may hop from one impurity to its neighbor even at low temperature. When this happens near the SET, the central artificial atom feels the transition as a change in effective gate voltage, changing the energy required to add an electron to the AA and perhaps even changing its occupancy by one. I'm not going to speculate much further on the origin of these switching events[2], but empirically they occur more in devices fabricated from some heterostructures than in those fabricated from others, and sometimes individual devices are particularly good or bad. My devices are rather bad from this perspective. In addition, most researchers study SETs in the weakly-coupled regime, so that peaks in conductance vs. gate voltage are sharp, with broad valleys in which conductance is unmeasurably small. A switch in such a valley may often not be noticeable. In contrast, I usually study my devices in the strongly-coupled regime, so that conductance is strongly modulated with gate voltage, but is

[1] In typical dilution refrigerator measurements of artificial atoms, the apparent "electron temperature" is 50–100 mK even when thermometers attest that the lattice temperature is below 10 mK!

[2] The physical origin of switching in a similar context has been studied in detail by David Cobden [113], with the conclusion that the two-state systems arise from defects or impurities.

never constant over a broad range of voltage. Hence, a switch is always manifested as a sudden jump in conductance versus gate voltage. All in all, this has allowed me a wonderful opportunity to observe switching events, and I can now classify them into several categories. Though all the details below pertain to my devices, I suspect the mechanisms for switching are similar in other SETs. A possible way to avoid switching altogether, essential for applications of SETs in computing, would be to suspend the SET structure away from its substrate [114].

1. The most common switches in my devices occur every time I sweep gate voltage from, say 0 mV to -100 mV. Either always at the same voltage, or in some small range of voltage, I see a jump in the $G - V_g$ curve, and then a jump back on the return sweep (at the same voltage, at a different voltage, over some range of voltage). See, for example, the jump at -40 mV in Figure 4-2(a), which occurred at the same voltage for nearly two weeks. That the system returns to the same state over and over again strongly suggests that the moving charge has only two (or in some cases several) possible states. As gate voltage is applied, the potential landscape is tilted, until the electron tunnels or rolls from one state to the other. This situation may persist for hours, days or weeks. These switches often maintain their position in plunger gate voltage even when I change the settings on other gates, allowing me to capacitively adjust the position of interesting features to regions of plunger gate voltage away from the switch(es).

2. A $G - V_g$ curve may be stable for minutes to days, then switch to a different curve, shifted in V_g by up to one peak spacing and sometimes slightly modified in shape. The new curve is again stable, until it switches back. There may even be a non-trivial duty cycle (90% of the time in state A, 10% in state B). Though the timing of these switches is unpredictable, I interpret the physics the same as for type (1), with the caveat that the tunneling rate between states is lower by orders of magnitude, preventing a switch from occuring every sweep.

3. Some switches can go back and forth many times during a sweep, generally in a certain range of gate voltage. I surmise that they are again transitions of an electron between two spatial states, but with high rate and low energy difference between the states, so that the switch doesn't simply occur once and for all as the potential landscape is tilted each sweep. This surmise is supported by the fact that this type of switch appears to spread over a larger range of V_g with increasing temperature, as more energy is available to overcome energy separation between the two states. In addition, these switches tend to shift the $G - V_g$ curve by much less than a full peak spacing, suggesting that the two states are either close to each other (accounting for

the high switching rate and low energy difference over a range of gate voltage) or both far from the artificial atom (at least accounting for the low energy difference).

The broader the range of gate voltage sweep, the more certainty that switches will occur. I figure (see (4) below) that, given time, the charge environment of the AA settles down to a state that is stable over a certain range of gate voltages. Empirically, I find that a sweep of 100 mV (covering four peaks) is the practical maximum that avoids major, non-reproducible switches. In addition, all of the types of switches described above can be triggered not only by changing V_g but also by applying high source-drain voltage V_{LR}, even though "high" means $|V_{LR}|$ =1 or 2 mV as compared to $|\Delta V_g|$ =100 mV. Even in steady state, a gate voltage more negative than -200 mV, or a difference of more than 100 mV between adjacent gates (with its concomitant high electric field over the 30–40 nm gap) dramatically increases the incidence of switches.

4. So far I've been speaking of steady-state and small adjustments to the potential landscape necessitated by sweeping the plunger gate voltage to cover a few conductance peaks. Of course, when one first cools down an SET, there are much larger changes required to reach typical operating voltages of -100 mV on all gates. I prefer to do this in steps of 10 to 20 mV, letting the device relax each time into a steady state. This relaxation may involve motion of many nearby charges, and until they find their collective ground state they may keep moving. You might consider my gradual change of gate voltage as annealing the glassy charge state that forms the SET's environment rather than subjecting it to a sudden shock. Even using this method, it takes days for the charge motion to settle down enough that the state of the SET remains steady for hours at a time, and the settling is repeated each time I make a significant change in any gate voltage, so a month of measurements on a single sample is more a necessity than a luxury.

In conclusion, though the uncertainty and randomness are frustrating, this thesis is proof that with proper care and patience interesting measurements can be made even on switchy samples.

Bibliography

[1] P. Drude. *Ann. der Phys.*, 3:369, 1900.

[2] N.W. Ashcroft and N.D. Mermin. *Solid State Physics.* Saunders College Publishing, first edition, 1976.

[3] A. C. Hewson. *The Kondo problem to heavy fermions.* Cambridge Studies in Magnetism. Cambridge University Press, Cambridge, 1993.

[4] M. Sarachik, E. Corenzwit, and L.D. Longinotti. *Physical Review A*, 135:1041–, 1964.

[5] G. Grüner and A. Zawadowski. Magnetic impurities in non-magnetic metals. *Rep. Prog. Phys.*, 37:1497–1583, 1974.

[6] C. M. Varma. Mixed-valence compounds. *Rev. Mod. Phys.*, 48:219–238, 1976.

[7] P. Nozières. A "Fermi liquid" description of the Kondo problem at low temperatures. *J. Low Temp. Phys.*, 17:31–42, 1974.

[8] J. Kondo. In Henry Ehrenreich and David Turnbull, editors, *Solid State Physics*, volume 23, page 183. Academic Press, New York, 1969.

[9] J. Weis, R.J. Haug, K. v. Klitzing, and K. Ploog. Competing channels in single-electron tunneling through a quantum dot. *Physical Review Letters*, 71:4019–4022, 1993.

[10] O. Klein et al. Exchange effects in an artificial atom in high magnetic fields. *Physical Review Letters*, 74:785, 1995.

[11] O. Klein, D. Goldhaber-Gordon, et al. Magnetic-field dependence of the level spacing of a small electron droplet. *Physical Review B*, 53:R4221, 1996.

[12] S. Tarucha, D.G. Austing, T. Honda, R.J. van der Hage, and L.P. Kouwenhoven. Shell filling and spin effects in a few electron quantum dot. *Physical Review Letters*, 77:3613–3616, 1996.

[13] R.C. Ashoori, H. Störmer, J. Weiner, L.N. Pfeiffer, S.J. Pearton, K.W. Baldwin, and K.W. West. Single-electron capacitance spectroscopy of discrete quantum levels. *Physical Review Letters*, 68:3088–3091, 1992.

[14] A. Yacoby, M. Heiblum, D. Mahalu, and H. Shtrikman. Coherence and phase-sensitive measurements in a quantum dot. *Physical Review Letters*, 74:4047–4050, 1995.

[15] E. Buks, R. Schuster M. Heiblum, D. Mahalu, and V. Umansky. Dephasing in electron interference by a 'which-path' detector. *Physical Review Letters*, 391:871–874, 1998.

[16] T.H. Oosterkamp, L.P. Kouwenhoven, A.E.A. Koolen, N.C. van der Vaart, and C.J.P.M. Harmans. Photon sidebands of the ground state and first excited state of a quantum dot. *Physical Review Letters*, 78:1536–1539, 1997.

[17] T. Fujisawa, T.H. Oosterkamp, W.G. van der Wiel, B.W. Broer, R. Aguado, S. Tarucha, and L.P. Kouwenhoven. Spontaneous emission spectrum in double quantum dot devices. *Science*, 282:932–935, 1998.

[18] D. Goldhaber-Gordon, Hadas Shtrikman, D. Mahalu, D. Abusch-Magder, U. Meirav, and M. A. Kastner. Kondo effect in a SET. *Nature*, 391:156–159, 1998.

[19] Ethan B. Foxman. *Single Electron Charging in Semiconductor Nanostructures.* PhD thesis, Massachusetts Institute of Technology, 1994.

[20] David Dixon. PhD thesis, University of California, Berkeley, 1998.

[21] Carol Livermore. PhD thesis, Harvard University, 1998.

[22] T.H. Oosterkamp. *Artificial atoms and molecules: on many body effects and coherence in semiconductor quantum dots.* PhD thesis, Technische Universiteit Delft, 1999.

[23] U. Meirav and E. B. Foxman. Single-electron phenomena in semiconductors. *Semiconductor Science and Technology*, 10:255–284, 1995.

[24] R.C. Ashoori. Electrons in artificial atoms. *Nature*, 379:413–419, 1996.

[25] L.P. Kouwenhoven, C.M. Marcus, P.L. McEuen, S. Tarucha, R.M. Westervelt, and N.S. Wingreen. Electron transport in quantum dots. In L.L. Sohn, G. Schön, and L.P. Kouwenhoven, editors, *Mesoscopic Electron Transport*, number 345 in NATO ASI Series E. Kluwer, 1997.

[26] W. Meissner and G. Voigt. *Ann. Physik*, 7:761, 892, 1930.

[27] Philip W. Anderson. *Concepts in Solids.* Addison-Wesley, 1982. 5th printing.

[28] J. Friedel. *Nuovo Cimento (Suppl)*, 7:287, 1958.

[29] P.W. Anderson. Localized magnetic states in metals. *Phys. Rev.*, 124:41, 1961.

[30] J. Kondo. *Prog. Theor. Phys.*, 32:37, 1964.

[31] A.P. Klein and A.J. Heeger. *Phys. Rev.*, 144:458, 1966.

[32] A.J. Heeger. Localized moments and nonmoments in metals. In Henry Ehrenreich and David Turnbull, editors, *Solid State Physics*, volume 23, page 283. Academic Press, New York, 1969.

[33] P.W. Anderson and A.M. Clogston. *Bull. Am. Phys. Soc.*, 144:458, 1966.

[34] J.R. Schrieffer and P.A. Wolff. *Phys. Rev.*, 149:491, 1966.

[35] D.C. Mattis. *Physical Review Letters*, 19:1478, 1967.

[36] K. G. Wilson. The renormalization group: critical phenomena and the Kondo problem. *Rev. Mod. Phys.*, 47:773–840, 1974.

[37] N. Andrei. Diagonalization of the Kondo Hamiltonian. *Physical Review Letters*, 45:379–382, 1980.

[38] P. B. Wiegmann. Towards an exact solution of the Anderson model. *Phys. Lett. A*, 80A:163–167, 1980.

[39] T. A. Costi and A. C. Hewson. Transport coefficients of the Anderson model via the numerical renormalization group. *J. Physics: Cond. Mat.*, 6:2519–2558, 1994.

[40] U. Meirav, M.A. Kastner, and S.J. Wind. Single-electron charging and periodic conductance resonances in GaAs nanostructures. *Physical Review Letters*, 65:771–774, 1990.

[41] B. Su, V.J. Goldman, and J.E. Cunningham. Observation of single-electron charging in double-barrier heterostructures. *Science*, 255:313–315, 1992.

[42] S. Tarucha, Y. Tokura, and Y. Hirayama. Resonant tunneling of 3-dimensional electrons into degenerate zero-dimensional levels. *Physical Review B*, 44:13815–13818, 1991.

[43] M.A. Reed, J.N. Randall, and J.H. Luscombe. Semiconductor quantum dot resonant tunneling spectroscopy. *Semicon. Sci. Tech.*, 7:B12–B14, 1992.

[44] P.H. Beton, L. Eaves, and P.C. Main. Quantum confinement in laterally squeezed resonant tunneling devices. *Physical Review Letters*, 69:2995, 1992.

[45] Y. Takahashi, M. Nagase, H. Namatsu, K. Kurihara, K. Iwadate, Y. Nakajima, S. Horiguchi, K. Murase, and M. Tabe. Fabrication technique for si single-electron transistor operating at room temperature. *Electronics Letters*, 31:136, 1995.

[46] Y. Takahashi, H. Namatsu, K. Kurihara, K. Iwadate, M. Nagase, and K. Murase. Size dependence of the characteristics of si single-electron transistors on simox substrates. *IEEE Transactions on Electron Devices*, 43:1213, 1996.

[47] D. Goldhaber-Gordon, M.S. Montemerlo, J.C. Love, G.J. Opiteck, and J.C. Ellenbogen. Overview of nanoelectronic devices. *Proc. of the IEEE*, 85:521–540, 1997.

[48] Alan Fowler. On some modern uses of the electron in logic and memory. *Physics Today*, October, 1997.

[49] Y. Meir, N. S. Wingreen, and P. A. Lee. Low-temperature transport through a quantum dot: the anderson model out of equilibrium. *Physical Review Letters*, 70:2601–2604, 1993.

[50] N. S. Wingreen and Y. Meir. Anderson model out of equilibrium: Noncrossing approximation approach to transport through a quantum dot. *Physical Review B*, 49:11040–11052, 1994.

[51] D.C. Ralph and R.A. Buhrman. Kondo-assisted and resonant tunneling via a single charge trap: a realization of the Anderson model out of equilibrium. *Physical Review Letters*, 72:3401–3404, 1994.

[52] V. Madhavan, W. Chen, T. Jamneala, M.F. Crommie, and N.S. Wingreen. Tunneling into a single magnetic atom: Spectroscopic evidence of the Kondo resonance. *Science*, 280:567, 1998. Fano and Kondo in tunneling through Co atom on Au.

[53] Y. Meir, N. S. Wingreen, and P. A. Lee. Low-temperature transport through a quantum dot: The Anderson model out of equilibrium. *Physical Review Letters*, 70:2601–2604, 1993.

[54] Wataru Izumida, Osamu Sakai, and Yukihiro Shimizu. Kondo effect in single quantum dot systems — study with numerical renormalization group method. *J. Phys. Soc. Jap.*, 67:2444–2454, 1998.

[55] D. Goldhaber-Gordon, Jörn Göres, Hadas Shtrikman, D. Mahalu, U. Meirav, and M. A. Kastner. From the kondo regime to the mixed-valence regime in a single-electron transistor. *Physical Review Letters*, 81:5225, 1998.

[56] B. J. van Wees, H. van Houten, C. W. J. Beenakker, J. G. Williamson, L. P. Kouwenhoven, D. van der Marel, and C. T. Foxon. Quantized conductance of point contacts in a two-dimensional electron gas. *Physical Review Letters*, 60:848–851, 1988.

[57] D.A. Wharam, T.J. Thornton, R. Newbury, M. Pepper, H. Ahmed, J.E.F. Frost, D.G. Hasko, D.C. Peacock, D.A. Ritchie, and G.A.C. Jones. One-dimensional transport and the quantisation of the ballistic resistance. *Journal of Physics C: Solid State Physics*, 21:L209–214, 1988.

[58] A.T. Johnson, L.P. Kouwenhoven, W. de Jong, N.C. van der Vaart, C.J.P.M. Harmans, and C.T. Foxon. Zero-dimensional states and single-electron charging in quantum dots. *Physical Review Letters*, 69:1592–1595, 1992.

[59] Hadas Shtrikman, D. Goldhaber-Gordon, and U. Meirav. To be published, 1997. Describes recent advances on fabricating shallow two-dimensional electron gas structures in GaAs/AlGaAs heterostructures.

[60] C. Dahl et al. Edge magnetoplasmons in single two-dimensional electron disks at microwave frequencies: Determination of the lateral depletion length. *Applied Physics Letters*, 66:2271–2273, 1995.

[61] D.J. Thouless. Maximum metallic resistance in thin wires. *Physical Review Letters*, 39:1167, 1977. Scaling theory of localization.

[62] Theo Costi. Private Communication, 1998.

[63] D. R. Hamann. *Phys. Rev.*, 158:570–, 1967.

[64] Tai Kai Ng and Patrick A. Lee. On-site Coulomb repulsion and resonant tunneling. *Physical Review Letters*, 61:1768–1771, 1988.

[65] L. I. Glazman and M. E. Raikh. Resonant Kondo transparency of a barrier with quasilocal impurity states. *JETP Letters*, 47:452–455, 1988.

[66] J.A. Folk, S.R. Patel, S.F. Godijn, A.G. Huibers, C.M. Marcus, K. Campman, and A.C. Gossard. Statistics and parametric correlations of coulomb blockade peak fluctuations in quantum dots. *Physical Review Letters*, 76:1699–1702, 1996.

[67] A.M. Chang, H.U. Baranger, L.N. Pfeiffer, K.W. West, and T.Y. Chang. Non-gaussian distribution of coulomb blockade peak heights in quantum dots. *Physical Review Letters*, 76:1695, 1996.

[68] U. Sivan, R. Berkovits, Y. Aloni, O. Prus, A. Auerbach, and G. Ben-Yoseph. Mesoscopic fluctuations in the ground state energy of disordered quantum dots. *prl*, 77:1123–1126, 1996.

[69] S.R. Patel, S.M. Cronenwett, D.R. Stewart, A.G. Huibers, C.M. Marcus, C.I. Duruoz, J.S. Harris, K. Campman, and A.C. Gossard. Statistics of coulomb blockade peak spacings. *Physical Review Letters*, 80:4522–4525, 1998.

[70] D.R. Stewart, D. Sprinzak, C.M. Marcus, C.I. Duruoz, and J.S. Harris. Correlations between ground and excited state spectra of a quantum dot. *Science*, 278:1784–1788, 1997.

[71] Charlie Marcus. Private Communication, 1999.

[72] Leonid Glazman. Private Communication, 1999.

[73] S.J. Tans S, M.H. Devoret, R.J.A. Groeneveld, and C. Dekker. Electron-electron correlations in carbon nanotubes. *Nature*, 394:761–764, 1998.

[74] E. B. Foxman, U. Meirav, P. L. McEuen, M. A. Kastner, P. A. Belk, D. M. Abusch, and S. J. Wind. Crossover from single-level to multilevel transport in artificial atoms. *Physical Review B*, 50:14193–9, 1994.

[75] Jürgen König, Jörg Schmid, Herbert Schoeller, and Gerd Schön. Resonant tunneling through ultrasmall quantum dots: Zero-bias anomalies, magnetic-field dependence, and boson-assisted transport. *Physical Review B*, 54:16820–16837, 1996.

[76] Selman Hershfield, John H. Davies, and John W. Wilkins. Probing the Kondo resonance by resonant tunneling through an Anderson impurity. *Physical Review Letters*, 67:3720–3723, 1991.

[77] L.Y.L. Shen and J.M. Rowell. *Phys. Rev.*, 165:566, 1968.

[78] M. Dobers, K. von Klitzing, and G. Weimann. Electron-spin resonance in the two-dimensional electron gas of GaAs-$Al_xGa_{1-x}As$ heterostructures. *Physical Review Letters*, 38:5453–5456, 1988.

[79] S. M. Cronenwett, T. H. Oosterkamp, and L. P. Kouwenhoven. A tunable Kondo effect in quantum dots. *Science*, 281:540–544, 1998.

[80] A. Kaminski, Yu.V. Nazarov, and L.I. Glazman. Suppression of Kondo effect in a quantum dot by external irradiation. *preprint*, 1999.

[81] C. M. Varma and Y. Yafet. Magnetic susceptibility of mixed-valence rare-earth compounds. *Physical Review B*, 13:2950–2954, 1976.

[82] N. E. Bickers. Thermodynamic, transport, and excitation properties of Ce impurities in a model metal: Kondo resonance and universality in the mixed-valent regime. *Physical Review Letters*, 54:230–233, 1985.

[83] J. Schmid, J. Weis, K. Eberl, and K. von Klitzing. A quantum dot in the limit of strong coupling to reservoirs. *Physica B*, 258:182–185, 1998.

[84] F. Simmel, R.H. Blick, J.P. Kotthaus, W. Wegscheider, and M. Bichler. Anomalous kondo-effect in quantum dot at non-zero bias. *LANL preprint archives*, pages cond–mat/9812153, 1998.

[85] F. D. M. Haldane. Scaling theory of the asymmetric Anderson model. *Physical Review Letters*, 40:416–419, 1978.

[86] Takeshi Inoshita, Yoshio Kuramoto, and Hiroyuki Sakaki. Nonlinear low-temperature transport of electrons through a multilevel quantum dot. *Superlattices and Microstructures*, 22:75–79, 1997.

[87] U. Fano. *Phys. Rev.*, 124:1866, 1961. Fano lineshapes.

[88] J.U. Nöckel and A.D. Stone. Resonance line-shapes in quasi-one-dimensional scattering. *Physical Review B*, 50:17415, 1994. Fano lineshapes in quasi 1D wires.

[89] E. Tekman and P.F. Bagwell. Fano resonances in quasi-one-dimensional electron wave-guides. *Physical Review B*, 48:2553, 1993. Fano lineshapes in quasi 1D wires.

[90] J. Göres, D. Goldhaber-Gordon, S. Heemeyer, M.A. Kastner, Hadas Shtrikman, D. Mahalu, and U. Meirav. Fano resonances in electronic transport through a single electron transistor. To be published, 1999.

[91] S. Heemeyer and X.G. Wen. To be published, 1999.

[92] C. Livermore, C.H. Crouch, R.M. Westervelt, K.L. Campman, and A.C. Gossard. The coulomb blockade in coupled quantum dots. *Science*, 274:1332–1335, 1996.

[93] N.C. van der Vaart, S.F. Godijn, Y.V. Nazarov, C.J.P.M. Harmans, J.E. Mooij, L.W. Molenkamp, and C.T. Foxon. Resonant-tunneling through 2 discrete energy-states. *Physical Review Letters*, 74:4702–4705, 1995.

[94] T.H. Oosterkamp, T. Fujisawa, W.G. van der Wiel, K. Ishibashi, R.V. Hijman, S. Tarucha, and L.P. Kouwenhoven. Microwave spectroscopy of a quantum-dot molecule. *Nature*, 395:873–876, 1998.

[95] Natan Andrei, Gergely T. Zimanyi, and Gerd Schoen. A new quantum phase transition in the coupled quantum dots system. *LANL preprint archives*, pages cond–mat/9711098, 1997.

[96] Y. Meir and A. Georges. Electronic correlations in transport through coupled quantum dots. *Physical Review Letters*, 82:3508–3511, 1999.

[97] C. Kittel. *Introduction to Solid State Physics.* John Wiley and Sons, fifth edition, 1976.

[98] D. Berman, N.B. Zhitenev, R.C. Ashoori, and M. Shayegan. Observation of quantum fluctuations of charge on a quantum dot. *Physical Review Letters*, 82:161–164, 1999.

[99] D.S. Duncan, C. Livermore, R.M. Westervelt, K.D. Maranowski, and A.C. Gossard. Direct measurement of the destruction of charge quantization in a single-electron box. *Appl. Phys. Lett.*, 74:1045–1047, 1999.

[100] R.H. Blick, D.W. van der Weide, R.J. Haug, and K. Eberl. Complex broadband millimeter wave response of a double quantum dot: Rabi oscillations in an artificial molecule. *Physical Review Letters*, 81:689–692, 1998.

[101] U. Meirav, M.A. Kastner, M. Heiblum, and S.J. Wind. One-dimensional electron-gas in GaAs — periodic conductance oscillations as a function of density. *Physical Review B*, 40:5871–5874, 1989.

[102] Z. Borsosfoldi et al. Spectroscopy of quantum dots in the few electron limit. *Surface Science*, 361:677–681, 1996.

[103] I.H. Chan et al. Ballistic conductance fluctuations in shape space. *Physical Review Letters*, 74:3876–3879, 1995.

[104] H. van Houten et al. Submicron conducting channels defined by shallow mesa etch in $GaAs-AlGaAs$ heterojunctions. *Applied Physics Letters*, 49:1781–1783, 1986.

[105] D.A. Wharam et al. Empirical relation between gate voltage and electrostatic potential in the one-dimensional electron gas of a split-gate device. *Physical Review B*, 39:6283–6286, 1989.

[106] J.E. Furneaux et al. The fractional quantum hall effect in Si MOSFETS: New results. In *Proceedings of the 18th International Conference on the Physics of Semiconductors*, pages 421–424, 1986.

[107] D. Abusch-Magder. Artificial atoms and electron puddles: Single and double barriers in a silicon MOS system. *PhD Thesis*, 1997.

[108] Yoshiji Horikoshi, Albrecht Fischer, Erdman F. Schubert, and Klaus Ploog. High-mobility two-dimensional electron gas from delta-doped asymmetric $Al_xGa_{1-x}/GaAs/Al_yGa_{1-y}As$ quantum wells. *Japanese Journal of Applied Physics*, 26:263–266, 1987.

[109] J.E.F. Frost, D.A. Ritchie, and G.A.C. Jones. The growth of shallow high mobility two-dimensional electron gas structures. *Journal of Crystal Growth*, 111:305–308, 1991.

[110] S.G. Ingram, D.A. Ritchie, and G.A.C. Jones. Effect of temperature changes during mbe of ultra-thin $GaAs/AlAs$ heterostructures on performance of Al gates grown *in situ*. *Semiconductor Science and Technology*, 7:968–971, 1992.

[111] M.C. Holland, E. Skuras, J.H. Davies, I.A. Larkin, A.R. Long, and C.R. Stanley. The effect of growth temperature, δ-doping and barrier composition on mobilities in shallow $AlGaAs - GaAs$ two-dimensional electron gases. *Journal of Crystal Growth*, 150:1215–1219, 1995.

[112] E. Skuras et al. Electron transport in shallow heterostructures with $AlGaAs$ and $AlAs$ barriers. *Semiconductor Science and Technology*, 10:922–929, 1995.

[113] D.H. Cobden, A. Savchenko, M. Pepper, M.K. Patel, D.A. Ritchie, J.E.F. Frost, and G.A.C. Jones. Time-irreversible random telegraph signal due to current along a single hopping chain. *Physical Review Letters*, 69:502–505, 1992.

[114] R.H. Blick, M.L. Roukes, W. Wegscheider, and M. Bichler. Freely suspended two-dimensional electron gases. *Physica B*, 251:784–787, 1998.

THESIS PROCESSING SLIP

FIXED FIELD: ill. _____ name _____

index _____ biblio _____

▶ COPIES: (Archives) Aero Dewey Eng Hum

Lindgren Music Rotch (Science)

TITLE VARIES: ▶[1] Strong Coupling and many body effects.

NAME VARIES: ▶[ ] _____

IMPRINT: (COPYRIGHT) _____

▶ COLLATION: 124 P

▶ ADD: DEGREE: _____ ▶ DEPT.: _____

SUPERVISORS: _____

NOTES: First 13 pages aren't numbered.

cat'r: date: page: 596

▶ DEPT: Phy

▶ YEAR: 1999 ▶ DEGREE: Ph. D.

▶ NAME: GOLDHABER-GORDON, David Joshua